

Synnøve Strand Jacobsen

**Investigation into the presence of polyphenols and carotenoids in the two seaweed species *Alaria esculenta* and *Saccharina latissima*, with a focus on extracting, purifying, and characterizing the xanthophyll fucoxanthin.**

Master's thesis in Biotechnology

Supervisor: Finn L. Aachmann

Co-supervisor: Leesa J. Klau

July 2021



Synnøve Strand Jacobsen

**Investigation into the presence of polyphenols and carotenoids in the two seaweed species *Alaria esculenta* and *Saccharina latissima*, with a focus on extracting, purifying, and characterizing the xanthophyll fucoxanthin.**

Master's thesis in Biotechnology  
Supervisor: Finn L. Aachmann  
Co-supervisor: Leesa J. Klau  
July 2021

Norwegian University of Science and Technology  
Faculty of Natural Sciences  
Department of Biotechnology and Food Science



# Abstract

In recent years, the cultivation and utilization of seaweed as a sustainable source of renewable resources has gained a lot of attention. Research on antioxidants such as carotenoids and polyphenols from brown seaweed has especially been of interest due to their potential bioactivities and health benefits. Investigation of the polyphenols and carotenoids present in seaweed and developing strategies to extract, purify, isolate, and analyze them, is a step towards a more efficient utilization of the seaweed plant. The main objective of this thesis has been to extract and structurally characterize carotenoids and polyphenols from brown seaweed by investigating the small molecules present in *Alaria esculenta* and *Saccharina latissima*.

In a small-scale experiment, seaweed material with two different pretreatments, 1) wet material freeze-dried and ground before extraction (FD) and 2) wet material treated with enzymes freeze-dried and ground before extraction (ET), were extracted in acetone and methanol. The crude extracts were compared with nuclear magnetic resonance spectroscopy (NMR) and liquid chromatography-mass spectrometry (LC-MS) to evaluate the extracts. Bulk extractions of wet material (W) with acetone and subsequently with methanol and of FD-material with acetone were conducted. Crude extracts were purified by liquid-liquid partitioning, adsorption resin (XAD-16), and liquid chromatography medium (LH-20). NMR and LC-MS were used to evaluate and guide the extraction and purification process and as a tool for structure elucidation.

FD- and ET-material from both species showed indications of polyphenols and carotenoids when extracted with methanol and acetone in the small-scale experiment. By comparing NMR data, extraction with acetone showed more signals indicating carotenoid and polyphenolic moieties than extraction with methanol. *Alaria esculenta* showed more signals and signals of higher intensity of these types of molecules compared to *Saccharina latissima*. Complete defatting, using *n*-hexane, was not achieved as lipids were still associated with the targeted compounds after defatting and signals of targeted compounds appeared in the hexane phase. Signals consistent with aldehydes were observed in both crude extract and hexane phase and could indicate oxidation and degradation of carotenoids.

Purification with XAD-16 resin can be an effective way of producing a fucoxanthin-rich extract as signals that indicate the presence of the carotenoid fucoxanthin were observed by NMR in W-material from *S. latissima* from the bulk extraction with acetone. However, fucoxanthin was unable to be purified using column chromatography (with LH-20). It is suspected this is due to oxidative degradation of fucoxanthin. Signals indicating polyphenolic moieties were observed in NMR data of some of the fractions eluted off the column. Further work is required for purification and structural characterization.

A compound was purified from *A. esculenta* FD-material from bulk extraction. The complete structure of the compound was characterized by correlations in  $^1\text{H}$ - $^{13}\text{C}$  HSQC,  $^1\text{H}$ - $^1\text{H}$  COSY and  $^1\text{H}$ - $^{13}\text{C}$  HMBC spectra and was determined to be fucoxanthin. The data also indicated the presence of lipids. It is suspected that fucoxanthin in the sample is acetylated with fatty acids and is present as a fucoxanthin ester. Additional purification steps are needed to purify fucoxanthin further to allow biological activity testing and deeper understanding of its functions.

In conclusion, further work is needed on methods to efficiently purify and characterize carotenoids and polyphenols from *A. esculenta* and *S. latissima*. These should include measures to prevent oxidation and degradation of the targeted compounds.

# Sammendrag

Kultivering og utnyttelse av tare som en bærekraftig kilde til fornybare ressurser har de siste årene fått mye oppmerksomhet. Forskning på antioksidanter som polyfenoler og karotenoider fra bruntare har spesielt fått mye oppmerksomhet på grunn av de potensielle bioaktive virkningene og positive helseeffektene de har. Undersøkelser av hvordan disse stoffene fra tare effektivt kan ekstraheres, renses, isoleres og analyseres, er et steg i retning av en mer effektiv bruk av hele tareplanten. Hovedmålet med denne masteroppgaven har derfor vært å ekstrahere og karakterisere karotenoider og polyfenoler fra bruntare ved å undersøke tilstedeværelsen av små molekyler i artene *Alaria esculenta* og *Saccharina latissima*.

Taremateriale med ulik forbehandling ble i et små-skala forsøk ekstrahert med aceton og metanol. De to ulike forbehandlingene var 1) materiale som ble frysetørket og kvernet og 2) materiale som ble behandlet med enzymer, frysetørket og kvernet. Råekstrakt ble analysert med kjernemagnetisk resonans spektroskopi (NMR) og væskechromatografi-masse spektrometri (LC-MS) og for å kunne sammenligne prøvene. Fersk tare (W) ble ekstrahert med acetone og påfølgende metanol, og FD-materiale ble ekstrahert med aceton i en bulk-ekstraksjon. Råekstrakt ble renset ved hjelp av væske-væske partitionering, adsorpsjons-resin (XAD-16), og væskechromatografi medium (LH-20). NMR og LC-MS ble brukt til å evaluere og veilede ekstraksjons- og renseprosessen og som analytisk verktøy for karakterisering.

FD og ET materialet fra begge artene viste indikasjoner på polyfenoler og karotenoider ved ekstraksjon med metanol og aceton i små-skala forsøket. Sammenligning av NMR dataen viste flere signaler som indikerte tilstedeværelsen av polyfenoler og karotenoider ved ekstraksjon med aceton enn med metanol. Flere og mer intense slike signaler ble observert i prøver av *Alaria esculenta* enn i *Saccharina latissima*. Avfetting, med bruk av *n*-heksan ble ikke oppnådd, da fettstoffer kunne sees i de avfattede prøvene etter partisjoneringen og signaler som indikerte polyfenoler og karotenoider ble observert i heksan-fasen. Signaler konsistente med aldehyder ble observert i både råekstrakt og i heksan-fasen, noe som kan være en indikasjon på oksidasjon og nedbrytning av karotenoider.

Rensing ved hjelp av XAD-16 resin kan være en effektiv måte å produsere fucoxanthin-rike prøver, da NMR data indikerte tilstedeværelse av karotenoidet fucoxanthin i W-materiale av *S. latissima* ekstrahert med aceton. Fucoxanthin kunne imidlertid ikke observeres i prøvene renset med kolonnechromatografi med (LH-20). Dette mistenkes å komme av oksidativ degradering av fucoxanthin. I fraksjonene eludert fra kolonnen kunne det observeres signaler som indikerte polyfenoler. Ytterligere arbeid trengs for å rense og karakterisere disse stoffene.

En forbindelse ble renset fra *A. esculenta* FD-materiale fra bulk-ekstraksjonen. Forbindelsen ble karakterisert ved korrelasjoner i  $^1\text{H}$ - $^{13}\text{C}$  HSQC,  $^1\text{H}$ - $^1\text{H}$  COSY og  $^1\text{H}$ - $^{13}\text{C}$  HMBC spekter og bestemt til å være fucoxanthin. Denne dataen indikerte også at fettstoffer var tilstede. Det mistenktes at fucoxanthin er acetyleret med fettstoffer og finnes som fucoxanthin ester. Ytterligere rensing behøves for å isolere fucoxanthin og kunne teste for biologisk aktivitet og en dypere forståelse av forbindelsen. Det ble ikke karakterisert noen polyfenoler.

Ytterligere forskning trengs for en effektiv rensing og karakterisering av karotenoider og polyfenoler fra *A. esculenta* og *S. latissima*. Disse burde fokusere på å hindre oksidering og nedbrytning av de ønskede stoffene.



# Preface

The following work has been carried out and documented by Synnøve Strand Jacobsen, master student in the program MSBIOTECH at the Department of Biotechnology and Food Science at Norwegian University of Science and Technology, NTNU. This master thesis is a part of, and funded by, the Norwegian Seaweed Biorefinery Platform (SBP-N), led by Professor Finn Lillelund Aachmann at NTNU. All samples have been prepared in NTNU's laboratories at the Department of Biotechnology and Food Science, at campus Gløshaugen in Trondheim, Norway. Supervisors has been Finn L. Aachmann and Leesa Jane Klau, and the work for this thesis has been completed in the timeframe of August 2020 to July 2021.

I want to thank Professor Finn L. Aachmann, SBP-N, and the Department of Biotechnology and Food Science for the opportunity to be a part of and complete this work. Thanks to Seaweed Solutions AS (SES) for delivering fresh and locally cultivated *Alaria esculenta* and *Saccharina latissima* and Maren Sæther at SES for answering all the questions I have had about the delivered seaweed. I want to thank my supervisors and the engineers in the laboratories for all their help, guidance, and expertise during this work. A special thanks to Leesa J. Klau for your close follow up and a lot of help with all aspects of the thesis. You have become a good friend.

Thanks to family and friends for keeping me motivated and helping me through this time. And maybe most important of all, I want to thank Rudi, for being there for me, supporting me, loving me, and keeping up with me every day. You are my "holdfast".



# Table of Contents

List of Figures .....	xiii
List of Abbreviations (or Symbols) .....	xv
1 INTRODUCTION.....	16
1.1 Macroalgae .....	16
1.2 Brown macroalgae .....	16
1.2.1 Chemical compounds.....	18
Carbohydrates .....	18
1.3 Extraction and purification of carotenoids and polyphenols.....	22
1.3.1 Solvents .....	22
1.3.2 Purification .....	23
1.4 Structural Characterisation/Structural elucidation .....	25
1.4.1 Nuclear Magnetic Resonance .....	25
1.5 Aim of the study .....	31
2 MATERIALS AND METHODS .....	32
2.1 Materials.....	32
2.1.1 Seaweed .....	32
2.1.2 Analytical reagents .....	32
2.2 Methods.....	32
2.2.1 Sample pretreatment .....	32
Wet material (W) .....	33
Freeze-dried material (FD) .....	33
2.2.2 Chemical extractions .....	33
2.2.3 Liquid-liquid partitioning .....	36
2.2.4 Macroporous resin.....	36
2.2.5 Column chromatography with Sephadex LH-20 .....	37
2.2.6 Characterisation .....	37
3 RESULTS .....	40
3.1 Comparison between small-scale extractions .....	40
3.1.1 Defatting .....	41
3.1.2 Extractions with acetone and methanol .....	44
3.2 Bulk extractions on wet material .....	49
3.3 Macroporous resin.....	54
3.4 Column chromatography with Sephadex LH-20 .....	60
3.4.1 <i>Combined fractions</i> .....	62
3.5 Freeze-dried material .....	66

4	DISCUSSION.....	74
4.1	Investigation of the presence of polyphenols and carotenoids.....	74
4.2	Purification steps.....	76
4.2.1	Defatting .....	76
4.2.2	XAD-16 resin.....	77
4.2.3	Sephadex LH-20 .....	77
4.3	Extraction and elucidation of fucoxanthin.....	78
4.4	Future perspectives .....	78
5	CONCLUSION .....	80

# List of Figures

Figure 1.1: <i>Alaria esculenta</i> (a) and <i>Saccharina latissima</i> (b).....	17
Figure 1.2: Structure of polysaccharides found in brown seaweed..	18
Figure 1.3: Chemical structures of carotenoids. ....	20
Figure 1.4: Some phenolic compounds derived from brown macroalgae. ....	22
Figure 1.5: Fourier transformation of FIDs in the time domain..	27
Figure 1.6: Illustration of which correlations COSY, HSQC and HMBC NMR spectra show... .....	28
Figure 1.7: Typical chemical shift of chemical moieties found in carotenoids. ....	30
Figure 1.8: Typical chemical shift of chemical moieties found in polyphenols.....	30
Figure 2.1: Schematic overview of the pretreatment of the seaweed material prior to extractions. ....	33
Figure 2.2: Schematic overview of the extractions and purification steps. ....	34
Figure 2.3: Schematic overview of the bulk extraction of wet material with aqueous acetone. ....	35
Figure 2.4: Schematic overview of the bulk extraction of wet material with aqueous acetone. ....	36
Figure 3.1: <sup>1</sup> H NMR spectra (0.7–2.5 ppm) of hexane fractions from defatting with <i>n</i> - hexane. ....	41
Figure 3.2: <sup>1</sup> H- <sup>13</sup> C HSQC (0.7–2.5 ppm) of hexane-fraction of freeze-dried material from <i>Alaria esculenta</i> .....	42
Figure 3.3: <sup>1</sup> H NMR spectra (4–10 ppm) of hexane fractions from defatting with <i>n</i> - hexane. ....	43
Figure 3.4: <sup>1</sup> H- <sup>13</sup> C HSQC (4.0–10.0 ppm) of hexane-fraction of freeze-dried material from <i>Alaria esculenta</i> .. ....	43
Figure 3.5: <sup>1</sup> H-NMR spectra (8.0–10.0 ppm) of acetone soluble fractions (A) and methanol soluble fractions (M) of freeze-dried (FD) and enzyme treated (ET) of <i>Alaria</i> <i>esculenta</i> (AE) and <i>Saccharina latissima</i> (SL). ....	44
Figure 3.6: <sup>1</sup> H- <sup>13</sup> C HSQC spectrum (8.0–10.0 ppm, 90.0–135.0 ppm) of enzyme treated material from <i>Alaria esculenta</i> extracted with acetone .....	45
Figure 3.7: <sup>1</sup> H-NMR spectra (8.0–10.0 ppm) of acetone soluble fractions (A) and methanol soluble fractions (M) of freeze-dried (FD) and enzyme treated (ET) of <i>Alaria</i> <i>esculenta</i> (AE) and <i>Saccharina latissima</i> (SL).. ....	46
Figure 3.8: <sup>1</sup> H- <sup>13</sup> C HSQC spectrum (5.0–8.0 ppm, 60.0–140.0 ppm) of freeze-dried material from <i>Alaria esculenta</i> extracted with acetone .....	47
Figure 3.9: <sup>1</sup> H NMR spectrum (0.5–4.5 ppm) of acetone soluble fractions (A) and methanol soluble fractions (M) of freeze-dried (FD) and enzyme treated (ET) of <i>Alaria</i> <i>esculenta</i> (AE) and <i>Saccharina latissima</i> (SL) .....	48
Figure 3.10: <sup>1</sup> H NMR spectrum (0.7–4.2 ppm) of W-Aq-A..	49
Figure 3.11: <sup>1</sup> H NMR spectrum (0.7–4.2 ppm) of W-Aq-M .....	50
Figure 3.12: <sup>1</sup> H NMR spectrum (5.7–8.7 ppm) of W-Aq-A .....	51
Figure 3.13: <sup>1</sup> H NMR spectrum (5.7–8.7 ppm) of W-Aq-M .....	52
Figure 3.14: Base peak chromatogram of W-Aq-A.....	53
Figure 3.15: Base peak chromatogram of W-Aq-M. ....	53
Figure 3.16: <sup>1</sup> H NMR spectra of elution fractions of acetone extract of <i>S. latissima</i> wet material purified with XAD-16 resin.. ....	54
Figure 3.17: <sup>1</sup> H- <sup>13</sup> C HSQC spectrum of SL-Ac100 fraction of <i>Saccharina latissima</i> .....	55
Figure 3.18: <sup>1</sup> H- <sup>13</sup> C HSQC spectrum of SL-Ac100 fraction of <i>Saccharina latissima</i> . ....	56

Figure 3.19: $^1\text{H}$ - $^{13}\text{C}$ HSQC spectrum of SL-Ac100 fraction of <i>Saccharina latissima</i> . .....	57
Figure 3.20: $^1\text{H}$ DOSY spectrum of SL-Ac100 fraction of <i>Saccharina latissima</i> .....	57
Figure 3.21: $^1\text{H}$ NMR spectra (0.7-4.2 ppm) of <i>A. esculenta</i> R0 and R2 fraction from purification with XAD-16 resin .....	58
Figure 3.22: $^1\text{H}$ NMR spectra (5.0-8.0 ppm) of <i>A. esculenta</i> R0 and R2 fraction from purification with XAD-16 resin .....	58
Figure 3.23: Base peak chromatograms of AE-R2 and SL-R2 from the purification with resin .....	59
Figure 3.24: $^1\text{H}$ - $^{13}\text{C}$ HSQC spectra of tryptophan in F-53 <i>A. esculenta</i> collected from column at ~500 mL. ....	61
Figure 3.25: $^1\text{H}$ NMR spectra of <i>Alaria esculenta</i> , sample P1-P4 .....	63
Figure 3.26: $^1\text{H}$ NMR spectra of <i>Saccharina latissima</i> , sample P5-P8.. .....	63
Figure 3.27: $^1\text{H}$ - $^{13}\text{C}$ HSQC and DOSY spectrum (5.8-8.8 ppm) of <i>Alaria esculenta</i> , P4. ..	64
Figure 3.28: $^1\text{H}$ - $^{13}\text{C}$ and DOSY spectra (5.8-8.8 ppm) of <i>Saccharina latissima</i> , P8.....	65
Figure 3.29: $^1\text{H}$ spectrum (6.0-7.2 ppm) of acetone extracted material from <i>Alaria esculenta</i> FD.....	66
Figure 3.30: $^1\text{H}$ spectrum (0.7-2.2 ppm) of FD <i>Alaria esculenta</i> extracted with acetone.	67
Figure 3.31: Partial structure of C9-C8' showing the typical acyclic conjugated chain in carotenoids.. .....	67
Figure 3.32: Part of $^1\text{H}$ - $^1\text{H}$ COSY spectrum of FD <i>Alaria esculenta</i> extracted with acetone .....	68
Figure 3.33: Partial structures and how they are connected to the conjugated chain.....	69
Figure 3.34: Panel with "slices" of $^1\text{H}$ - $^{13}\text{C}$ HMBC spectrum of <i>A. esculenta</i> FD.....	69
Figure 3.35: $^1\text{H}$ - $^{13}\text{C}$ HMBC of C-1 and C-1' in compound from <i>Alaria esculenta</i> FD.....	70
Figure 3.36: $^1\text{H}$ - $^{13}\text{C}$ HMBC spectra of correlations from C8 ( $\delta_{\text{C}}197.9$ ).....	70
Figure 3.37: $^1\text{H}$ - $^{13}\text{C}$ HMBC of C-21' in compound from <i>Alaria esculenta</i> FD.....	71
Figure 3.38: Fucoxanthin structure with atom numbers, COSY correlations, and HMBC correlations. ....	71

## List of Abbreviations (or Symbols)

(CD <sub>3</sub> ) <sub>2</sub> CO	Deuterated acetone, acetone-d <sub>6</sub>
CD <sub>3</sub> DO	Deuterated methanol, methanol-d <sub>4</sub>
CDCl <sub>3</sub>	Deuterated chloroform, chloroform-d
COSY	Correlation Spectroscopy
d	Doublet
dd	Doublet of doublets
ddd	Doublet of doublet of doublets
DOSY	Diffusion Ordered Spectroscopy
DW	Dry weight
ET	Enzyme treated
FD	Freeze dried
FPLC	Fast protein liquid chromatography
HMBC	Heteronuclear Multiple Bond coherence
HSQC	Heteronuclear Single Quantum Coherence
LC-MS	Liquid Chromatography Mass Spectrometry
m	Multiplet
MS	Mass spectrometry
MW	Molecular weight
NMR	Nuclear Magnetic Resonance
ppm	Parts per million
q	Quartet
s	Singlet
t	Triplet
W	Wet
WW	Wet weight

# 1 INTRODUCTION

Due to the world's growing population and the increase in environmental challenges, which has been addressed as a worldwide issue for several decades (UNFCCC, 1992; UNFCCC, 1998; UNITED NATIONS, s.a.), there is a high demand of new, sustainable resources for food and energy. The interest in the unexploited, quick-growing, and low trophic biomass of seaweed and its potential use in the production of food, medicines, supplements, biomaterials, bulk chemicals, and biogas, has thus increased.

## 1.1 Macroalgae

Marine macroalgae, or seaweed, are multicellular photosynthetic organisms that can be divided into three main groups: green algae (class: Chlorophyceae), red algae (class: Rhodophyceae), and brown algae (class: Phaeophyceae), depending on the nature of the pigments present (Rueness, 1998; UiO, 2011). The size, shape, and structure of seaweed varies between species. The plants generally consists of a hapter (holdfast), stipes (stem), and lamina (blade(s)) (figure 1.1), through which it can absorb water, nutrients, and dissolved gasses (Dawes, 2016; Rueness, 1998). As described by Pavluk and bij de Vaate (2017), the trophic level is defined as «the position of an organism in the food chain and ranges from a value of 1 for primary producers to 5 for marine mammals and humans. Macroalgae, which need only sunlight and nutrients from the sea to grow, is at the lowest trophic level. Cultivation of species at the lowest trophic level is predicted to contribute significantly to meet the increasing demand of food, feed, materials, chemicals, and pharmaceuticals (Skjeremo *et al.*, 2014).

Seaweed has been utilized as a source of nutrition throughout the world for centuries, and the tradition origins from Asian countries where it can be traced back to the 4<sup>th</sup> century (McHugh, 2003). Today, seaweeds are exploited worldwide for algal hydrocolloids such as agar, alginate, and carrageenans, used as thickeners and stabilizers in food and pharmaceuticals, among other industries (Domínguez, 2013; Holdt and Kraan, 2011). In recent years, the cultivation and utilization of seaweed as a sustainable source of renewable resources has gained a lot of attention. Research on antioxidants such as carotenoids and polyphenols from brown seaweed has especially been of interest because of their potential bioactivities and health benefits (Holdt and Kraan, 2011; Li *et al.*, 2011; Vo *et al.*, 2012). Strategies for effective utilization of the raw material are still lacking, and more than half of the dry matter is returned to the sea (Brandslet, 2019). Today, researchers are working to get a better overview of the possibilities with seaweed, with the goal of utilizing more of the substances contained in them.

## 1.2 Brown macroalgae

Of the three group Phaeophyceae, the brown seaweeds, contains the largest species better known as kelps (Rueness, 1998). These are dominating in the Norwegian waters. The kelps are some of the fastest growing plants in the world and can produce a huge biomass in a short period of time. Of these, the species *Alaria esculenta* and *Saccharina latissima* (figure 1.1) are of especially high interest in Norway because of their natural



occurrence and potential for cultivating in the cold-temperate and arctic zones (Skjermo *et al.*, 2014).

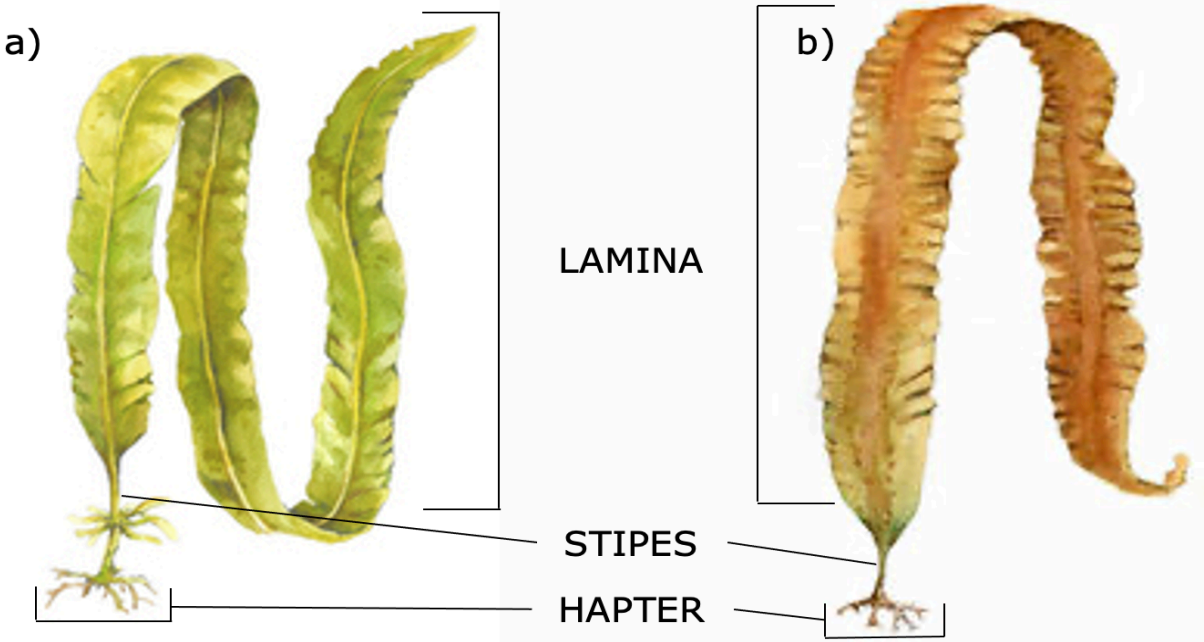


**Figure 1.1: *Alaria esculenta* (a) and *Saccharina latissima* (b).** Showing the different parts of the plant, including lamina, stipes and hapter. Adapted from Stein Mortensen at Miljølære.no.

### 1.2.1 Chemical compounds

Fresh seaweed has a high moisture content, which can account for up to 94 % of the wet weight in some species (Holdt and Kraan, 2011). In addition to water, seaweed consist of carbohydrates, proteins, lipids, vitamins, and minerals. The content of these components can vary between the different parts of the plant, species, habitats, and seasons (Misurcova, 2011).

#### Carbohydrates

Brown seaweeds are mainly comprised of carbohydrates that are found as cell wall polysaccharides, mucopolysaccharides, and storage polysaccharides. Some of the main carbohydrates documented (Holdt and Kraan, 2011) in brown seaweed include structural polysaccharides, like alginates and cellulose, and storage carbohydrates, like the polysaccharide laminarin and the sugar alcohol mannitol.

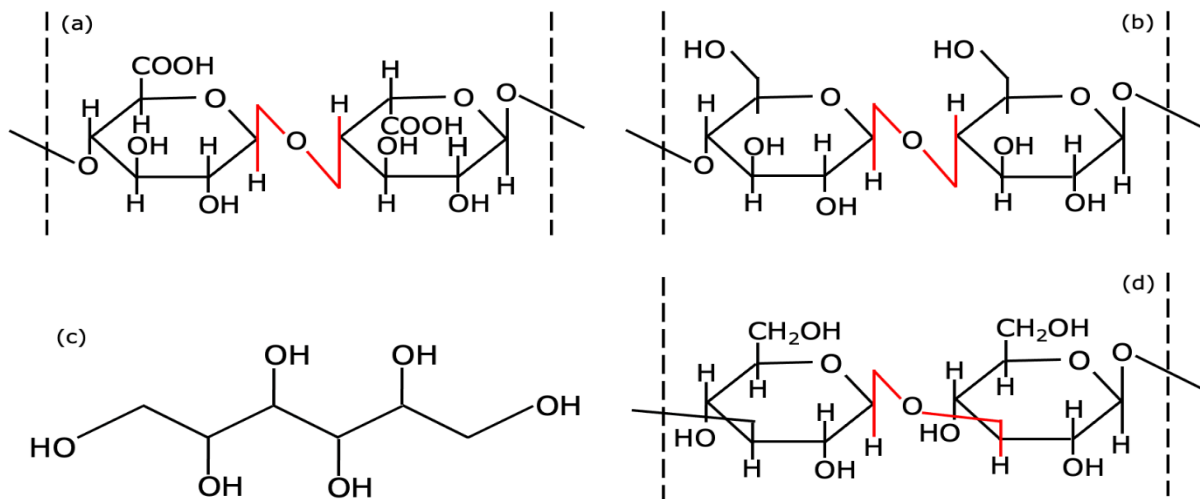


**Figure 1.2: Structure of polysaccharides found in brown seaweed.** a) Structure of alginate, consisting of  $\beta$ -D-mannuronic acid and  $\alpha$ -L-guluronic acid. b) Structure of cellulose, consisting of 1 $\rightarrow$ 4 linked  $\beta$ -D-glucose monomers. c) Structure of mannitol. d) Structure of laminarin, consisting of 1 $\rightarrow$ 3 linked  $\beta$ -D-glucan (branched 1 $\rightarrow$ 6 linkages not shown).

Alginates are linear polymers containing two different monomers,  $\beta$ -D-mannuronic acid and  $\alpha$ -L-guluronic acid (see figure 1.2a) (Draget *et al.*, 2005; Skjåk-Bræk, 1988). These can account for up to 40 % of the dry weight and make up most of the carbohydrates found in brown seaweed. Specifically, Schiener *et al.* (2015) found that the average amount of alginates in *Alaria esculenta* and *Saccharina latissima* was  $37.4 \pm 4.0$  % and  $28.5 \pm 3.9$  %, respectively. The acid form of alginates, alginic acids, are of high interest for many industries, such as food, pharmaceuticals, feed, and cosmetics, due to its many bioactive properties, including protection against carcinogens, clearing the digestion system, and lowering the concentration of cholesterol .

Cellulose is a linear polymer of 1 $\rightarrow$ 4 linked  $\beta$ -D-glucose monomers (see figure 1.2b) and is generally insoluble in water and organic solvents (Christensen, 2015). It works as a structural component and is found in the cell walls of brown seaweed. Schiener *et al.* (2015) found that the average content of cellulose in *A. esculenta* and *S. latissima* was

11.3 ± 1.0 % and 11.0 ± 1.4 %, respectively, and that the content of cellulose remained stable throughout the different seasons.

Other carbohydrates found in brown seaweed are mannitol (see figure 1.2c), an important sugar alcohol used in both pharmaceuticals and food, among other industries (Holdt and Kraan, 2011), laminarin (see figure 1.2d), consisting of 1→3 linked β-D-glucan with branched 1→6 linkages (Moldoveanu, 2021), and fucoidan, a family of polysaccharides composed of sulfated L-fucose (Holdt and Kraan, 2011).

Both mannitol and laminarin are storage carbohydrates that have shown to vary in amount depending on the season. The average content of mannitol and laminarin in *A. esculenta* and *S. latissima* is found to be 12.1 ± 3.5 % and 18.6 ± 4.7 %, and 11.1 ± 7.2 % and 8.2 ± 5.3 %, respectively. The mannitol content in *A. esculenta* and *S. latissima* has been found to accumulate during the months of summer (northern hemisphere) and have the highest yield during autumn (Schiener *et al.*, 2015).

### **Proteins**

Compared to green and red seaweeds, brown seaweeds have low protein content that range from about 3 – 21 % of dry weight (Fleurence, 2004; Holdt and Kraan, 2011; Schiener *et al.*, 2015). The protein content has also been found to vary with species and seasons, and the average total protein content in *A. esculenta* and *S. latissima* was found to be 11.0 ± 1.4 % and 7.1 ± 1.7 %, respectively, with the highest levels in the first quarter of the year (Schiener *et al.*, 2015). Most seaweed species contain all the essential amino acids, including tryptophan, the precursor of the important neurotransmitter serotonin (Pratt and Cornley, 2014).

### **Lipids**

The lipid fraction of brown seaweed includes phospholipids, glycolipids, neutral lipids, carotenoids, tocopherols, and sterols. Seaweeds contain only a small amount of lipids, varying from about 1-5 % (dw) (Makkar *et al.*, 2016). Holdt and Kraan (2011) reports that lipids may represent up to 4.5 % (dry weight) of the seaweed, but that the fatty acid fraction varies with season and other environmental factors. The majority of lipids found in seaweed are polyunsaturated fatty acids (PUFAs), like the two important n-3 fatty acids eicosapentaenoic acid (EPA) and docosahexaenoic acid (DHA) (Narayan *et al.*, 2006).

### **Carotenoids**

Carotenoids are pigments chemically classified as terpenoids, a group of naturally occurring compounds made up of isoprene units, unsaturated hydrocarbons with five carbons (figure 1.3a). Of the terpenoids, carotenoids are tetraterpenoids, consisting of eight isoprene units (*i.e.* containing 40 carbon atoms). All naturally occurring carotenoids can exist in a number of geometrical (*cis/trans* or *E/Z*) isomeric forms and contain an extended delocalized π-electron system (Britton *et al.*, 2008). In this central acyclic region (C-11 to C-11'), the double bonds are in the *trans* conformation which gives the carotenoid molecule an elongated shape (figure 1.3b) (Coulter, 2016). The extensive system of conjugated double bonds is responsible for the light absorption of carotenoids, but also makes them extremely susceptible to isomerization and oxidation by light, heat, or acids (Britton *et al.*, 2008). The end-group of the chain can either be acyclic (*e.g.* lycopene, figure 1.3c), cyclic at one end (*e.g.* γ-carotene, figure 1.3d), or cyclic at both ends (*e.g.* fucoxanthin, figure 1.3e).

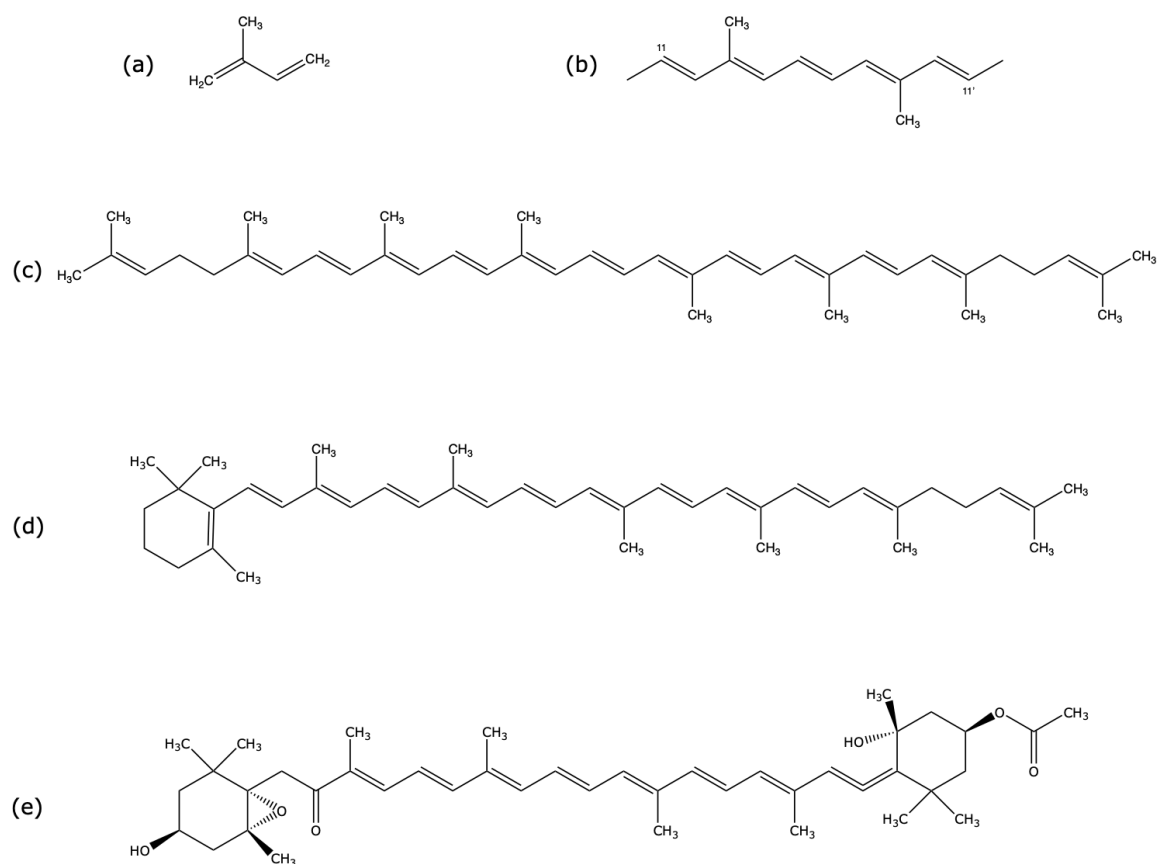


**Figure 1.3: Chemical structures of carotenoids.** a) Isoprene unit, an unsaturated hydrocarbon with five carbons. b) The central acyclic region (C11 to C11') common for all carotenoids. c) Lycopene, carotenoid with acyclic end groups. d)  $\gamma$ -carotene, carotenoid cyclic at one end. e) Fucoxanthin, carotenoid cyclic at both ends.

Carotenoids are divided into two main groups, 1) carotenes, which are hydrocarbons without oxygen, and 2) xanthophylls, which contain oxygen and arise initially by hydroxylation of carotenes (Coulter, 2016). Haugan and Liaen-Jensen (1994b) identified  $\beta,\beta$ -carotene as the only carotene present in brown seaweed, which accounted for 6 % of the total carotenoid content in the species *Saccharina latissima*. One of the most abundant carotenoids in nature is fucoxanthin, estimated to contribute to more than 10 % of the total natural carotenoid production (Peng *et al.*, 2011). Fucoxanthin, which is the main carotenoid in brown seaweed (Haugan and Liaen-Jensen, 1994b), is a xanthophyll with a unique structure containing a 5,6-monoepoxide and an unusual allenic bond. The molecular weight of fucoxanthin is 658.91 g/mol. In their study on isomers of fucoxanthin, Haugan and Liaen-Jensen (1994a) found the all-*trans*-(6'*R*)-isomer to be the naturally occurring isomer of fucoxanthin in brown seaweed. They also found four allenic (6'*S*)-isomers, all-*trans*-(6'*S*)-, 9'-*cis*-(6'*S*)-, 13'-*cis*-(6'*S*)-, and 13-*cis*-(6'*S*)-isomers.

Fucoxanthin has been investigated for bioactive properties, and it has been found to exhibit several biological effects (Holdt and Kraan, 2011; Peng *et al.*, 2011). Fucoxanthin has shown antioxidant activity (Sachindra *et al.*, 2007), where the effect has been suggested to be related to the allenic bond. Studies have also shown that fucoxanthin exhibit anti-inflammatory activity (Heo *et al.*, 2008; Kim *et al.*, 2010), anticancer activity (Hosokawa *et al.*, 2004), anti-obesity activity (Maeda *et al.*, 2005), among others. It is metabolized into fucoxanthinol and amarouciaxanthin after absorption (Sangeetha *et al.*,

2009), and it has been discussed whether the bioactivity documented of fucoxanthin (Holdt and Kraan, 2011) is actually the bioactivity of its primary metabolite fucoxanthinol (Sugawara *et al.*, 2002).

### **Polyphenols**

The WBSSH definition (from White, Bate-Smith, Swain, and Haslam), defines polyphenols as: "1) water-soluble compounds, 2) with molecular weight of 500–4000 Da, 3) possessing 12 to 16 phenolic hydroxy groups on five to seven aromatic rings per 1000 Da of relative molecular mass, and 4) polyphenols possess the ability to form complexes with other biomolecules, such as proteins and alkaloids to form precipitates" (Tsimogiannis and Oreopoulou, 2019). The true definition of what the term "polyphenols" should include is however much discussed. In need of a new and more comprehensive definition of the term, Quideau *et al.* (2011), proposed the following: "*The term "polyphenol" should be used to define plant secondary metabolites derived exclusively from the shikimate-derived phenylpropanoid and/or the polyketide pathway(s), featuring more than one phenolic ring and being devoid of any nitrogen-based functional group in their most basic structural expression*". In lack of an explicit definition of what polyphenols are, they will in this thesis be referred to as a large heterogenous group of phenolic compounds, chemically made up of hydroxylated phenyl moieties, and which consist of two or more aromatic rings bearing one or more hydroxyl substituents (Tsimogiannis and Oreopoulou, 2019).

Polyphenols occur in plants as secondary metabolites, small organic molecules not essential for growth, development, or reproduction (Barrios-González, 2018), but one of the most important groups of natural and chemo-preventative agents found in the human diet (Chedea and Pop, 2019). Previous research on the total phenolic content (TPC) in brown seaweeds (Connan *et al.*, 2004; Roleda *et al.*, 2019; Schiener *et al.*, 2015) have shown that variation in polyphenols are largely specie-specific and seasonal.

The major polyphenolic class found in brown seaweed is the phlorotannins (Cotas *et al.*, 2020), accounting for about 5-12 % of the dry mass (Venkatesan *et al.*, 2019). Phlorotannins are oligomers formed by polymerization of phloroglucinol monomer units (figure 1.3a), and are highly hydrophilic components with a wide range of molecular sizes (Cotas *et al.*, 2020; Imbs and Zvyagintseva, 2018; Singh and Sidana, 2013; Venkatesan *et al.*, 2019). Phlorotannin compounds can be classified into four subclasses based on their linkage; 1) Fuhalols and phlorethols, phlorotannins with an ether linkage, 2) fucols, phlorotannins with a phenyl linkage, 3) fucophloroethols, phlorotannins with an ether and a phenyl linkage, and 4) eckols, phlorotannins with a dibenzodioxin linkage (Sang *et al.*, 2012). A representation of phlorotannins structures by some previously characterized phlorotannins from brown macroalgae (Freile-Pelegrin and Robledo, 2014; Glombitza and Zieprath, 1989; Keusgen and Glombitza, 1995) is displayed in figure 1.4.

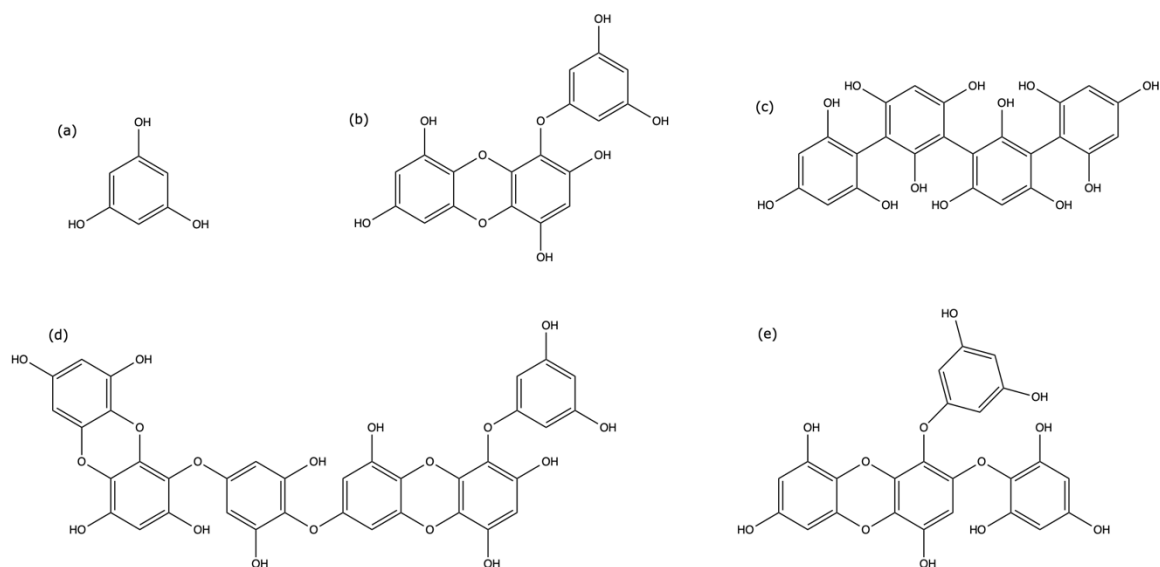


**Figure 1.4: Some phenolic compounds derived from brown macroalgae.** a) Phloroglucinol monomer. b) Eckol. c) Tetrafulcol A. d) Dieckol. e) 2-phloroeckol.

### 1.3 Extraction and purification of carotenoids and polyphenols

Extraction is the first step in the process of separating targeted molecules from the raw material. Methods for extraction include conventional methods based on solid-liquid extractions with various solvents, like Soxhlet extraction, maceration, percolation, turbo-extraction, and sonication (Sticher, 2008; Zhang *et al.*, 2018), and more novel methods like ultrasound assisted extraction (UAE), microwave assisted extraction (MAE), supercritical fluid extraction (SFE), pressurized liquid extraction (PLE), subcritical water extraction (SWE), and enzyme-assisted extraction (EAE) (Oreopoulou *et al.*, 2019). These newer extraction techniques are a result of an increasing demand of more environmentally friendly, faster, and efficient methods.

The reduction of particle size, by chopping, grinding, or milling the material prior to extraction, ruptures the cell walls and increases the diffusivity of the compounds (Alsaud and Farid, 2020). For plant-derived antioxidants, like carotenoids and polyphenols, solvent extraction is the most widely used method (Sultana *et al.*, 2009; Zhang *et al.*, 2018). Solvent extraction is based on the penetration of solvent into the solid matrix where the solute dissolves, and finally diffuse out of the solid matrix. The extraction efficiency is dependent on the properties of the extraction solvent, the particle size of the raw-materials, the solvent-to-solid ratio, the extraction temperature, pH, and the duration of extraction (Shannon and Abu-Ghannam, 2017; Sultana *et al.*, 2009; Zhang *et al.*, 2018).

#### 1.3.1 Solvents

Due to the presence of different compounds of varied chemical characteristic and polarities in plant material, the extract yield of the extracted compounds are strongly dependent on the nature of the extracting solvent (Sultana *et al.*, 2009). Based on the rule that "like dissolve like", solvents with a polarity near to the polarity of the solute are more efficient than solvents less similar. Several solvents have been used to extract

carotenoids and polyphenols from plant tissue previously, including acetone, ethanol, methanol, ethyl acetate, hexane, chloroform, diethyl ether, and aqueous solutions of these (Mourtzinou and Goula, 2019).

Phenolic compounds are usually most soluble in extractant less polar than water, and mixtures of water with methanol, ethanol, or acetone are generally recommended (Koivikko *et al.*, 2005). However, extraction of different phenolic compounds from different plant material requires different polarities. Pinelo *et al.* (2005) found methanol to be the most selective solvent for the extraction of phenolic compounds from grape byproducts, compared to ethanol and water, while Koivikko *et al.* (2005) found 70 % aqueous acetone to be the most effective extractant for phlorotannins from the brown alga *Fucus vesiculosus*.

Carotenoids are usually extracted using organic solvents due to their hydrophobic nature. However, carotenoids also exhibit different polarities, complicating the selection of appropriate solvent. Generally, non-polar solvents such as hexane are commonly used to extract non-polar carotenoids like the carotenes, while polar solvents such as acetone and ethanol are used to extract polar carotenoids, like the xanthophylls (Amorim-Carrilho *et al.*, 2014). Shannon and Abu-Ghannam (2017) found 62.2 % acetone to be the optimum solvent by RSM (response surface methodology) for extraction of the xanthophyll fucoxanthin from the blade of brown seaweed.

Due to the wide diversity of compounds of both polyphenols and carotenoids, there is no straight forward answer in the literature for extraction of such compounds. Overall, the most efficient solvent and extraction method is dependent on several factors, including the targeted molecules and type of plant material.

### 1.3.2 Purification

In the process of isolation and characterization of pure compounds from plant material purification of the extracts are important. Plant extracts usually occur as a complex combination of various type of compounds of different polarities, and separation of these can be challenging (Rodríguez-Amaya and Kimura, 2004). Before further purification, a defatting step is a common way to remove nonpolar compounds such as lipid, oils, waxes, and chlorophyll pigments from the crude extract (Tan *et al.*, 2013).

Various techniques exist for separation and purification of plant material mixtures, and choice of method is based on the properties of the analytes (Zhang *et al.*, 2018). Chromatography, a chemical separation method which allow for separation of molecules based on differences in properties like size, charge, and polarity (Thieman and Palladino, 2009), is the main method for separation of products from complex natural mixtures. Column chromatography is based on a two-phase system, a column filled with a stationary phase and elution with a mobile phase. The sample to be separated is loaded onto the column with the mobile phase, which could be a gas or a liquid, and elute from the column at different retention time based on the interactions between the compounds in the sample and the stationary phase (Nelson and Cox, 2013).

#### **Adsorptive macroporous resin**

Due to its simplicity, high capacity, and low-cost adsorbents, such as macroporous resins, adsorption column chromatography is often used for separation of natural products in the initial stages of separation. The principle of adsorptive macroporous resins is to separate compounds in solution by adsorption. The material to be adsorbed must thus be able to migrate through the pores of the resin to the adsorption surface.

Differences in molecular weight, polarity, or shape of different molecules leads to different affinity for the adsorbent, which is important to consider when choosing the right adsorption resin. Many different types of resin exist today, including synthetic polymeric adsorbents, of either hydrophilic or hydrophobic nature, such as polystyrene-divinylbenzene copolymers, polymethacrylate, divinylbenzene-ethyl vinylbenzene copolymers, and vinyl pyridine (Soto *et al.*, 2011).

Adsorptive macroporous resins have been found to be useful for the purification of numerous constituents from natural products, including polyphenols, glycosides, saponins, taxols, carotenoids, serotonin, and fatty alcohols (Li and Chase, 2010). Novel non-ionic macroporous resins are usually produced from styrene-divinylbenzene (SDVB) or acrylic-based polymers in the presence of porogens, which give rise to the discrete macropores. The three key parameters that characterize an adsorptive macroporous resin is 1) internal surface area, 2) pore diameter, and 3) surface polarity. According to Li and Chase (2010) the internal surface area for a dried resins are usually in the range of 100 to 1000 m<sup>2</sup>/g, with pore diameters ranging from 100 to 300 Å. The polarity is dependent of the monomer used in the synthesis of the resin or by additional polymerization.

Amberlite XAD-16 is a non-polar, hydrophobic, polymeric adsorption resin with a pore radius of 105 Å. This resin is generally used for adsorption of organic substances of small to medium molecular weight, from aqueous systems and organic solvents. In this way, the resin can be used to remove non-polar compounds from polar solvents (Silva *et al.*, 2007).

### **Gel filtration chromatography**

Sephadex LH-20 is a liquid chromatography medium made up of beaded, cross-linked hydroxypropylated dextran. Its structure gives it both hydrophilic and lipophilic properties, which allows it to swell in water and several organic solvents and gives it a unique chromatographic selectivity. The medium is made for molecular sizing of natural products and can be used for the preparation of closely related molecular species. Sephadex LH-20 has been employed in the purification strategy of several different flavonoids from specifically plant material. Mottaghipisheh and Iriti (2020) reported that 190 flavonoid derivatives have been isolated or purified from various plants by using LH-20.

### **Liquid chromatography-mass spectrometry**

LC-MS (Liquid Chromatography-Mass Spectrometry) is an analytical technique combined of the two separate techniques: high pressure-liquid chromatography (HPLC) and mass spectrometry (MS). HPLC is an advanced type of liquid-chromatography, where a mixture can be separated through a column packed with a stationary phase by elution with a mobile phase under high pressure (Herbert and Johnstone, 2003). The high pressure reduces the time of separation, and compounds of the mixture elute from the column based on their retention time. MS is a method where the sample is converted to a gaseous phase, ionized, and separated according to their mass/charge ratio (Mellon, 2003). Ionization may be accomplished by a variety of techniques, including electron ionization (EI), chemical ionization (CI), fast atom bombardment (FAB), electrospray ionization (ESI), atmospheric pressure chemical ionization (APCI), and matrix-assisted laser desorption ionization (MALDI), among others.

The combination of HPLC and MS is known as LC-MS and involves both the separation of mixtures according to their physical and chemical properties and identification of the



compounds based on their charges. The mass spectrometer analyzes the ions produced by the ionization, and as the component elutes off the column, a mass spectrum is recorded. By adding multiple ionization steps, known as tandem mass spectrometry (LC-MS/MS), further specificity can be obtained.

Ionization often results in the formation of adduct ions. An adduct ion is defined as an "ion formed by the interaction of a *precursor ion* with one or more atoms or molecules to form an ion containing all the constituent atoms of the precursor ion as well as the additional atoms from the associated atoms or molecules" (Murray *et al.*, 2013). The molecule can interact with a proton to form protonated molecules  $[M+H]^+$  and deprotonated molecules  $[M-H]^-$  in the positive and negative ion modes respectively, where M represent the molecule. For some molecules that undergo ionization, cationized molecules like  $[M+Na]^+$ ,  $[M+K]^+$ , and  $[M+NH_4]^+$  can form in the positive ion mode, and anionized molecules like  $[M-Cl]^-$ . Loss of a water molecule during the ionization process result in water-loss fragments  $[M+H-H_2O]^+$  or  $[M-H-H_2O]^-$ . Such adducts frequently appear in the mass spectrum and can suppress the analyte signal.

LC-MS methods has previously been used to successfully identify several carotenoids (de Rosso and Mercadante, 2007; Matsumoto *et al.*, 2007) and polyphenols (Boros *et al.*, 2010; Ma *et al.*, 2004). The similar chemical configurations of many carotenoids and polyphenols complicates the identification process. LC-MS, due to its sensitivity, has thus become an important tool to simultaneously detect several polyphenols and carotenoids, and to confirm that a peak corresponds to a component of the isomeric set for a particular carotenoid (Britton *et al.*, 2008).

## 1.4 Structural Characterisation/Structural elucidation

A key to understanding the molecular function of a compound is to know its molecular structure. Structural elucidation is the process of determining the molecular structure of a compound (Nature Portfolio, s.a.), including assessment of the constitution, spatial descriptors, conformation, and configuration (Niessen and Honing, 2015). Techniques used for structural elucidation includes novel chromatography and spectroscopy technology such as LC-MS (Liquid Chromatography Mass Spectrometry), GCMS (Gas Chromatography-Mass Spectrometry), NMR (Nuclear Magnetic Resonance spectrometry), and FTIR (Fourier-Transform Infrared Spectroscopy) (Amagata, 2010; Niessen and Honing, 2015)

### 1.4.1 Nuclear Magnetic Resonance

Nuclear magnetic resonance (NMR) spectroscopy is an analytical technique used in structural elucidation, which relies on the magnetic properties of the atomic nucleus (Günther, 2013; Jacobsen, 2007). An NMR spectrometer is a system containing a superconductive magnet, a probe, a console, and a computer, which together provides detailed information about the chemistry of a sample.

The principle of NMR is based on the Rutherford-Bohr model that all atomic nuclei have an electric charge and that electrons surround the nucleus in planetary orbits (Podgoršak, 2016). By applying electromagnetic energy to an atomic nucleus, the nucleus can be excited and emit a magnetic signal called a free induction decay (FID) that can be detected. For the NMR signal to be observable the sample must contain a magnetically active nuclide. This activity is caused by the presence of magnetic moment in the nucleus, nuclear spin (Simpson, 2008). Nuclei where the atomic mass and the atomic number are even, e.g. carbon-12, do not have this spin. A nuclide of the same

chemical element, e.g. carbon-13, would however possess this spin and thus be observable by NMR.

When a dissolved sample is placed in a homogenous magnetic field, the spins are influenced to align along the direction of the magnet field, either partially parallel ( $\alpha$  spin state) or antiparallel ( $\beta$  spin state) (Simpson, 2008; Wu, 2011). With increasing magnetic field, the difference between the energies of the  $\alpha$  spin state and the  $\beta$  spin state will increase. To induce transitions between the allowed spin states, photons with the same energy as the unique energy difference between the spin state of each NMR active nuclide must be applied. The frequency at which these photons can induce the transition is called the Larmor frequency, also known as the NMR frequency (Simpson, 2008).

The resonant frequency of a nucleus is affected by the atom's chemical environment, such as associated and nearby electrons, and intervening chemical bonds. Electrons resist to the applied magnetic field and thus shields the nucleus (chemical shielding). The more electrons surrounding the nucleus, the more protected from the applied field it is, which decrease the resonance frequency. Contrary to this, the less electrons surrounding the nucleus, the less protected it is, which increase the resonance frequency. This phenomenon is known as the chemical shift, a unitless quantity denoted  $\delta$  (Simpson, 2008). Nuclear spins can interact with each other is by indirect spin-spin coupling, also known as  $J$ -coupling, described by a coupling tensor  $J$ .  $J$  leads to a splitting of the resonance of the coupling spins, and thus provide important information about the structure. Several spin interactions may act simultaneously, and the respective coupling energies are added to the frequencies. The distribution of resonance frequencies forms the NMR spectrum, which works as a fingerprint of the molecular structure as magnetically inequivalent chemical groups possess different chemical shifts (Blümich, 2005).

Deuterated solvents, solvents where one or more hydrogens ( $^1\text{H}$ ) in the compound is changed with the isotope deuterium ( $^2\text{H}$ ), is required for NMR. This is to avoid a huge solvent signal that would dominate the spectrum and to stabilize the magnetic field strength. Common solvents to use are acetone- $d_6$  ( $(\text{CD}_3)_2\text{CO}$ ), chloroform- $d$  ( $\text{CDCl}_3$ ), dimethyl sulfoxide- $d_6$  (DMSO,  $\text{C}_2\text{D}_6\text{SO}$ ), methanol- $d_4$  ( $\text{CD}_3\text{OD}$ ), and deuterated water ( $\text{D}_2\text{O}$ ), and their suitability are based on several factors, e.g. polarity, temperature, and the chemical shift of the solvent (Claridge, 2016b). Some solvents, such as  $\text{D}_2\text{O}$ , are protic and will exchange its  $^2\text{H}$  atoms with  $^1\text{H}$  atoms at certain sites in the sample, e.g. low  $\text{pK}_a$ -values or Lewis base sites, making protons at these sites not observable (Simpson, 2008). These protons are often referred to as exchangeable protons and the proton exchange often leads to a broadening of signals (Claridge, 2016a).

Interpretation of NMR spectra can be used to molecular identifications of known and unknown structures. In addition to the chemical shift and spin coupling, which give information about the chemical environments, the integrals of the signals are important to consider. In  $^1\text{H}$  spectra the peak intensity is directly proportional to the number of protons. Spectral aliasing and folding, two phenomena which occur when the resonances fall outside the chosen spectral width and is characterized with incorrect frequencies (Claridge, 2016c) is also important to consider. When the peak occur at a position in the spectrum that is exactly one position away from its real position it is called spectral aliasing, while folding is when the peak occur at the position mirrored about the spectrum boundary (Vranken *et al.*, 2005). Both aliased and folded signals can also appear with sign inversion.

Many different NMR experiments have been developed to give useful information about the molecules in a sample. The experiments relevant for this thesis will be described in short below.

### One-dimensional NMR spectroscopy

In a one-dimensional NMR spectrum, the FID signal generated by the excited nuclei is detected and converted from a time domain to a frequency domain by the Fourier transform (FT). The signal is thus displayed in an NMR spectrum as amplitude as a function of frequency, where each frequency is assigned a peak (figure 1.5). One-dimensional NMR spectra is often displayed with the frequency axis as the chemical shift axis in parts per million (ppm) (Simpson, 2008). The more shielded the nucleus is the lower chemical shift in ppm it has, and it will appear further to the right side of the spectrum. Contrary, less shielded nuclei will appear at a higher chemical shift.

Two of the most common 1-D NMR experiments to perform is the  $^1\text{H}$ -NMR and  $^{13}\text{C}$ -NMR-spectrum, which provides information about the chemical shift of the protons and carbons, respectively.

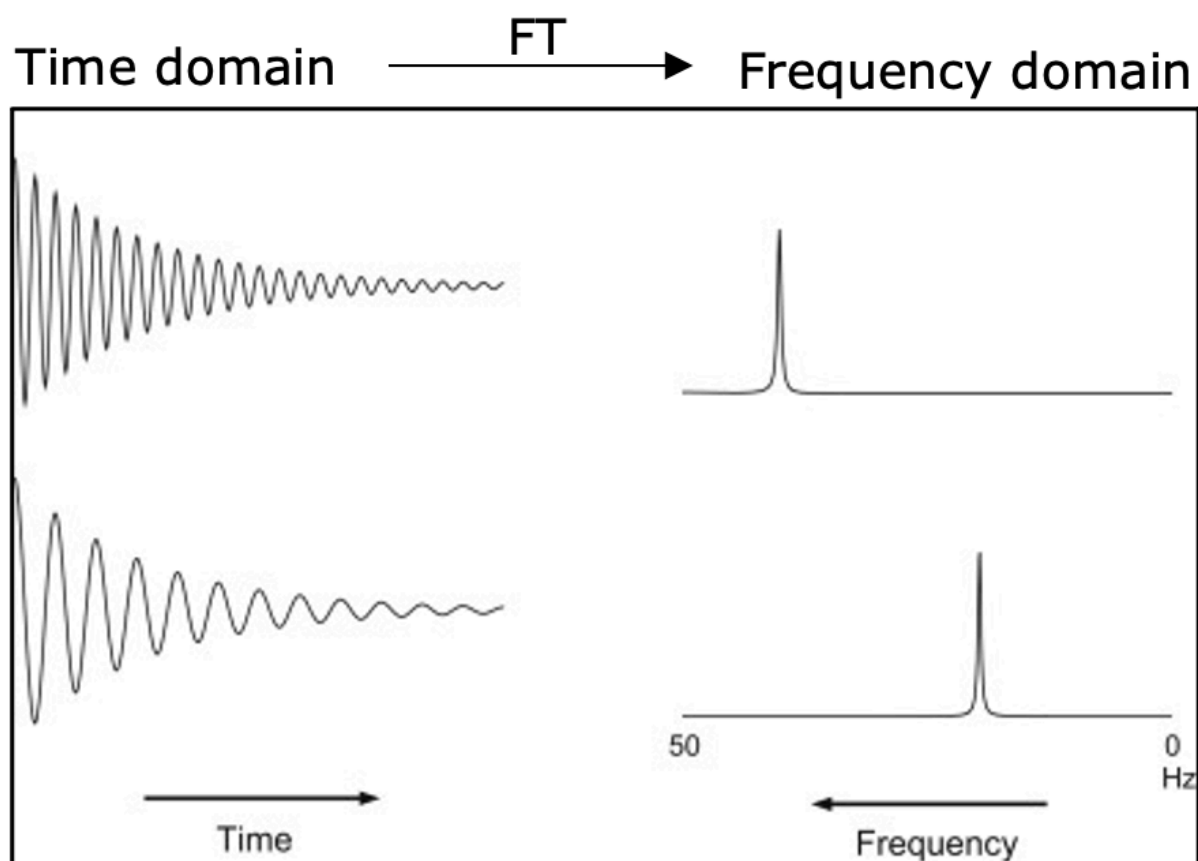


**Figure 1.5: Fourier transformation of FIDs in the time domain.** By applying the Fourier transform to FID signals detected in the time domain they are mathematically converted to signals in the frequency domain. Adapted from Claridge (2016a).

## Two-dimensional NMR spectroscopy

In a two-dimensional (2D) NMR spectrum there is two frequency domains (two frequency axis),  $f_1$  and  $f_2$ , representing any combination of chemical shifts and/or scalar products (Claridge, 2016c). 2D experiments can be divided into homonuclear and heteronuclear. Homonuclear experiments transfer magnetization from one nucleus to another nucleus of the same type, usually  $^1\text{H}$  to  $^1\text{H}$ , while heteronuclear experiments transfer magnetization between two different types of nuclei, *e.g.*  $^1\text{H}$  and  $^{13}\text{C}$  (Jacobsen, 2007). Correlation Spectroscopy (COSY) is a common homonuclear experiment, while heteronuclear experiment includes Heteronuclear Single Quantum Coherence (HSQC) and Heteronuclear Multiple Bond Correlation (HMBC), among others.

The COSY experiment is the simplest 2D experiment and show correlations between protons ( $^1\text{H}$ ) via a single  $J$  coupling (Jacobsen, 2007). This can be done due to magnetization transfer between coupled spins, where magnetization associated with one spin is transferred to a coupled spin by the pulse sequence (Claridge, 2016c). The  $J$  coupling are often two-bond (geminal) or three-bond (vicinal), but may in rare cases be long-range, up to four-five bonds. In a COSY spectrum both  $F_2$  and  $F_1$  display chemical shift for the protons.

HSQC experiments show single bond correlations between protons and carbons (figure 1.6). HSQC with multiplicity editing allows the determination of the number of protons attached to one carbon, where the CH and  $\text{CH}_3$  groups will phase the same (positive) and the  $\text{CH}_2$  groups will phase oppositely (negative) (Bruker, 2018). HMBC experiments show longer-range correlations between protons and carbons. Typically these are two- three correlations but can sometimes show four-bond correlations (figure 1.6). The single-bond correlations, observed in HSQC spectra, in such experiments are suppressed. In both HSQC and HMBC spectra chemical shift for the protons are displayed along the  $F_2$  (x-axis) and the carbons along the  $F_1$  (y-axis).

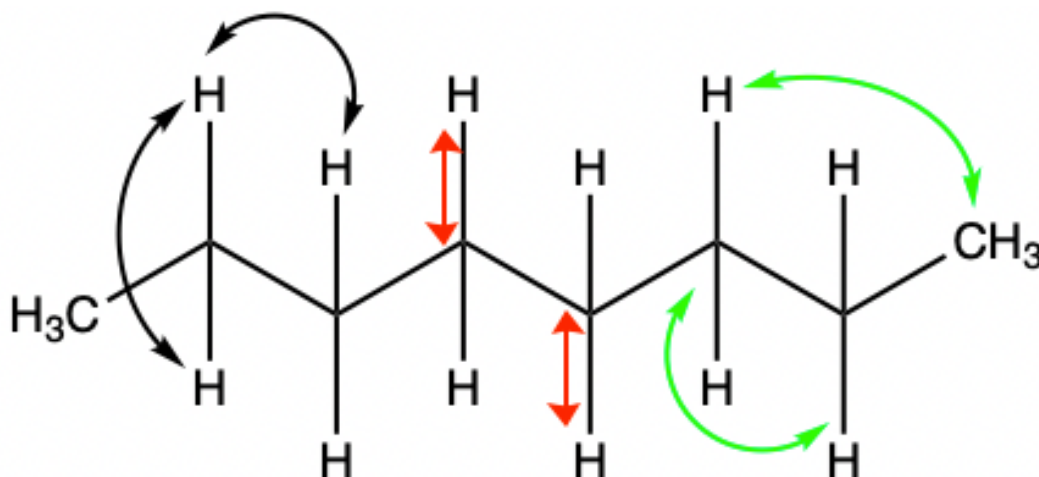


**Figure 1.6: Illustration of which correlations COSY, HSQC and HMBC NMR spectra show.** COSY correlations (black arrows) show protons two-three bonds away. HSQC (red arrows) show single bond correlation between protons and carbons. HMBC (green arrows) show multiple bond correlations between protons and carbons.

NMR can also be used to calculate other properties of molecules, such as diffusion coefficient. Diffusion-Ordered Spectroscopy (DOSY) experiments show which NMR signals belong to different molecules based on their diffusion coefficient. The rate of diffusion of a molecule is related to their size and shape, and since the diffusion coefficient of a given molecule is characteristic, all signals from a given molecule should appear at the same diffusion coefficient (Claridge, 2016d). In this way the DOSY spectrum can be useful in assessing mixtures by providing information about their complexity. In a DOSY spectrum, chemical shift for protons is displayed along the F2, while the diffusion coefficients are displayed along F1.

### **Characterisation of carotenoids and polyphenols**

Since its origin in 1945, nuclear magnetic resonance spectroscopy has become one of the most important analytical techniques in chemistry and overlapping subdisciplines. For researchers probing chemical structures, NMR is generally the tool of choice due to its fast, non-disruptive, and non-invasive means for the observation of matter (American Chemical Society, s.a.) NMR was early recognized as a technique with great potential for identification, characterization, and structure determination of carotenoids and other bioactive compounds from natural products (Moss, 1976; Pauli *et al.*, 2005). In the work of understanding the chemical composition of the molecules found in brown seaweed, NMR has been used quantitatively and qualitatively to study the presence and structures of carotenoids and polyphenols. This work includes the quantification and identification of phlorotannin structures (Ford *et al.*, 2019) and carotenoids, such as the xanthophyll fucoxanthin (Haugan and Liaaen-Jensen, 1994b).

In carotenoids, the atoms in the extensive system of conjugated double bonds (central acyclic region) are highly influenced of the movement of the  $\pi$ -electrons. This movement creates a "pulling" force within the  $\pi$ -bond of the double bond, and the alkenyl hydrogens becomes less shielded (Chemistry LibreText, 2020). These hydrogens usually occur between 6-7 ppm (Englert, 1985). In phlorotannins, several groups of protons show a tendency in their chemical shifts, making it possible to establish the structure of different phlorotannins based on the aromatic protons of different rings (Singh and Sidana, 2013). The aromatic protons in the middle rings typically show up at  $\delta_{\text{H}}$ 7.14-7.19, while those in the terminal rings show up at a slightly lower chemical shift at  $\delta_{\text{H}}$ 6.95-7.05. The acetyl groups on the middle rings are strongly shielded by biphenyl bonds in the structure, giving them a chemical shift of  $\delta_{\text{H}}$ 1.65-1.69, while the terminal ring located in the *para*- and *ortho*-position to the biphenyl bond, usually show up at a higher chemical shift  $\delta_{\text{H}}$ 2.27-2.28 and  $\delta_{\text{H}}$ 2.01-2.07, respectively (Singh and Sidana, 2013).

Typical chemical shifts of proton-carbon correlations in moieties found in carotenoids (figure 1.7) and polyphenols (figure 1.8) have been pooled from the literature of previously characterized compounds (Englert, 1985; Human Metabolome Database, s.a.-b; Organic Chemistry Data, 2005b; Singh and Sidana, 2013).

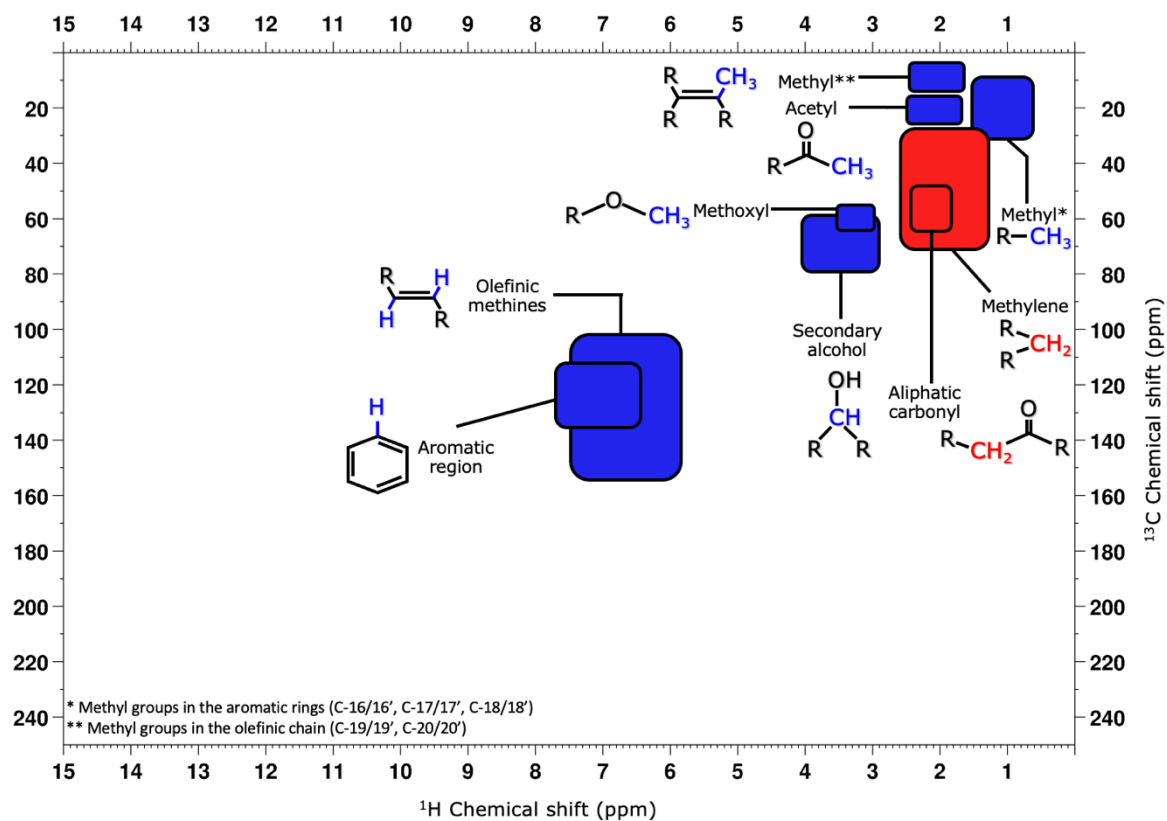


**Figure 1.7: Typical chemical shift of chemical moieties found in carotenoids.** The moieties are represented by blue ( $\text{CH}$  and  $\text{CH}_3$ ) and red ( $\text{CH}_2$ ) squares. The values are not accurate, but a representation of chemical shifts found in the literature.

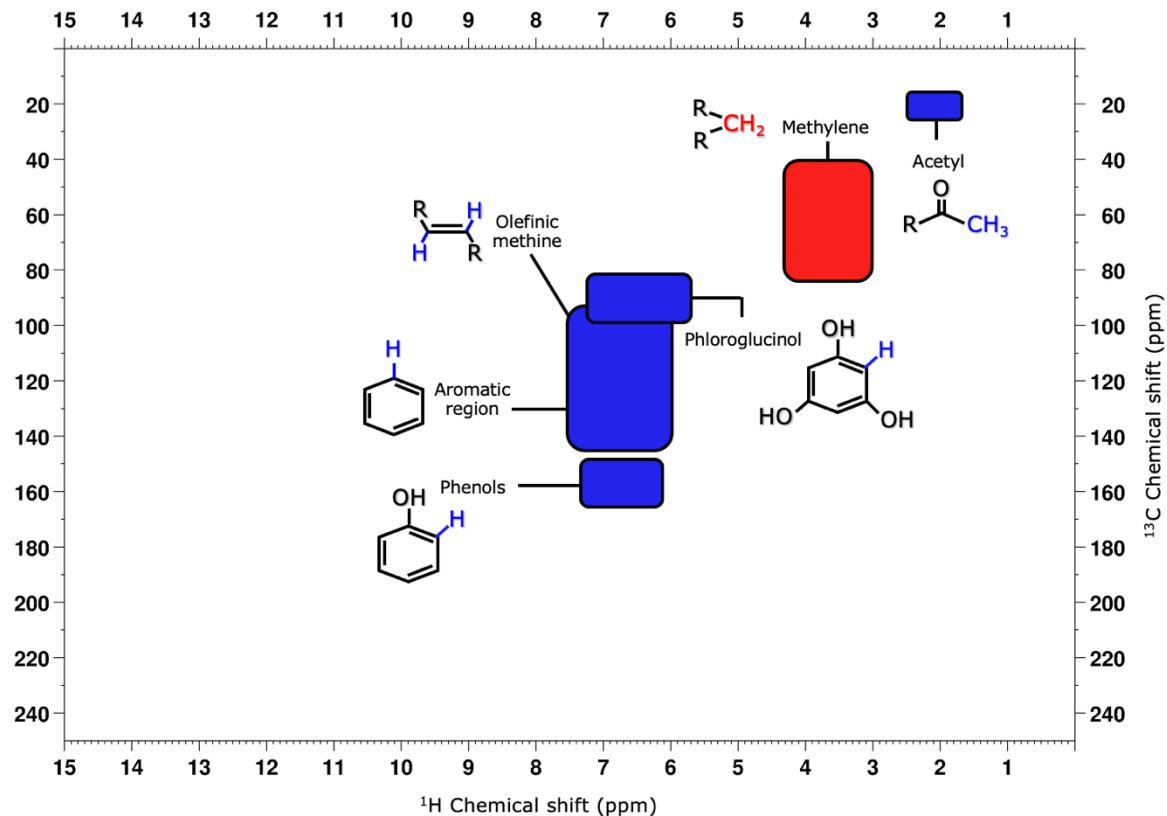


**Figure 1.8: Typical chemical shift of chemical moieties found in polyphenols.** The moieties are represented by blue ( $\text{CH}$  and  $\text{CH}_3$ ) and red ( $\text{CH}_2$ ) squares. The values are not accurate, but a representation of chemical shifts found in the literature.

## 1.5 Aim of the study

The main objective of this work is to extract and structurally characterize carotenoids and polyphenols from brown macroalgae. This is done by investigating the small molecules present in the two cultivated species of macroalgae, *Alaria esculenta* and *Saccharina latissima* with the following subgoals:

1. Investigate the presence of carotenoids and polyphenols in *Alaria esculenta* and *Saccharina latissima*.
2. Purify the samples through a set of purification steps.
3. Extract and isolate the carotenoid fucoxanthin.

Seaweed material with different pretreatment is extracted in solvents of different polarity and purified using macroporous resin (XAD-16) and liquid chromatography medium (LH-20). NMR spectroscopy and LC-MS is used to evaluate and guide the extraction process and for structure elucidation.

## 2 MATERIALS AND METHODS

### 2.1 Materials

#### 2.1.1 Seaweed

The two species of seaweed, *Alaria esculenta* and *Saccharina latissima*, were delivered to the lab at NTNU by Seaweed Solutions (SES) on June 9<sup>th</sup>, 2020. *A. esculenta* and *S. latissima* had been cultivated at SES Seaweed's farm located at Frøya (N63° 42.279' E8° 52.232') from 06.01.2020 to 11.05.2020 and from 17.01.2020 to 19.05.2020, respectively. The seaweed was harvested directly into 1000 L tanks with circulating seawater and transferred to the processing factory at Hitra (HitraMat) where it was vacuum-packed and frozen before transported to NTNU.

#### 2.1.2 Analytical reagents

Analytical graded solvents for extractions and partitioning were purchased from VWR Chemicals. These were acetone ( $\geq 99.8\%$ , CAS: 67-64-1), *n*-hexane ( $\geq 95\%$ , CAS: 110-54-3), and methanol ( $\geq 99.8\%$ , CAS: 67-56-1). Sodium Acetate (NaAc, 100 %, CAS: 127-09-3) was also purchased from VWR Chemicals. Acetic Acid (HAc, 100 %, CAS: 64-19-7) was purchased from Merck Life Sciences (Sigma-Aldrich). NovoZymes' Cellic<sup>®</sup> CTec2 was a kind gift from NovoZymes.

Deuterated solvents for NMR spectroscopy were purchased from Merck Life Sciences (Sigma-Aldrich). These were acetone-*d*6 (99.9 atom % D, CAS: 666-52-4), chloroform-*d* (99.8 atom % D, 0.05% v/v TMS, CAS: 865-49-6), deuterium oxide (99.9 atom % D, CAS: 7789-20-0), and methanol-*d*4 ( $\geq 99.8\%$  atom % D, CAS: 811-98-3).

Amberlite XAD-16 resin (CAS: 104219-63-8) was bought from Alfa Aesar<sup>™</sup> by Thermo Fisher Scientific. XAD-16 has a surface area of 800 m<sup>2</sup>/g, average pore diameter of 105 Å, a wet density of 1.02 g/cm<sup>3</sup>, mesh size of 20-60, and a moisture content of 62 %.

Sephadex<sup>®</sup> LH-20 resin was purchased from Merck Life Sciences (Cytiva).

### 2.2 Methods

#### 2.2.1 Sample pretreatment

Raw material from both species was weighed and separated into three different batches; one to be extracted directly from the wet material (W), one to be freeze-dried (FD), and one to be treated with enzymes (ET). The FD- and ET-material were freeze dried (Martin Christ Beta 1-8 LD plus, Edwards vacuum pump type E2M18) and ground (Janke & Kunkel IKA-WERK DCFH 48 mill, MF 2.0 sieve Ø 2.0 mm) before extraction. A schematic overview of the different pretreatments is displayed in figure 2.1, and the different pretreatments are described in detail below.



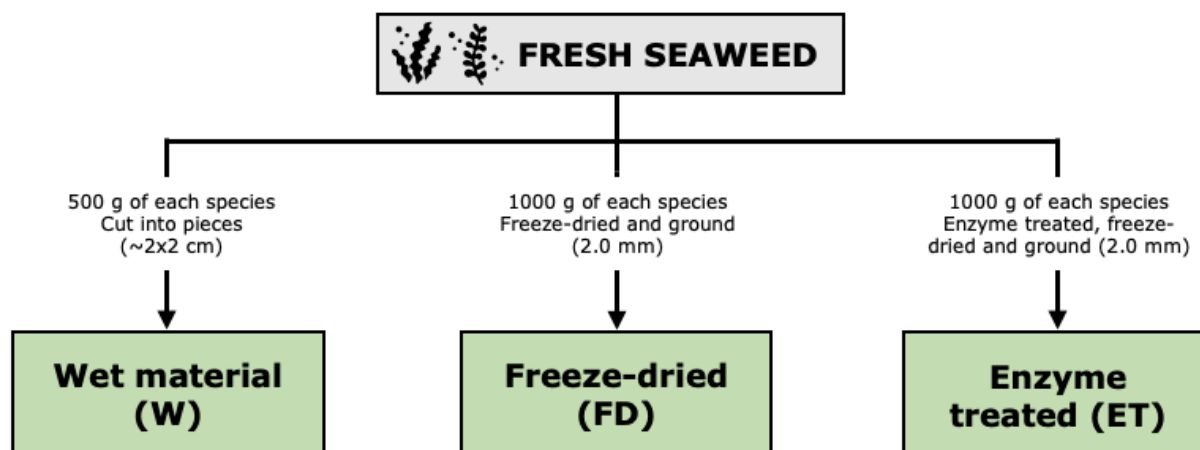


**Figure 2.1: Schematic overview of the pretreatment of the seaweed material prior to extractions.** The pretreatment resulted in three different batches of material from both species, wet (W), freeze-dried (FD), and enzyme-treated (ET).

### Wet material (W)

For each species 500 g fresh seaweed was cut into small pieces ( $\sim 2 \times 2$  cm<sup>2</sup>) and transferred to blue-top-bottles for extraction.

### Freeze-dried material (FD)

For each species 1 kg (2 x 500 g) fresh seaweed was placed in zip-lock bags. All samples were freeze dried and ground down to 2.0 mm.

### Enzyme treated material (ET)

For each species 500 g fresh seaweed was cut by hand into small pieces ( $\sim 2 \times 2$  cm<sup>2</sup>) and put in dialysis buckets. A volume of 1.2 L buffer (0.05 M NaAc/HAc) was added, and the buckets were placed in an incubator (New Brunswick™) for 30 minutes to reach room temperature before 1.2 mL enzyme (NovoZymes® Cellic CTec 2) was added. The buckets were then put back into the incubator (22 °C, 15 hours, 142 r.p.m., dark)

After incubation, the solid biomass was separated from the buffer and soluble fraction by filtration through a cheese cloth. The solid biomass was placed in zip-lock bags and freeze dried and ground down to 2.0 mm. The soluble fraction was filtered using vacuum filtration to remove particles, before concentrated using a rotary evaporator and freeze-dried.

## 2.2.2 Chemical extractions

For chemical extractions two different approaches were developed and performed. One approach was a small-scale extraction on the freeze-dried and the enzyme-treated material, consisting of a defatting-step with *n*-hexane, before extracting with acetone or methanol. The other approach was a bulk extraction with aqueous acetone of the wet material (W-Ac) and freeze-dried material (FD-Ac). The solid fraction of W-Ac was further extracted with methanol (W-M). The soluble fractions were portioned with *n*-hexane to defat, then purified using macroporous resin (Amberlite XAD-16 resin, see section 2.2.4). Selected fractions were chromatographically run on a column (Sephadex LH-20, see section 2.2.5). A schematic overview of the extraction process is displayed in figure 2.2.

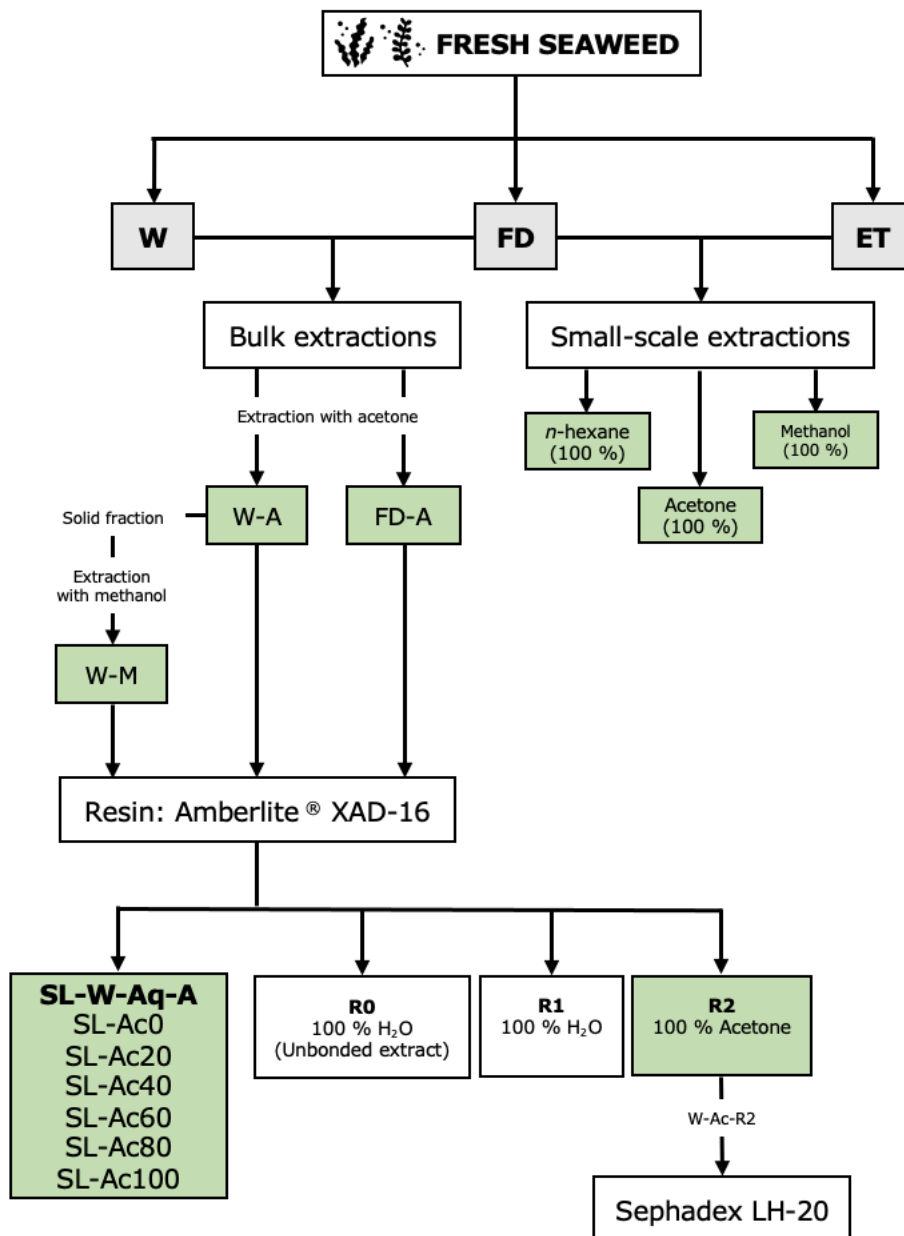


**Figure 2.2: Schematic overview of the extractions and purification steps.** W: Wet material, FD: Freeze-dried material, ET: Enzyme treated material, Ac: Acetone, Me: Methanol. Bulk extractions were performed on W- and FD-material. Small-scale extractions were performed on FD- and ET-material. Solid material of W-Ac was further extracted with methanol. Fractions from bulk extraction was purified with XAD-16 resin. R2-fractions (SL-W and AE-W) were chromatographically run on a column with Sephadex LH-20.

### Small-scale extractions

Freeze-dried (FD) and enzyme treated (ET) dried and ground material (two parallels of ~1 g of each specie and treatment, SL-FD-A, SL-FD-B, AE-FD-A, AE-FD-B) was submerged in 10 mL of *n*-hexane (100 %) and sonicated for 10 minutes. The solution was decanted off and filtered through a filter-paper (Whatman 113, 30 µm). The process was repeated three times with a total volume of 30 mL hexane and 30 minutes sonicating to extract lipids from the material.

After defatting, fractions A and B of each species was extracted with 10 mL of acetone (100 %) and methanol (100 %), respectively, and sonicated for 10 minutes. The solution was decanted off and filtered through a filter-paper (Whatman 113, 30 µm). The process was repeated five times, with a total volume of 50 mL methanol or acetone and 50 minutes sonicating.

All the soluble fractions were dried using a rotary evaporator and analyzed by NMR and LC-MS.

### Bulk extraction with aqueous acetone and methanol

#### Freeze-dried material

Ground freeze-dried material was covered with acetone (100 %) and sonicated for 15 minutes. The solution was decanted off and filtered through a filter-paper (Whatman 113, 30 µm). The process was repeated eight times. The extract was dried by rotary evaporator. A schematic overview is displayed in figure 2.3.

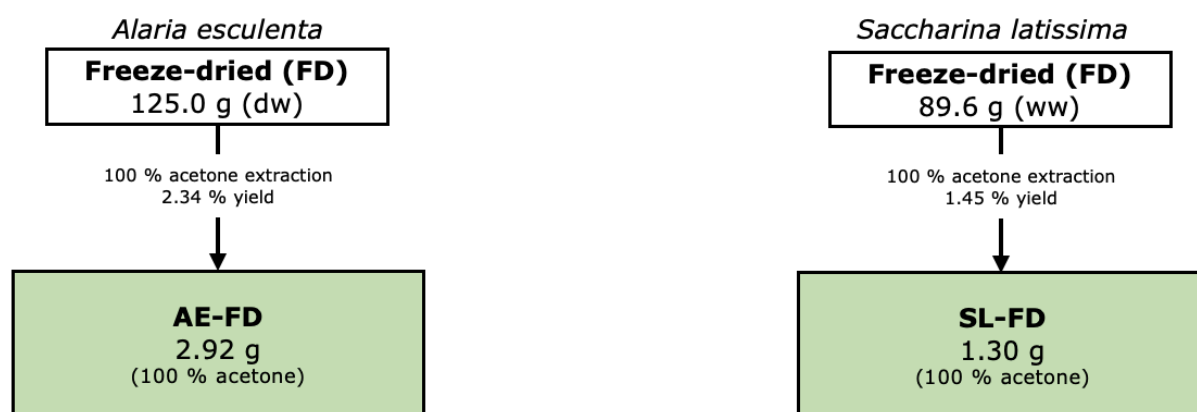


**Figure 2.3: Schematic overview of the bulk extraction of wet material with aqueous acetone.**

#### Wet material

Chopped seaweed material was submerged in 1 L of aqueous acetone (62.5 % v/v), covered in foil, and left to extract for 18 hours. After 18 hours the acetone-solutions were sonicated for 10 minutes. The solution was decanted off and filtered through a filter-paper (Whatman 113, 30 µm). The material was extracted further two times by adding 250 mL 62.5% aqueous acetone, sonicating for 10 minutes, and decanting and filtering the solution. A schematic overview is displayed in figure 2.4. The soluble fraction was

defatted as described in section 2.2.3 below and dried using a rotary evaporator. A subsample was analyzed by NMR and LC-MS. The solid fraction was frozen for further processing.

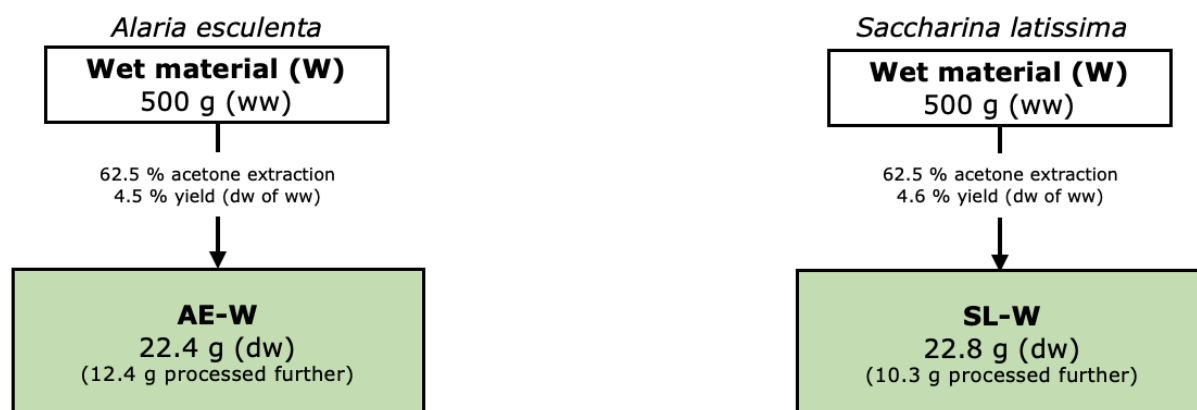


**Figure 2.4: Schematic overview of the bulk extraction of wet material with aqueous acetone.**

The wet seaweed material previously extracted with aqueous acetone was submerged in 700 mL methanol (100 %) and left to extract for 18 hours. After 18 hours the methanol-solutions were sonicated for 15 minutes. The soluble fraction was decanted off and concentrated on the rotavapor. The material was extracted further five times by adding 700 mL methanol, sonicating for 15 minutes, and decanting and filtering the solution. The soluble fraction was defatted as described in section 2.2.3 below and dried using a rotary evaporator. A subsample was analyzed by NMR and LC-MS.

### 2.2.3 Liquid-liquid partitioning

To remove lipids aqueous samples were portioned against *n*-hexane. Liquid-liquid partitioning was performed using a separating funnel.

#### Freeze-dried material

Crude extract from the bulk extraction with acetone (100 %) was resuspended 60 mL 1:2 reverse osmosis water (RO-water, Omnipure filter Co.):acetone, and defatted in a three-phase solvent system of *n*-hexane-RO-water-acetone in the volume ratio 3:1:2. Aqueous phase (FD-Aq) was recovered and dried.

#### Wet material

The soluble fractions from the bulk extractions with aqueous acetone (62.5 %) were defatted with a two-phase solvent system of *n*-hexane-RO-water in the volume ratio 1:1. Aqueous phase (W-Aq-A) was recovered and dried.

The soluble fractions from the extractions with methanol (100 %) were defatted with a three-phase solvent system of *n*-hexane-methanol-RO-water in the volume ratio 4:1:1. Aqueous phase (W-Aq-M) was recovered and dried.

### 2.2.4 Macroporous resin

Dried samples from the liquid-liquid partitioning (FD-Aq, W-Aq-A) were redissolved in RO-water in the ratio 1:2 (w/v). XAD-16 resin was washed thoroughly first with acetone

then with RO water, before added to a sintered glass funnel with a valve and a vacuum pump attached. The samples were then added to the resin in the ratio 1:5 (dried sample:resin).

Two different elution schemes (A and B) were used:

**A)** W-Aq-A: First to determine which percentage of acetone to use for elution a gradient elution with aqueous acetone was performed with ratios of 0:1, 1:4, 2:3, 3:2, 4:1, and 1:0 acetone:RO-water. The fractions were collected as Ac0, Ac20, Ac40, Ac60, Ac80 and Ac100 respectively.

**B)** FD-Aq, W-Aq-A: All subsequent samples were eluted as follows: The sample was loaded onto the resin and the flow through (unbonded extract still suspended in RO-water) was collected (R0). The resin was washed with RO-water and collected (R1). Finally, the sample was eluted with acetone (100 %) and collected (R2).

The collected fractions were dried using a rotary evaporator and selected fractions were analyzed by NMR. A subsample of the Ac100 and R2 fractions were also analyzed by LC-MS. FD-Aq was sent to Aalborg University in Denmark for further purification.

### 2.2.5 Column chromatography with Sephadex LH-20

Sephadex LH-20 (100 g) was packed in methanol (100 %) according to the protocol in appendix 1, in a solvent resistant column (2.6 cm x 100 cm). The column was attached to a GE ÄKTA Start protein purification system (FPLC) with an UV-detector (280 nm) and a Frac30 fraction collector. The elution buffer was 100 % methanol. UNICORN™ start 1.0 software from GE Healthcare Bio-Sciences AB was used to monitor the process and evaluate the results.

Dried fractions collected from the elution with acetone off the XAD-16 resin (R2) were redissolved in methanol and run chromatographically on the column packed with Sephadex LH-20. The elution was isocratic, and the total elution volume was 650 mL with a volumetric flow rate of 1 mL/min. The first 50 mL of eluent was not collected. The next 300 mL of eluent was collected as fractions of 10 mL in centrifuge tubes (15 mL, SARSTEDT) and dried using SpeedVac Concentrator (Savant SC250 EXP, Thermo Scientific) with Refrigerated Vapor Trap (Savant RVT5105, Thermo Scientific) and Vacuum Pump (OFP400, Thermo Scientific). Based on the UV-peaks in the chromatograms, selected fractions were analyzed by NMR and LC-MS.

### 2.2.6 Characterisation

#### **NMR**

NMR was used to analyze the structural composition of samples collected throughout this work. Samples were dissolved in either 180  $\mu$ L suitable solvent and transferred to a 3 mm WILMAN WG-1000 NMR tube (VWR) (800 MHz) or 600  $\mu$ L suitable solvent and transferred to a 5 mm WILMAN WG-1000 NMR tube (VWR) (600 MHz). The solvents used was either acetone- $d_6$  ( $\geq 99.9$  % atom D), chloroform- $d$  (99.8 atom % D, 0.05% v/v TMS), methanol- $d_4$  ( $\geq 99.8$  % atom D), or deuterium oxide ( $> 99.9$  % atom D). The specific solvent used for each experiment is defined in the respective results.

The  $^1\text{H}$  NMR and  $^1\text{H}$ - $^{13}\text{C}$  HSQC spectra, except of the fractions listed in table 1, and  $^1\text{H}$  NMR,  $^{13}\text{C}$  NMR,  $^1\text{H}$ - $^{13}\text{C}$  HSQC,  $^1\text{H}$ - $^1\text{H}$  COSY, and  $^1\text{H}$ - $^{13}\text{C}$  HMBC spectra of freeze-dried material sent to Aalborg University (Denmark) for further processing (and recording)

were recorded at 298.0-298.1 K (24.85-24.95 °C) on a Bruker Ultrashield 600 MHz magnet and with Avance III HD equipped with a 5-mm cryogenic CP-TCI z-gradient probe and SampleCase.

The  $^1\text{H}$  NMR and  $^1\text{H}$ - $^{13}\text{C}$  HSQC spectra of the fractions listed in table 1 and all  $^1\text{H}$  DOSY spectra were recorded at 298.1 K on a Bruker Ascend 800 MHz magnet and with Avance III HD equipped with a 5-mm cryogenic CP-TCI z-gradient probe and SampleJet.

The spectra were recorded, processed using TopSpin® 3.5 pl7, and analyzed using TopSpin® 4.0.9 software from Bruker. Chemical shifts are given in ppm. The following abbreviations are used for the characterization of NMR signals: s=singlet, d=doublet, t=triplet, q=quartet, and m=multiplet.

### LC-MS

Analyses were performed with an ACQUITY UPLC system consisting of a column manager (CM), flow through needle (FTN) injector and a binary solvent manager (BSM). The UHPLC was coupled to a Synapt G2-S HDMS mass spectrometer (Waters, Milford, MA, USA) equipped with an ESI source operating in positive and negative ion mode.

The chromatographic column was a Waters Premier Atlantis C18AX (95Å, 150×2.1 mm L×I.D. 1.7 µm, part.no 186009369) column, and the column manager was set to 45 °C. Mobile phase consisted of (A) water + 0.1% formic acid and (B) acetonitrile + 0.1% formic acid, and flow rate was set at 0.30 mL/min. Gradient was started at 99.0% A and held for one minute, then a linear gradient was programmed for 6.0 minutes down to 5.0% A, then held for 7.0 minutes, before it was brought back to 99.0% A in 0.50 minutes. Finally, the column was equilibrated for 1.50 minutes before starting a new injection. Total run time was 16.0 minutes. Ethanol was used as wash solvent for the FTN injector and water containing 10% acetonitrile was used as seal wash for the BSM system. The injection volume was 5 µL.

MS and MS/MS analyses were performed under constant ESI conditions. The flow from the UHPLC was directed to waste using the diverter valve for the first 0.6 minutes to prevent salt originating from samples to enter the ion source. The capillary voltage, cone voltage and source offset voltages in positive/negative mode were set at 2.5/-2.5 kV, 40/-40 V and 60/-60 V, respectively. The source temperature was maintained at 150 °C, desolvation gas temperature at 500 °C, and flow rate was set at 1000 L/h in both polarities. The cone gas flow rate was fixed at 50 L/h and the nebulizer gas flow maintained at 6 bar. The collision gas flow was set to 2 mL/min of argon.

Samples were analyzed in MS<sup>E</sup> mode, which yields both the scan spectrum and the MS/MS spectrum from the same chromatographic run. Mass range was set to 50-2000 Da (the same range as the valid calibration performed with Na-formate). The MS<sup>E</sup> was performed with low (4 V)/high (ramp 25-45V) energy applied to the trap cell. Data was collected in resolution mode with scan time set to 0.1 s. Resolution mode yields 20,000 FWHM for m/z 956 and is calibrated to a mass accuracy of 2 ppm. During the analysis, a lock mass flow of 20 µL/min leucine enkephalin (200 pg/mL) was infused into the ion source to correct the mass axis on the fly. Lock spray capillary voltage was set to 2.0/-2.0 and cone voltage to 50/-50 for positive and negative mode, respectively. The voltages are optimized to give approximately 100,000 counts and the dynamic range enhancement (DRE) setting is adjusted by the lock mass setup algorithm in IntelliStart

within the MassLynx software. UHPLC– qTOF data were acquired and processed using MassLynx software (v4.1, SCN957) and Progenesis QI (version 3.0.7600.27622).

LC-MS operations, including instrument handling, setting instrumental parameters, and running the samples were done by Kåre Andre Kristiansen, senior engineer at the Mass Spectrometry Lab at Faculty of Natural Sciences at NTNU. The method description is also adapted from his work.

## 3 RESULTS

### 3.1 Comparison between small-scale extractions

To compare species, extraction solvents and pretreatments, freeze-dried (FD) and enzyme-treated (ET) seaweed material from both species, *Alaria esculenta* (AE) and *Saccharina latissima* (SL), were defatted and extracted with acetone and methanol in a small-scale experiment. Two parallels of approximately 1 g (dw) of the freeze-dried (FD) and enzyme-treated (ET) material (SL-FD-1, SL-FD-2, AE-FD-1, AE-FD-2) were defatted with *n*-hexane. After defatting, fractions 1 and 2 were extracted with acetone and methanol, respectively.

The yield (in mg and % of dw) of each extraction is listed in table 1. Extraction of freeze-dried material with methanol resulted in the highest yield from both species, 14.63 % (dw/dw) and 14.41 % (dw/dw) of the extracted biomass of *A. esculenta* and *S. latissima* respectively. An aliquot of each sample was dried and analyzed by NMR. All NMR spectra can be seen in appendix B.

**Table 1: The yield from the small-scale extractions.** Pretreatments: FD=freeze-dried, ET=enzyme treated. The starting weight (in g) is the dry weight of the starting material, weights of the extract (in mg) is the dry weight of the extracted fractions. The yield is given as both weight and percentage (dw/dw) of the starting material.

	<i>Alaria esculenta</i>				<i>Saccharina latissima</i>			
Pretreatment	FD-1	FD-2	ET-1	ET-2	FD-1	FD-2	ET-1	ET-2
Starting weight	1.001 g	1.001 g	1.000 g	1.001 g	1.002 g	1.005 g	1.001 g	1.000 g
Defatting	3.8 mg 0.38 %	8.6 mg 0.86 %	1.6 mg 0.16 %	2.9 mg 0.29 %	3.3 mg 0.33 %	2.4 mg 0.24 %	3.0 mg 0.30 %	3.1 mg 0.31 %
Extraction	7.5 mg 0.75 %	146.4 mg 14.63 %	6.1 mg 0.61 %	24.9 mg 2.49 %	7.1 mg 0.71 %	144.8 mg 14.41 %	2.6 mg 0.26 %	52.5 mg 5.25 %



### 3.1.1 Defatting

Lipids were removed by extracting seaweed material with *n*-hexane.  $^1\text{H}$  NMR spectra (figure 3.1) of the hexane-soluble fractions indicate the presence of lipids. Chemical shifts at approximately 0.95-1.00 ppm are typical for the protons in the methyl-group (omega end), 1.20-1.25 ppm for the protons in the alkene chain, and 1.60-1.65 and 2.30-2.36 ppm for the protons in the methylene group at  $\gamma$ -carbon and  $\beta$ -carbon (alpha end) respectively. Both species and pretreatments have similar profiles.

The  $^1\text{H}$ - $^{13}\text{C}$  HSQC spectrum of the same area (figure 3.2) of freeze-dried material from *A. esculenta* confirms the presence of lipids. The annotated proton-carbon spin pairs ( $\delta_{\text{H}}0.86$   $\delta_{\text{C}}14.1$ ,  $\delta_{\text{H}}1.23$   $\delta_{\text{C}}32.1$ ,  $\delta_{\text{H}}1.65$   $\delta_{\text{C}}24.6$ ,  $\delta_{\text{H}}2.33$   $\delta_{\text{C}}33.9$ ) are consistent with the groups mentioned above in aliphatic fatty acids.

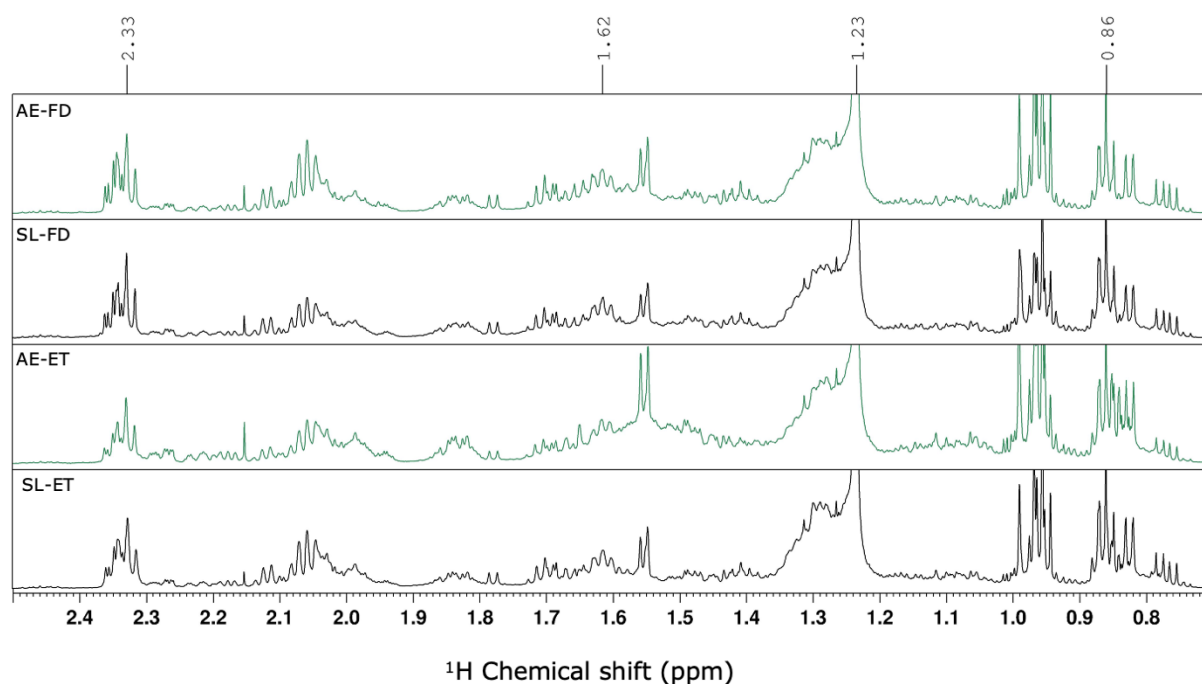


**Figure 3.1:  $^1\text{H}$  NMR spectra (0.7–2.5 ppm) of hexane fractions from defatting with *n*-hexane.** AE: *Alaria esculenta*, SL: *Saccharina latissima*, FD: freeze-dried material, ET: enzyme treated material. Signals in the region 0.7–2.5 ppm that could indicate protons in an aliphatic fatty acid, like the assigned peaks at 2.33, 1.62, 1.23, and 0.86 ppm. The samples were dissolved in deuterated chloroform ( $\text{CDCl}_3$ ) and run at 298.1K on 600 MHz.

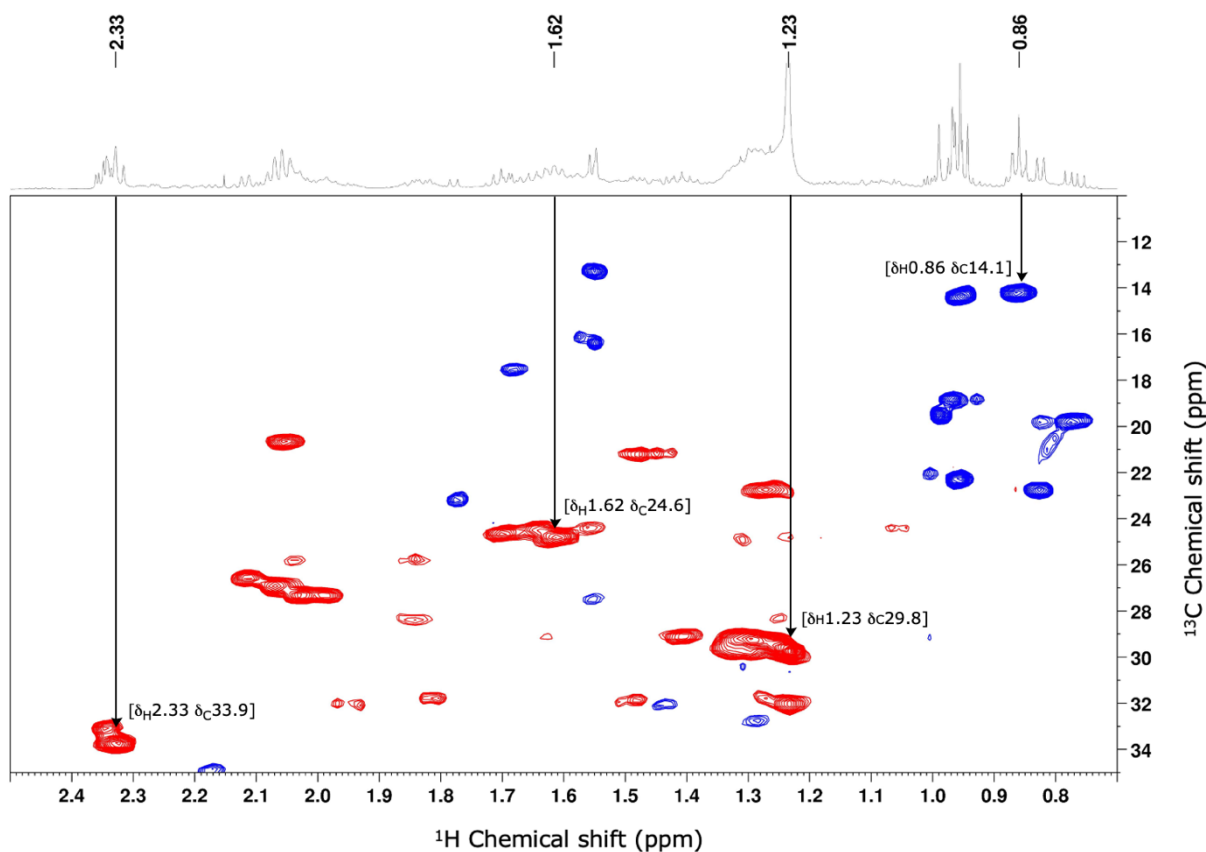


**Figure 3.2:  $^1\text{H}$ - $^{13}\text{C}$  HSQC (0.7-2.5 ppm) of hexane-fraction of freeze-dried material from *Alaria esculenta*.** The spectrum shows the proton-carbon spin pairs (in brackets [ ]) consistent with correlations in the methyl-group (omega end,  $\delta_{\text{H}}0.86$   $\delta_{\text{C}}14.1$ ), in the alkene chain ( $\delta_{\text{H}}1.23$   $\delta_{\text{C}}29.8$ ), and in the methylene group at  $\gamma$ -carbon ( $\delta_{\text{H}}1.62$   $\delta_{\text{C}}24.6$ ) and  $\beta$ -carbon ( $\delta_{\text{H}}2.33$   $\delta_{\text{C}}33.9$ ) (alpha end) of lipids. The sample were dissolved in deuterated chloroform ( $\text{CDCl}_3$ ) and run at 298.1K on 600 MHz.

In addition to lipids, the  $^1\text{H}$ -NMR spectra (figure 3.3) show signals at higher chemical shifts that are consistent with aldehydes (typically  $\geq 9$  ppm), aromatic protons (typically 7-8 ppm), phenolic protons (typically  $\sim 5$ -7 ppm), and olefinic protons (typically  $\sim 4.5$  ppm). The  $^1\text{H}$ - $^{13}\text{C}$  HSQC spectrum of the same area (figure 3.4) of *A. esculenta* FD show proton-carbon spin pairs consistent with folded aldehyde moieties ( $\delta_{\text{H}}9.51$   $\delta_{\text{C}}104.6$ ,  $\delta_{\text{H}}9.38$   $\delta_{\text{C}}97.8$ ,  $\delta_{\text{H}}8.53$   $\delta_{\text{C}}93.3$ ), substituted aromatic moieties ( $\delta_{\text{H}}7.99$   $\delta_{\text{C}}129.5$ ) and methylene groups ( $\delta_{\text{H}}5.36$   $\delta_{\text{C}}128.0$ ).

As the NMR spectra of the hexane-phase clearly show signals consistent with lipids, the defatting step seems to work well for removing lipids. However, other and more hydrophobic molecules are clearly also extracted with the hexane.

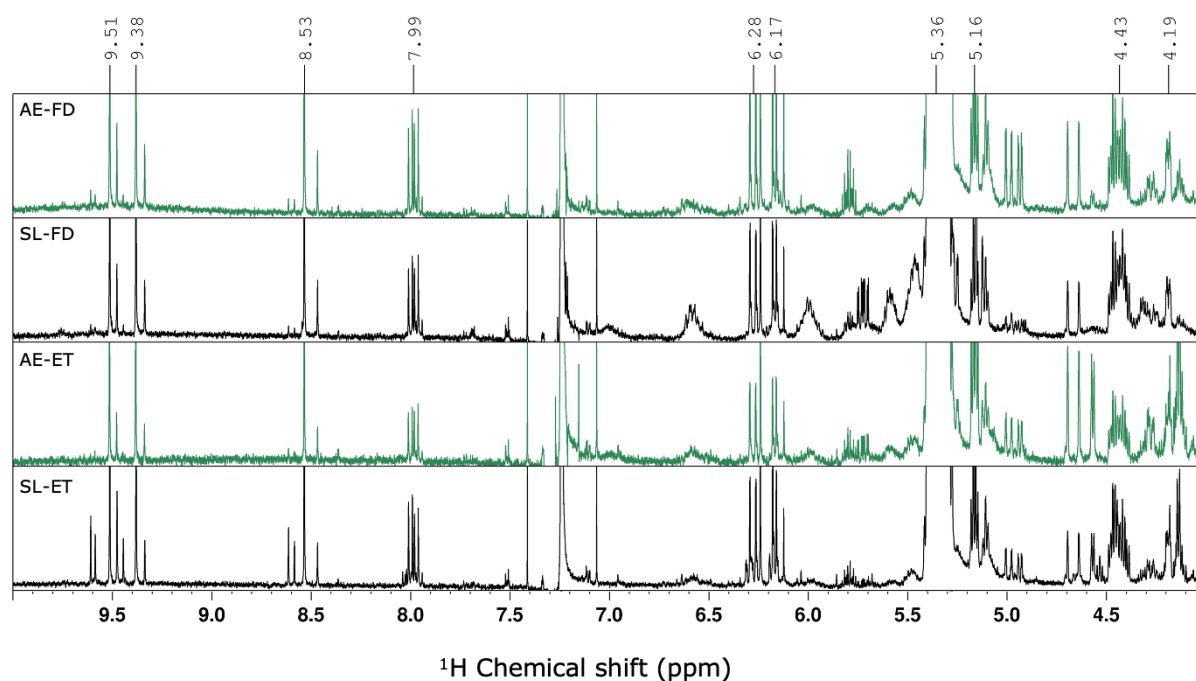


**Figure 3.3:  $^1\text{H}$  NMR spectra (4–10 ppm) of hexane fractions from defatting with *n*-hexane.** AE: *Alaria esculenta*, SL: *Saccharina latissima*, FD: freeze-dried material, ET: enzyme treated material. These signals indicate the presence of aldehydes ( $\sim 9.5$  ppm), aromatic protons ( $\sim 7$ – $7.5$  ppm), phenolic protons ( $\sim 5$ – $7$  ppm), and olefinic protons ( $\sim 4$ – $5$  ppm). The samples were dissolved in deuterated chloroform ( $\text{CDCl}_3$ ) and run at 298.1K on 600 MHz.

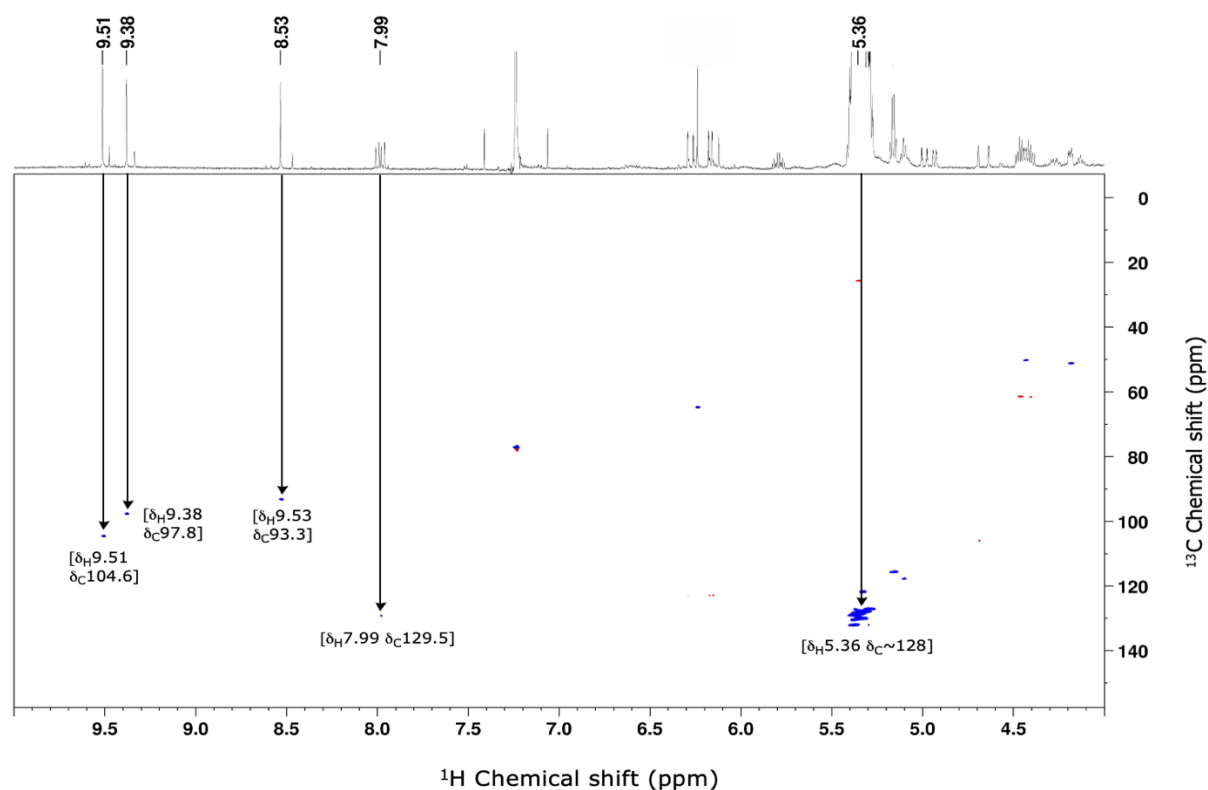


**Figure 3.4:  $^1\text{H}$ - $^{13}\text{C}$  HSQC (4.0–10.0 ppm) of hexane-fraction of freeze-dried material from *Alaria esculenta*.** The spectrum shows the proton-carbon spin pairs (in brackets [ ]) consistent with correlations in folded aldehyde moieties ( $\delta_{\text{H}}9.51$   $\delta_{\text{C}}104.6$ ,  $\delta_{\text{H}}9.38$   $\delta_{\text{C}}97.8$ ,  $\delta_{\text{H}}8.53$   $\delta_{\text{C}}93.3$ ), substituted aromatic moieties ( $\delta_{\text{H}}7.99$   $\delta_{\text{C}}129.5$ ) and methylene groups ( $\delta_{\text{H}}5.36$   $\delta_{\text{C}}128$ ). The sample was dissolved in deuterated chloroform ( $\text{CDCl}_3$ ) and run at 298.1K on 600 MHz.

### 3.1.2 Extractions with acetone and methanol

The defatted material was further extracted with acetone (100%) and methanol (100 %). The extracted fractions were analyzed by NMR and LC-MS. The NMR spectra of freeze-dried (FD) and enzyme treated (ET) material is compared with each other.

The  $^1\text{H}$  spectra of the acetone soluble fractions and methanol soluble fractions of freeze-dried (FD) and enzyme-treated (ET) material (figure 3.5) show signals between 8.0 ppm and 10 ppm for both species. These signals could indicate the presence of aldehydes (typically  $\geq 9$  ppm) and aromatic or heteroaromatic protons ( $< 9$  ppm). Samples extracted with acetone (A) show several and more intense signals in this area than samples extracted with methanol (M). The  $^1\text{H}$ - $^{13}\text{C}$  HSQC of the same area of enzyme treated material from *Alaria esculenta* extracted with acetone (figure 3.6) show four proton-carbon spin pairs, where three pairs ( $\delta_{\text{H}}9.83$   $\delta_{\text{C}}105.5$ ,  $\delta_{\text{H}}9.55$   $\delta_{\text{C}}98.0$ , and  $\delta_{\text{H}}8.92$ ,  $\delta_{\text{C}}94.6$ ) are consistent with folded aldehyde signals, and one pair ( $\delta_{\text{H}}8.20$   $\delta_{\text{C}}129.9$ ) is consistent with a heteroaromatic moiety.

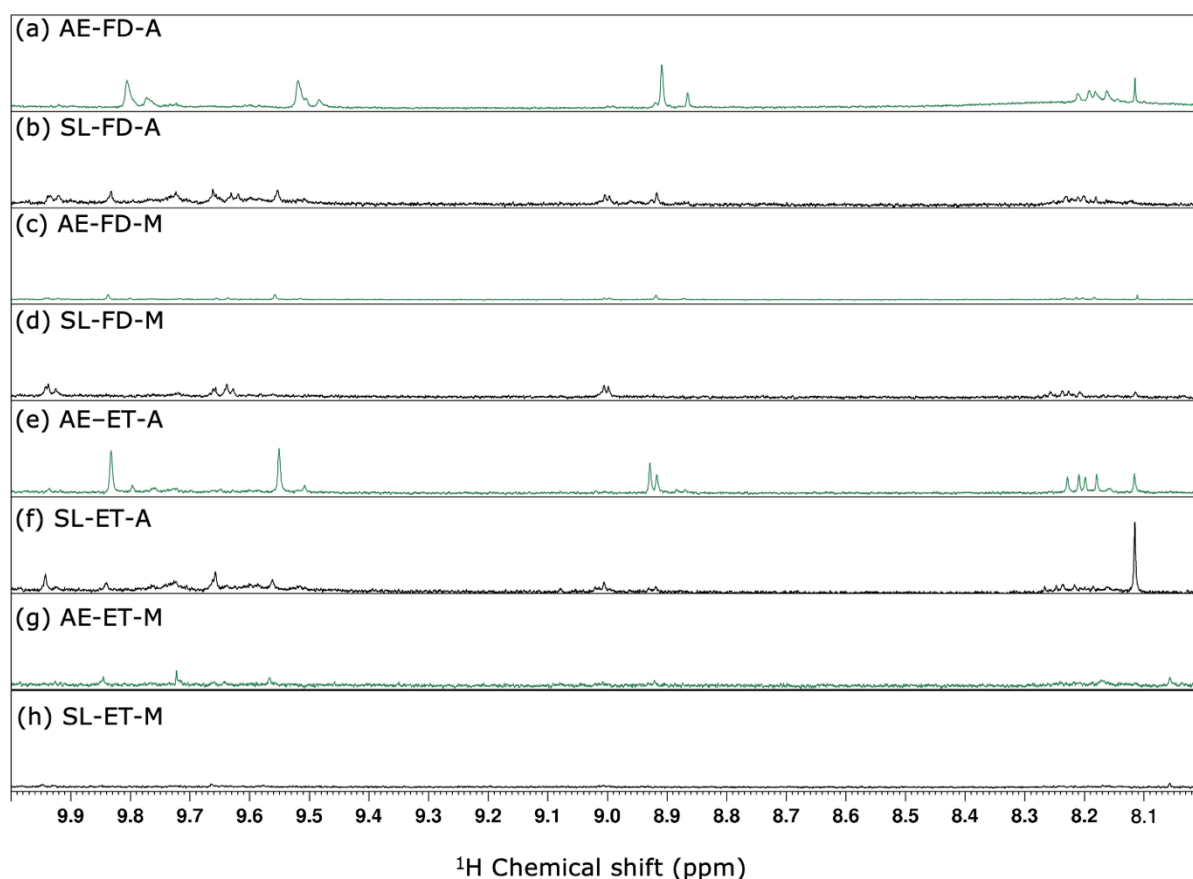


**Figure 3.5:**  $^1\text{H}$ -NMR spectra (8.0-10.0 ppm) of acetone soluble fractions (A) and methanol soluble fractions (M) of freeze-dried (FD) and enzyme treated (ET) of *Alaria esculenta* (AE) and *Saccharina latissima* (SL). The samples were dissolved in deuterated acetone ( $(\text{CD}_3)_2\text{CO}$ ) and run at 298.0 K at 600 MHz.

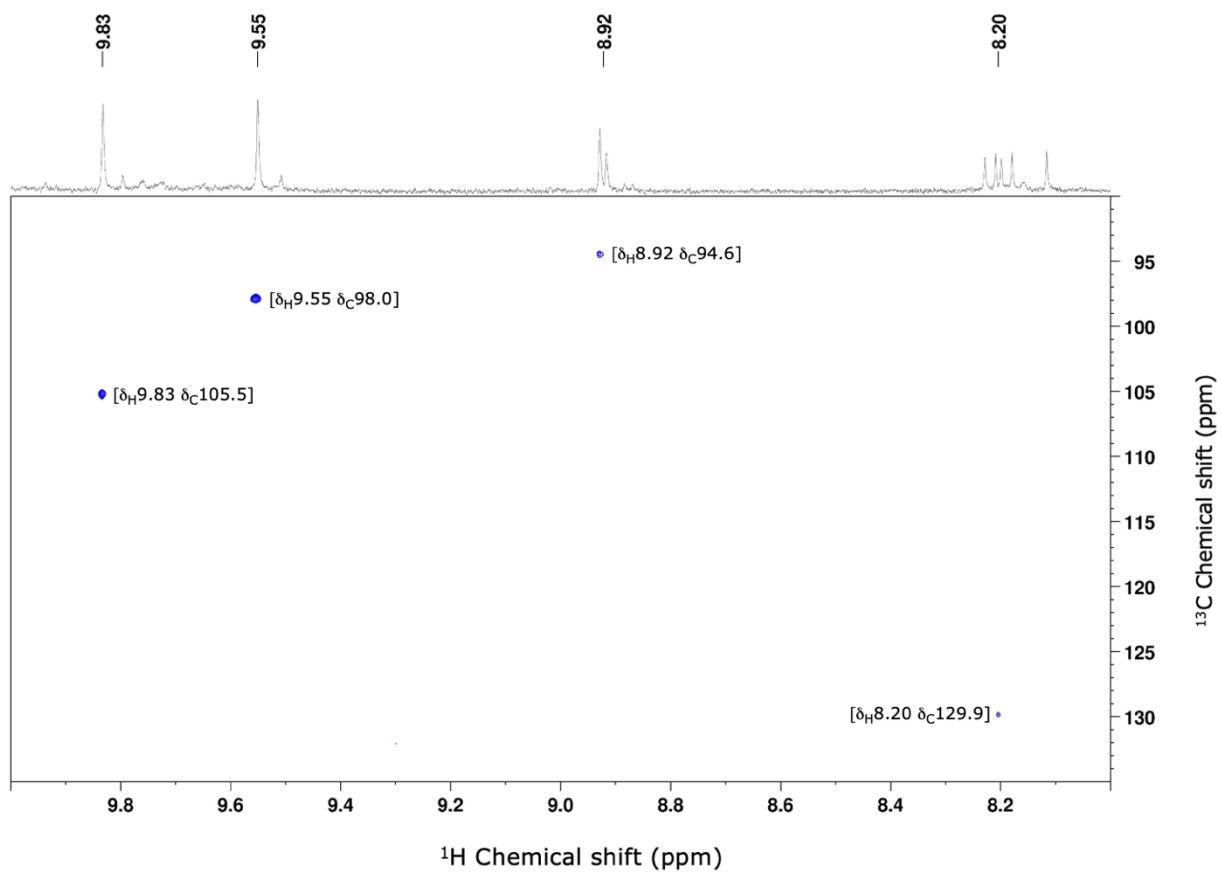


**Figure 3.6:**  $^1\text{H}$ - $^{13}\text{C}$  HSQC spectrum (8.0-10.0 ppm, 90.0-135.0 ppm) of enzyme treated material from *Alaria esculenta* extracted with acetone. The sample was dissolved in deuterated acetone ( $(\text{CD}_3)_2\text{CO}$ ) and run at 298.0 K at 600 MHz.

Between 5.0-8.0 ppm (figure 3.7) the spectra show signals indicating the presence of aromatic, phenolic and olefinic protons. The signals between approximately 6-7 ppm are typical for the protons in a conjugated chain, like the central acyclic region (C-11 to C11') common for all carotenoids. The spectrum of enzyme treated material from *Alaria esculenta* extracted with acetone (e, AE-ET-A) stands out with its signals between 6.8-8.0 ppm. Overall, more signals consistent with carotenoid-like and polyphenol-like signals can be seen in samples extracted with acetone. The spectra of enzyme treated material of *Alaria esculenta* have more diverse and intense signals than the other samples, and *A. esculenta* show more of the signals consistent with carotenoid-like and polyphenol-like signals than *Saccharina latissima*.

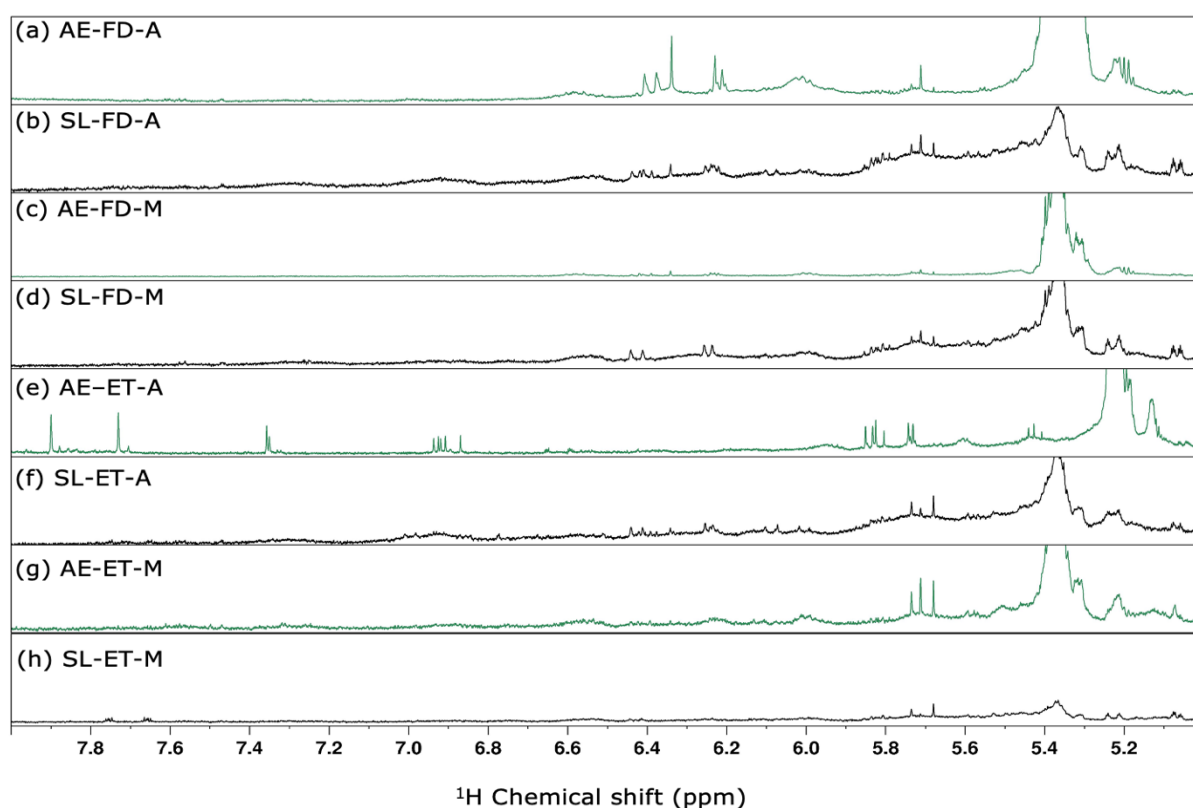


**Figure 3.7: <sup>1</sup>H-NMR spectra (8.0-10.0 ppm) of acetone soluble fractions (A) and methanol soluble fractions (M) of freeze-dried (FD) and enzyme treated (ET) of *Alaria esculenta* (AE) and *Saccharina latissima* (SL).** The samples were dissolved in deuterated acetone ((CD<sub>3</sub>)<sub>2</sub>CO) and run at 298.0 K at 600 MHz.

The  $^1\text{H}$ - $^{13}\text{C}$  HSQC spectrum of freeze-dried *Alaria esculenta* material extracted with acetone (figure 3.8) show the clearest proton-carbon spin pairs in the same area. The correlations at approximately 6 ppm could indicate a phloroglucinol moiety ( $\delta_{\text{H}}6.34$   $\delta_{\text{C}}65.7$ ) and oxygenated methylene groups ( $\delta_{\text{H}}6.31$   $\delta_{\text{C}}123.1$ , and  $\delta_{\text{H}}6.22$ ,  $\delta_{\text{C}}123.4$ ). The correlations at approximately 5 ppm indicate methines with electron delocalization ( $\delta_{\text{H}}5.19$   $\delta_{\text{C}}116.4$ ,  $\delta_{\text{H}}5.31$   $\delta_{\text{C}}121.6$ , and  $\delta_{\text{H}}5.37$ ,  $\delta_{\text{C}}130.0$ ) and oxygenated methines ( $\delta_{\text{H}}5.22$   $\delta_{\text{C}}71.2$ ).

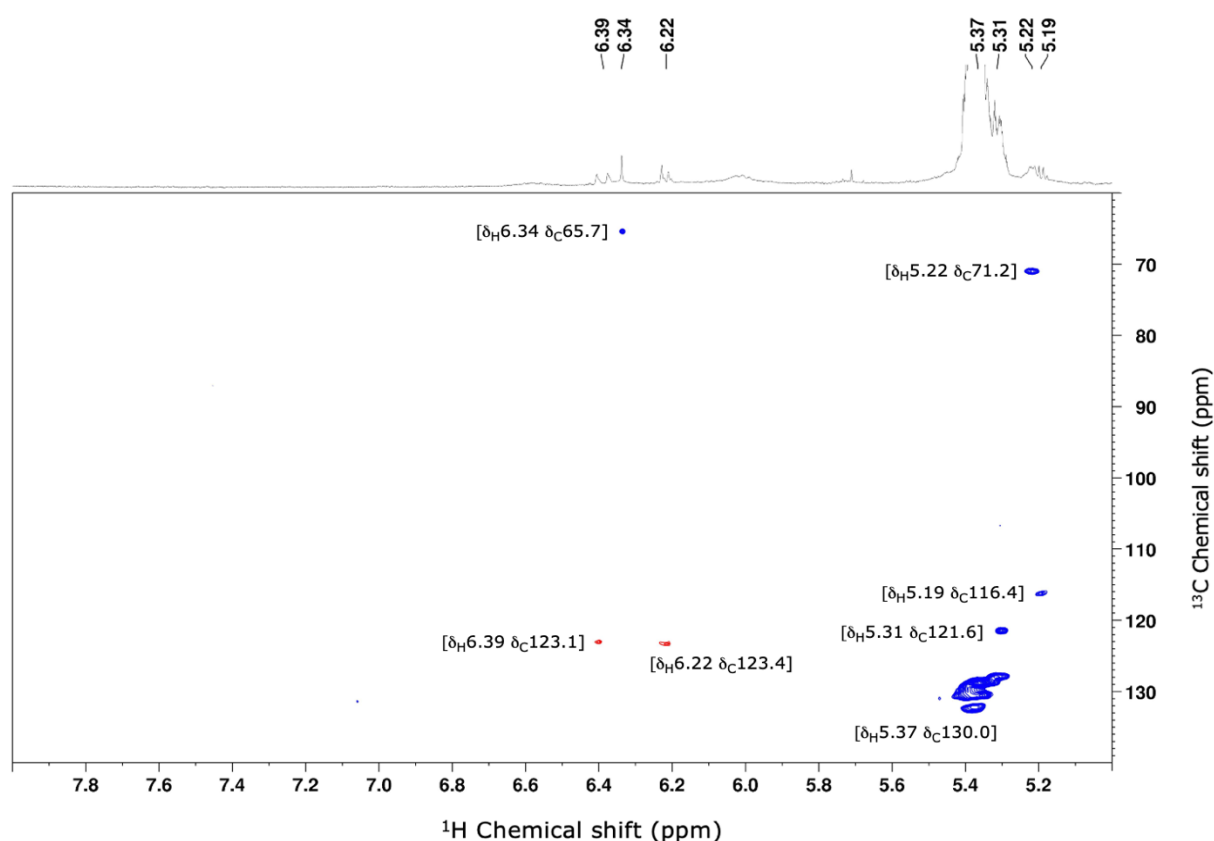


**Figure 3.8:**  $^1\text{H}$ - $^{13}\text{C}$  HSQC spectrum (5.0-8.0 ppm, 60.0-140.0 ppm) of freeze-dried material from *Alaria esculenta* extracted with acetone. The sample was dissolved in deuterated acetone ( $(\text{CD}_3)_2\text{CO}$ ) and run at 298.0 K at 600 MHz.

Between 0.5-4.5 ppm (figure 3.9) the  $^1\text{H}$  NMR spectra show signals indicating secondary alcohols and methylene protons ( $\sim 2\text{-}4$  ppm) and methyl protons ( $\sim 0.5\text{-}2$  ppm). The spectra also show signals consistent with lipids, as seen in the hexane-fraction (section 3.1.1) indicating that the samples were not completely defatted by extraction with *n*-hexane.

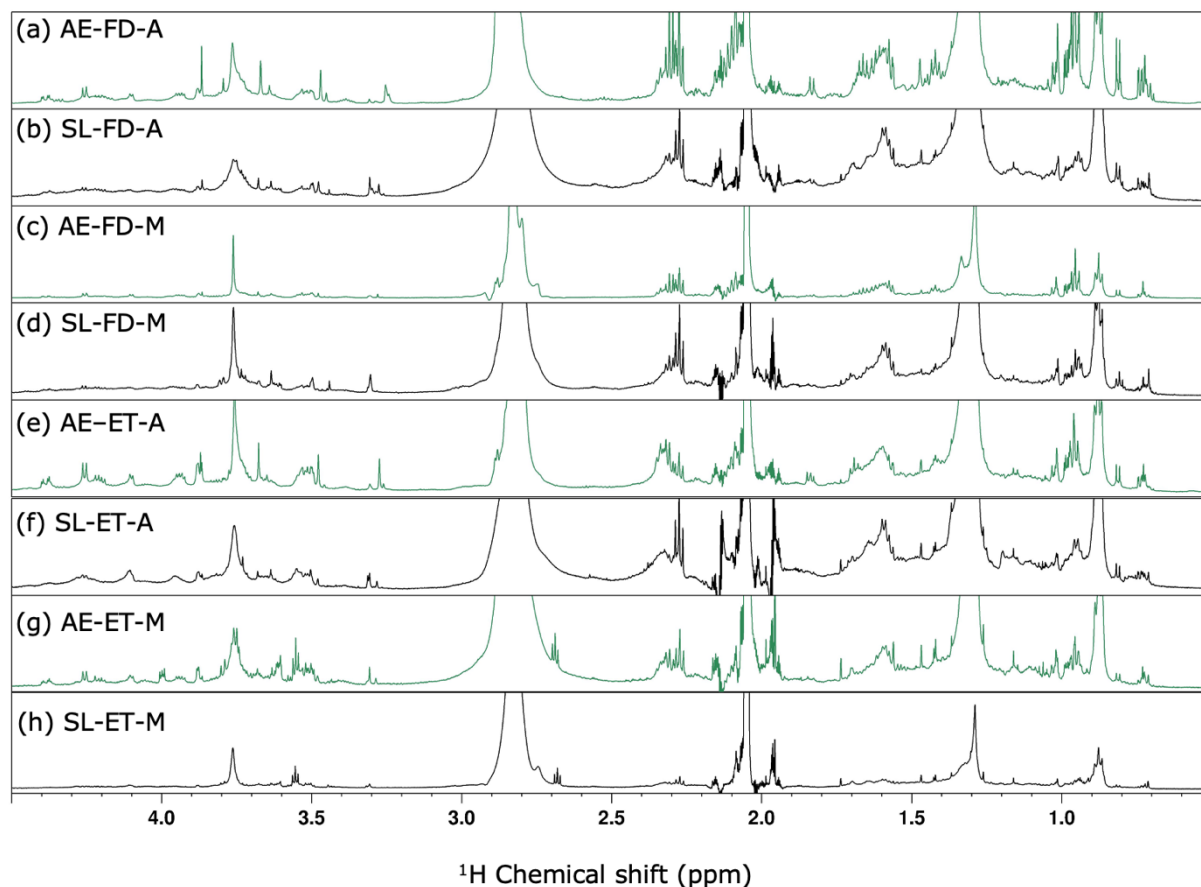


**Figure 3.9:  $^1\text{H}$  NMR spectrum (0.5-4.5 ppm) of acetone soluble fractions (A) and methanol soluble fractions (M) of freeze-dried (FD) and enzyme treated (ET) of *Alaria esculenta* (AE) and *Saccharina latissima* (SL).** Residual solvent signal at 2.05 ppm. The samples were dissolved in deuterated acetone ( $(\text{CD}_3)_2\text{CO}$ ) and run at 298.0 K at 600 MHz.



## 3.2 Bulk extractions on wet material

Chopped seaweed material with no previous pretreatment (W) was exhaustively extracted with aqueous acetone. The solid material was further extracted with methanol in a sequential extraction. The extracts were defatted, and the aqueous phases (W-Aq-A and W-Aq-M) was recovered and dried. Dried aliquots of W-Aq-A and W-Aq-M were analyzed by NMR and LC-MS. Full plots the NMR spectra can be seen in appendix C.

The  $^1\text{H}$  NMR spectrum between 0.7–4.2 ppm (figure 3.10) show a high content of the sugar alcohol mannitol ( $\sim 3.5\text{--}4.0$  ppm) in the acetone extracts. Mannitol was confirmed by comparing the  $^1\text{H}$  spectrum with the reported data for this compound in the literature (Human Metabolome Database, s.a.-a) (see appendix C figure C-3 and C-4). Approximately the same signals can be seen for both species.

The  $^1\text{H}$  NMR spectra of methanol extracts from the same material (figure 3.11) also show signals between 0.7–4.2 ppm. Signals between 3–4 ppm, indicating aliphatic hydrocarbons, can be seen in the methanol extracts, but mannitol was however not characterized from these fractions. Both acetone and methanol extracts show signals consistent with protons in secondary alcohols ( $\sim 3.0\text{--}3.5$  ppm), methylene groups ( $\sim 1.5\text{--}3.0$  ppm) or methyl groups ( $\sim 0.9\text{--}3$  ppm). Approximately the same signals can be seen for both species.

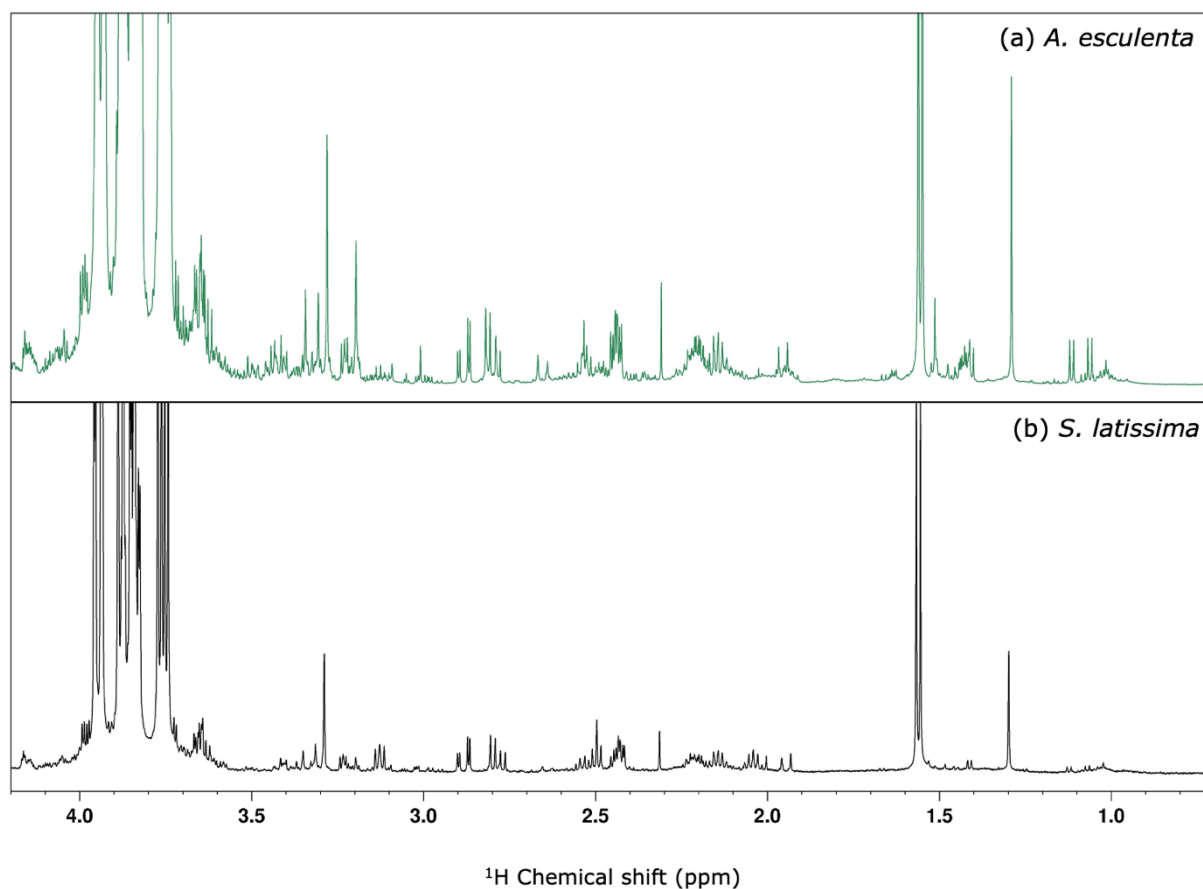


**Figure 3.10:**  $^1\text{H}$  NMR spectrum (0.7–4.2 ppm) of W-Aq-A. Defatted, aqueous fraction from bulk extraction with acetone on wet material. (a) *Alaria esculenta* (b) *Saccharina latissima*. Samples were dissolved in deuterium oxide ( $\text{D}_2\text{O}$ ) and run at 298.1 K on 600 MHz.

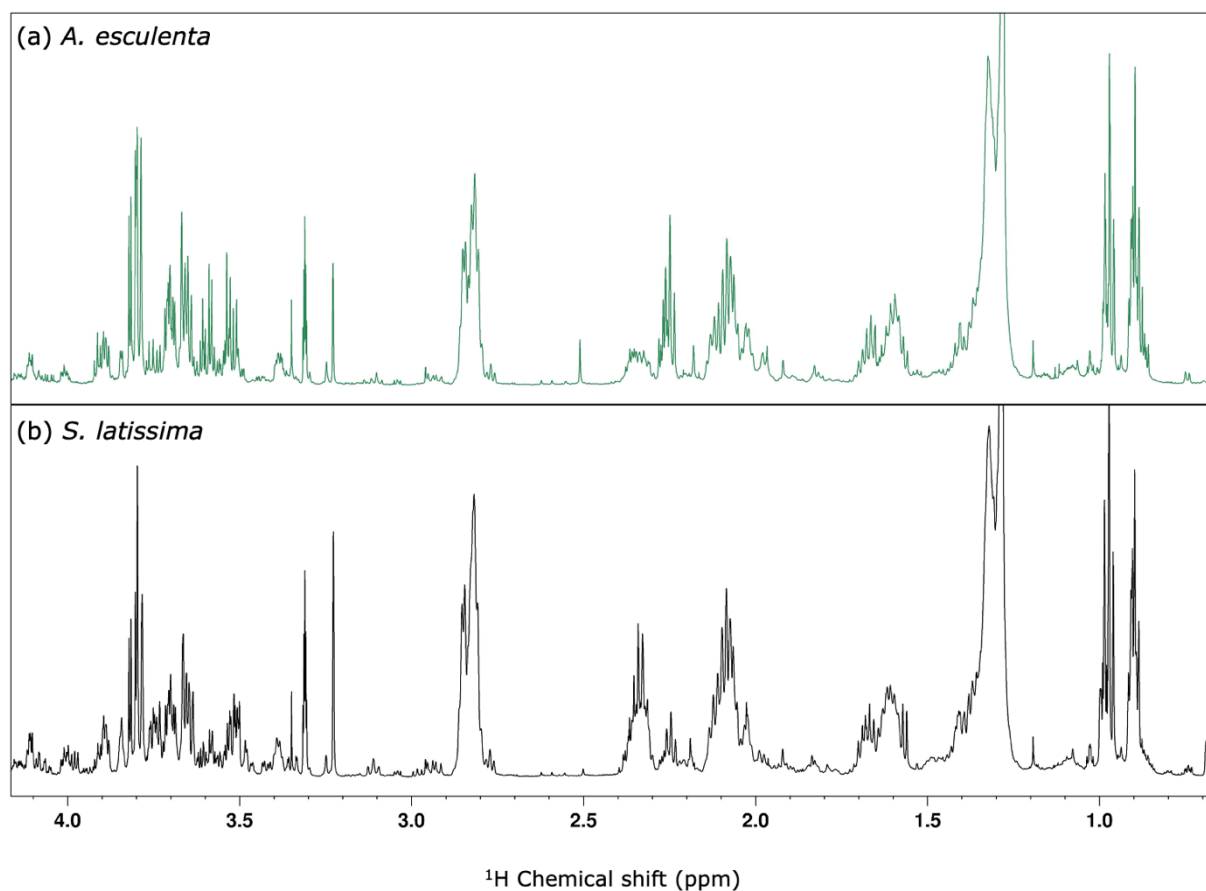


**Figure 3.11:  $^1\text{H}$  NMR spectrum (0.7–4.2 ppm) of W-Aq-M.** Defatted, aqueous fraction from bulk extraction with methanol on wet material. (a) *Alaria esculenta* (b) *Saccharina latissima*. Samples were dissolved in deuterated methanol ( $\text{CD}_3\text{OD}$ ) and run at 298.1 K on 600 MHz.

The  $^1\text{H}$  NMR spectra between 5.7–8.7 ppm show signals consistent with aromatic and heteroaromatic moieties ( $\sim 7$ –8.7 ppm), and olefinic methines or phenyl moieties ( $\sim 6$ –7 ppm) in both acetone extracts and methanol extracts. These signals are consistent with carotenoid-like and polyphenol-like signals.

In the spectra of the acetone extracts (figure 3.12), the spectrum of *Alaria esculenta* show signals higher intensities than *Saccharina latissima*. In the spectra of the methanol extracts both species show approximately the same signals.

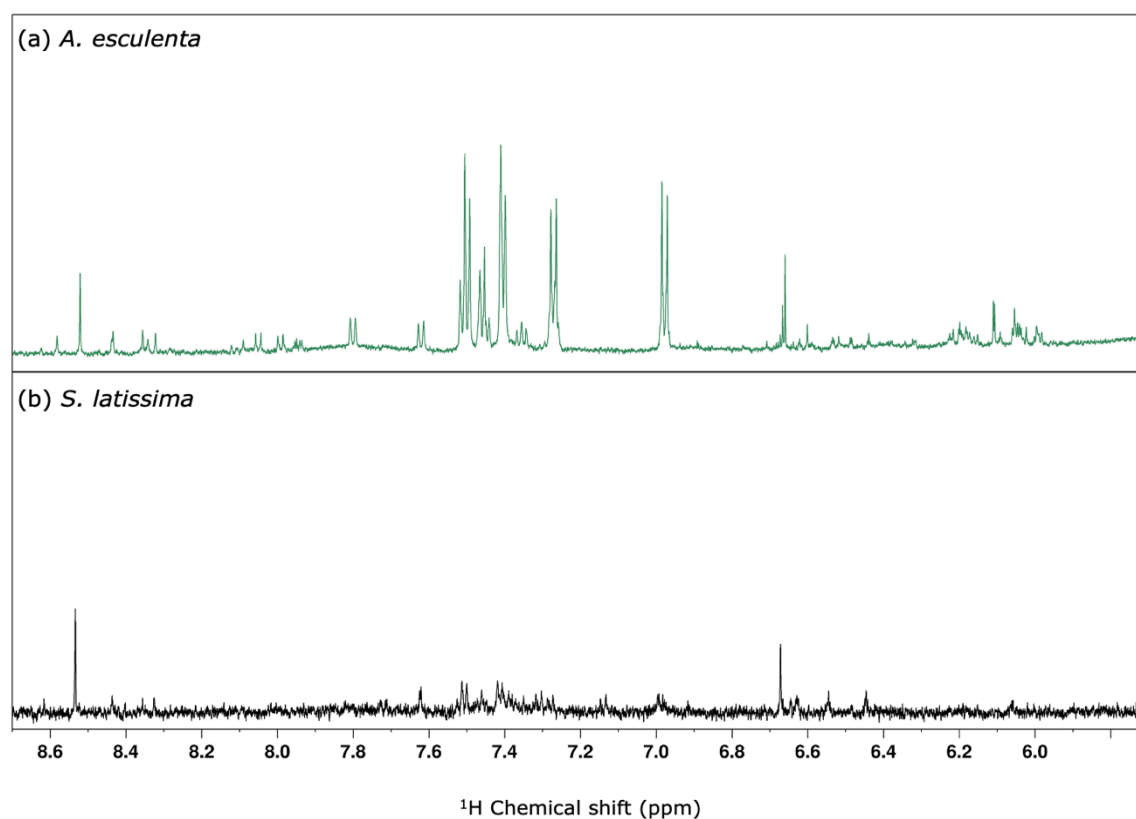


**Figure 3.12:  $^1\text{H}$  NMR spectrum (5.7–8.7 ppm) of W-Aq-A.** Defatted, aqueous fraction from bulk extraction with acetone on wet material. (a) *Alaria esculenta* (b) *Saccharina latissima*. Samples were dissolved in deuterium oxide ( $\text{D}_2\text{O}$ ) and run at 298.1 K on 600 MHz.

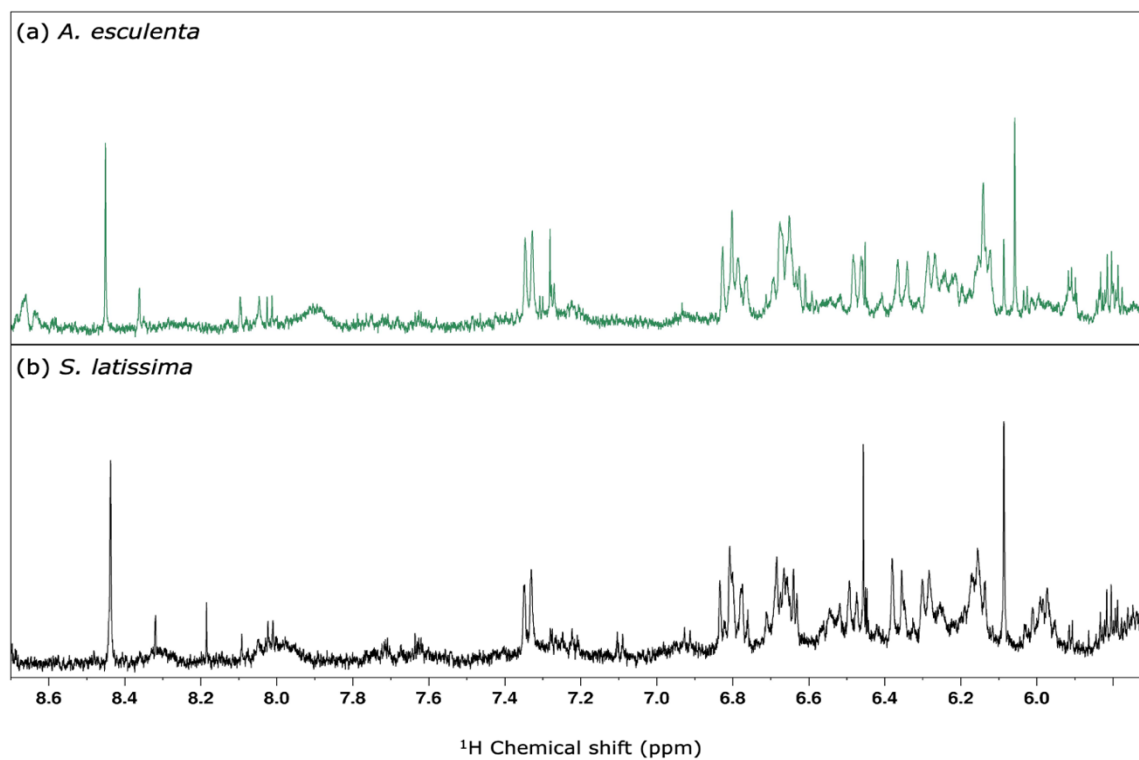


**Figure 3.13:  $^1\text{H}$  NMR spectrum (5.7–8.7 ppm) of W-Aq-M.** Defatted, aqueous fraction from bulk extraction with methanol on wet material. (a) *Alaria esculenta* (b) *Saccharina latissima*. Samples were dissolved in deuterated methanol ( $\text{CD}_3\text{OD}$ ) and run at 298.1 K on 600 MHz.

The base peak (BP) chromatograms from analytical LC-MS of the acetone extracts (figure 3.14) show various  $m/z$  values ranging between approximately 120–450 Da. The chromatograms show approximately similar  $m/z$  values for both species. The BP-chromatograms of the methanol extracts (figure 3.15) show various  $m/z$  values ranging between approximately 180–980 Da. The chromatograms differ greatly between the two species. *Alaria esculenta* (figure 3.15a) show more peaks with higher  $m/z$  values than *Saccharina latissima* (figure 3.15b).

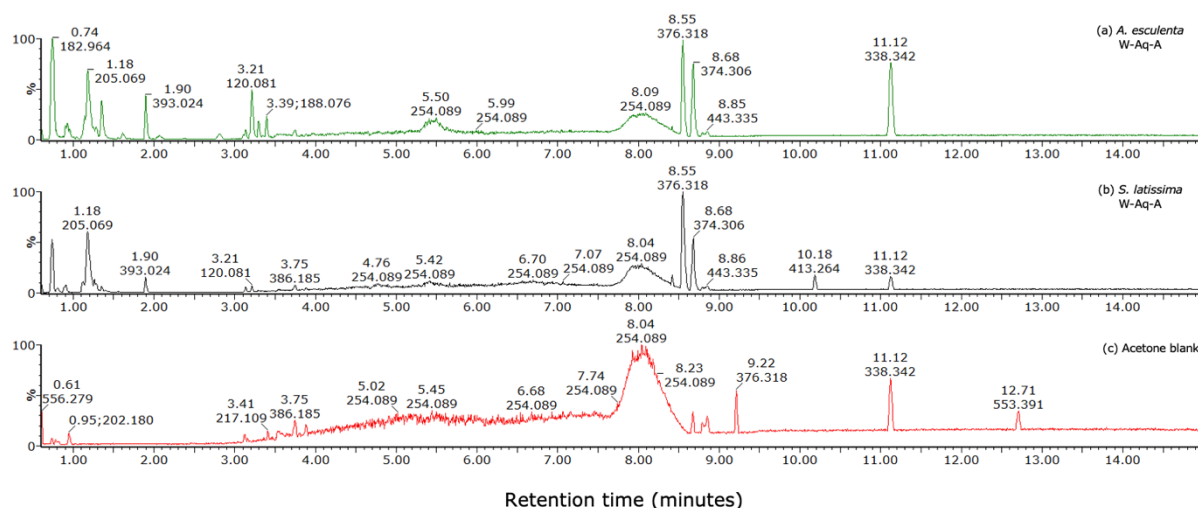


**Figure 3.14: Base peak chromatogram of W-Aq-A.** a) *Alaria esculenta*. b) *Saccharina latissima*. c) Acetone blank (from acetone used for extractions, put through filter paper and syringe filter). The x-axis is showing the retention time in minutes. The y-axis is showing the base peak intensity in percentage (%). The chromatogram was recorded in positive ion mode.

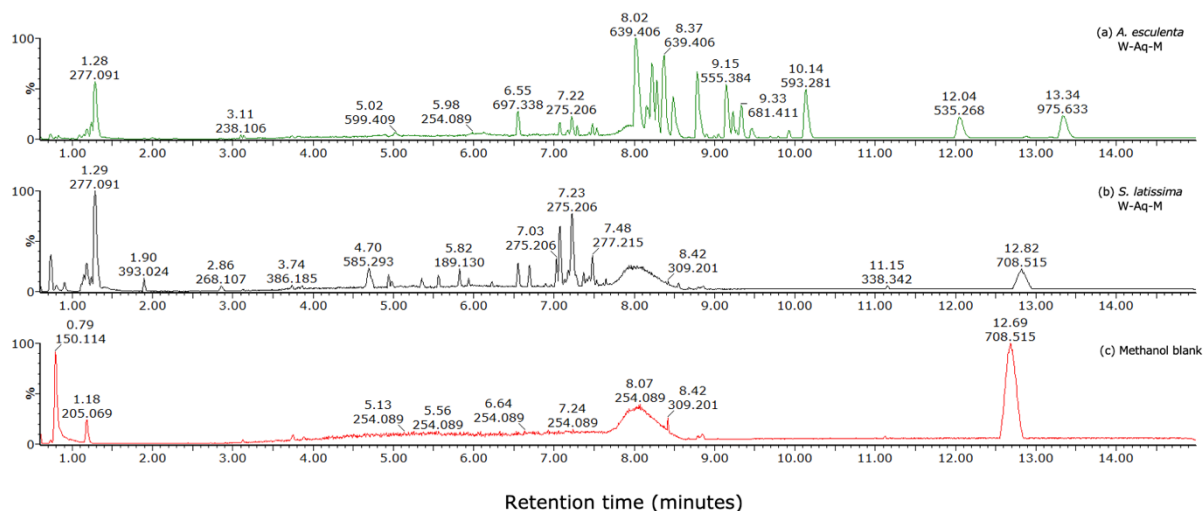


**Figure 3.15: Base peak chromatogram of W-Aq-M.** a) *Alaria esculenta*. b) *Saccharina latissima*. c) Methanol blank (methanol used for extractions, put through filtration paper and syringe filter). The x-axis is showing the retention time in minutes. The y-axis is showing the base peak intensity in percentage (%).

### 3.3 Macroporous resin

Due to the intensity and amount of carotenoid-like and polyphenol-like signals observed by NMR of wet material extracted with acetone, these were further purified. First, the extracts were defatted by liquid-liquid partitioning and the aqueous fractions (Aq) were added to XAD-16 resin for further separation.

Aqueous fraction of *Saccharina latissima* SL-W-Aq were eluted with six different ratios of RO-water and acetone to determine which ratio of acetone will elute components with carotenoid and polyphenol moieties. The ratios were as following 0:1, 1:4, 2:3, 3:2, 4:1, and 1:0 acetone:RO-water, and these were collected as Ac0, Ac20, Ac40, Ac60, Ac80 and Ac100 respectively. Subsamples were analyzed by NMR.

Fraction SL-Ac60, SL-Ac80, and SL-Ac100 show signals (figure 3.16) consistent with signals from carotenoids and polyphenols. Full plot of each spectrum can be seen in appendix D, figure D-1 and D-2. Based on the diversity and intensity of especially the carotenoid-like signals ( $\sim 6\text{-}7$  ppm) seen in the fraction eluted with 100 % acetone, and to a certain degree in the fraction eluted with 80 % acetone (figure 3.16b-c), an elution with 100 % acetone was determined to be used. From this result another elution scheme was developed consisting of two elution fractions, 100 % RO-water (R1) and 100 % acetone (R2).

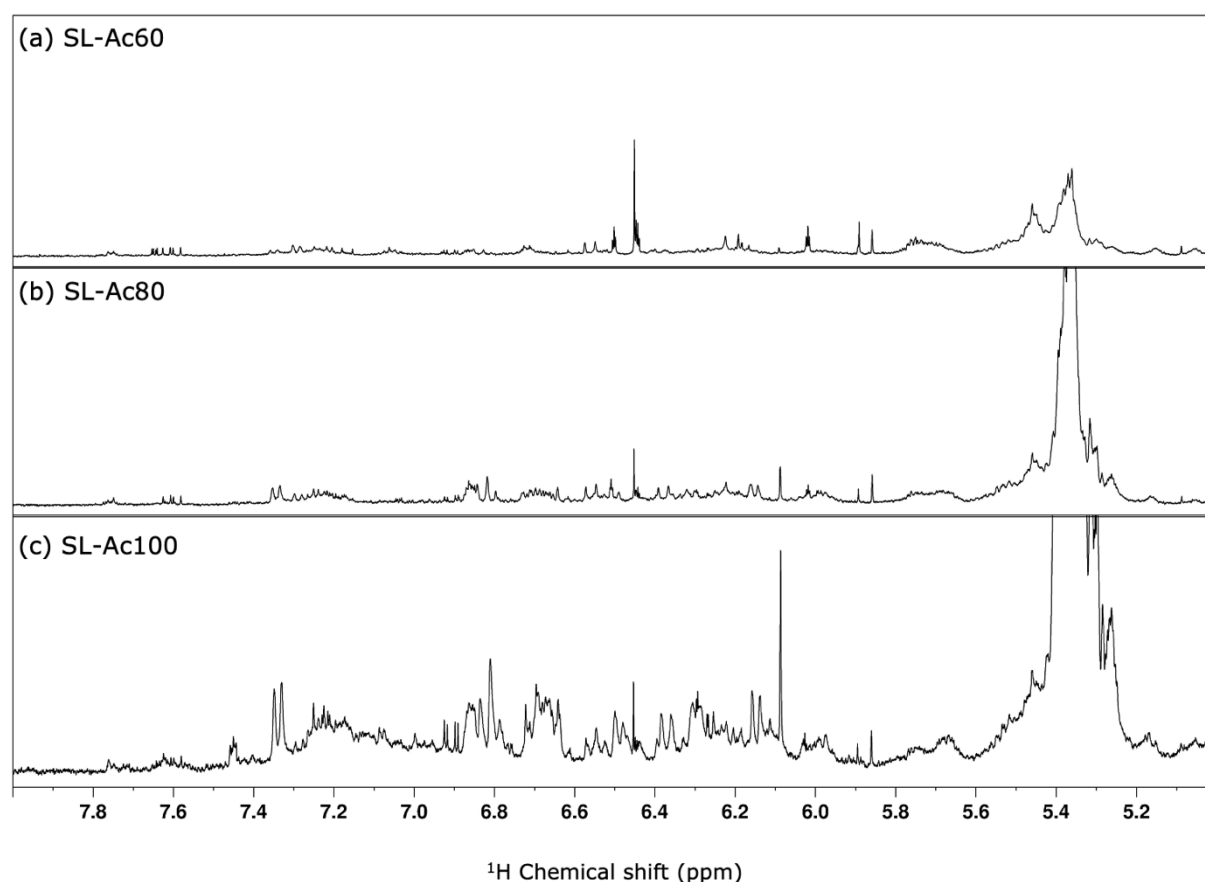


**Figure 3.16:  $^1\text{H}$  NMR spectra of elution fractions of acetone extract of *S. latissima* wet material purified with XAD-16 resin.** a) SL-Ac60, ratio 3:2 acetone:RO-water (60 % acetone). b) SL-Ac80, ratio 4:1 acetone:RO-water (80 % acetone). c) SL-Ac100, ratio 1:0 acetone:RO-water (100 % acetone). The samples were dissolved in deuterated methanol ( $\text{CD}_3\text{OD}$ ) and run at 298.1 K on 600 MHz.

Fraction SL-Ac100 was investigated further and the  $^1\text{H}$ - $^{13}\text{C}$  HSQC (figures 3.17-3.19) show the presence of chemical moieties that are consistent with fucoxanthin-like structures. The proton-carbon spin pairs that can be observed between 6.0-7.5 ppm ( $^1\text{H}$ ) and 100-150 ppm ( $^{13}\text{C}$ ) in the  $^1\text{H}$ - $^{13}\text{C}$  HSQC spectrum (figure 3.17) is consistent with the central acyclic region (C10-C8') of carotenoids, consisting of conjugated double bonds. The proton-carbon spin pairs that can be observed between 1.2-1.85 ppm ( $^1\text{H}$ ) and 41-49 ppm ( $^{13}\text{C}$ ) (figure 3.18) are consistent with the methylene groups at C7 and at C2, C2', C4, and C4' in the end rings of fucoxanthin. The proton-carbon spin pairs that can be observed between 0.9-2.1 ppm ( $^1\text{H}$ ) and 10-35 ppm ( $^{13}\text{C}$ ) (figure 3.20) are consistent with the methyl groups in carotenoids, and could be the C16-C20, C16'-C20', and C22' in fucoxanthin. The DOSY spectrum (figure 3.20) show that the SL-Ac100 fraction is still a mixture consisting of several compounds, as the signals detected at different rates of diffusion. Further purification is needed to isolate any carotenoid compounds from this sample.

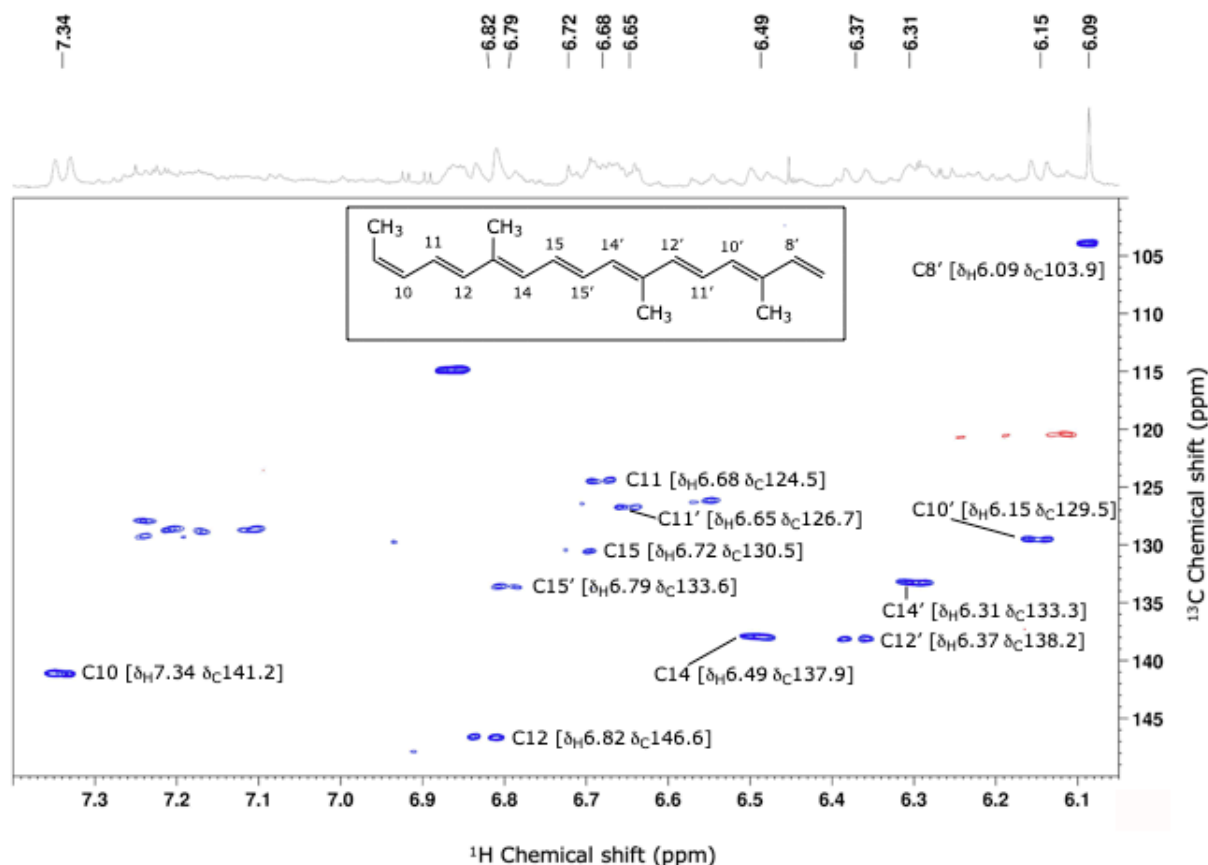


**Figure 3.17:**  $^1\text{H}$ - $^{13}\text{C}$  HSQC spectrum of SL-Ac100 fraction of *Saccharina latissima*. The annotated signals show the proton-carbon spin pairs of the central acyclic region (C10-C8') found in carotenoids. The partial structure is given in the spectrum. The sample was dissolved in deuterated methanol ( $\text{CD}_3\text{OD}$ ) and run at 298.1 K on 600 MHz.

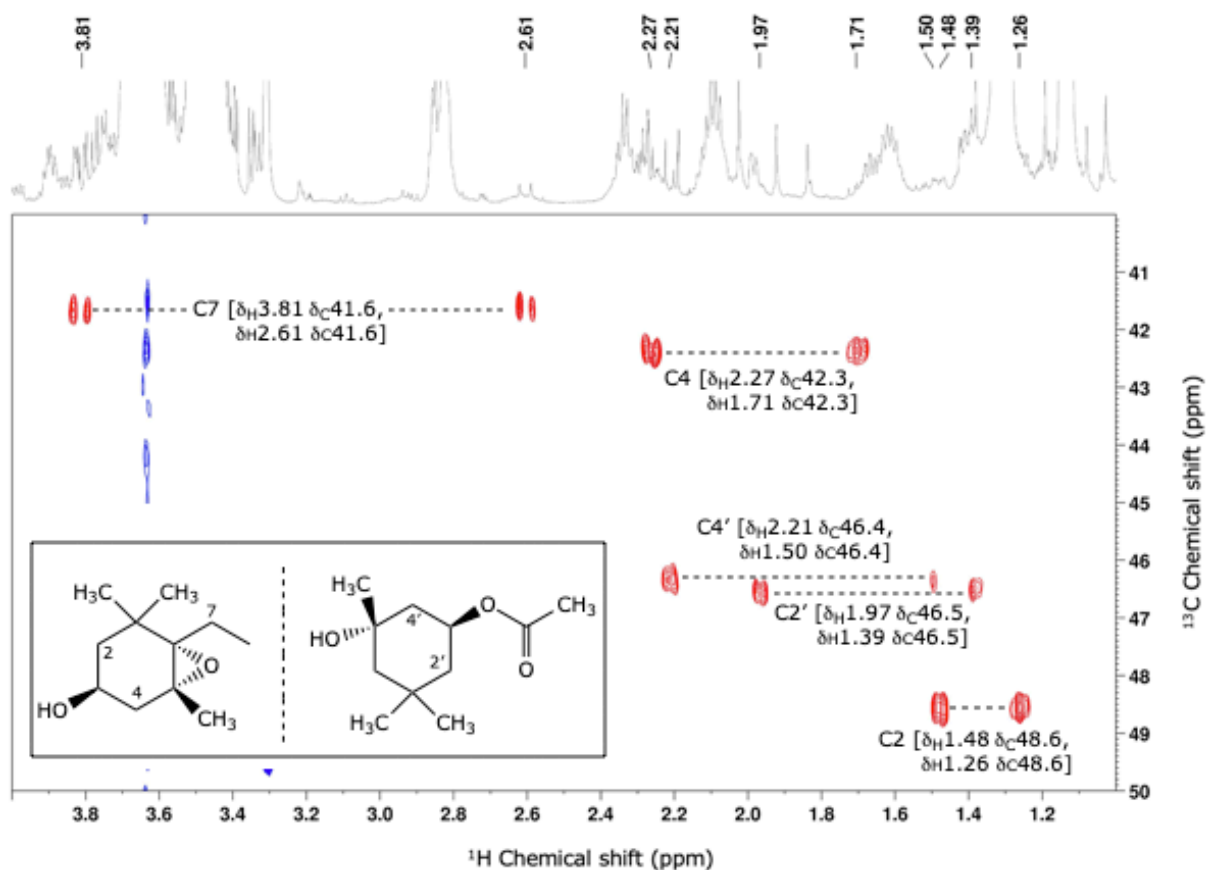


**Figure 3.18:**  $^1\text{H}$ - $^{13}\text{C}$  HSQC spectrum of SL-Ac100 fraction of *Saccharina latissima*. The annotated signals show the proton-carbon spin pairs consistent with the methylene groups (C2, C4, C7, C2', and C4') found in fucoxanthin. The structure of the end rings including C2, C4, C2' and C4' and the bond to C7 is given in the spectrum. The sample was dissolved in deuterated methanol ( $\text{CD}_3\text{OD}$ ) and run at 298.1 K on 600 MHz.



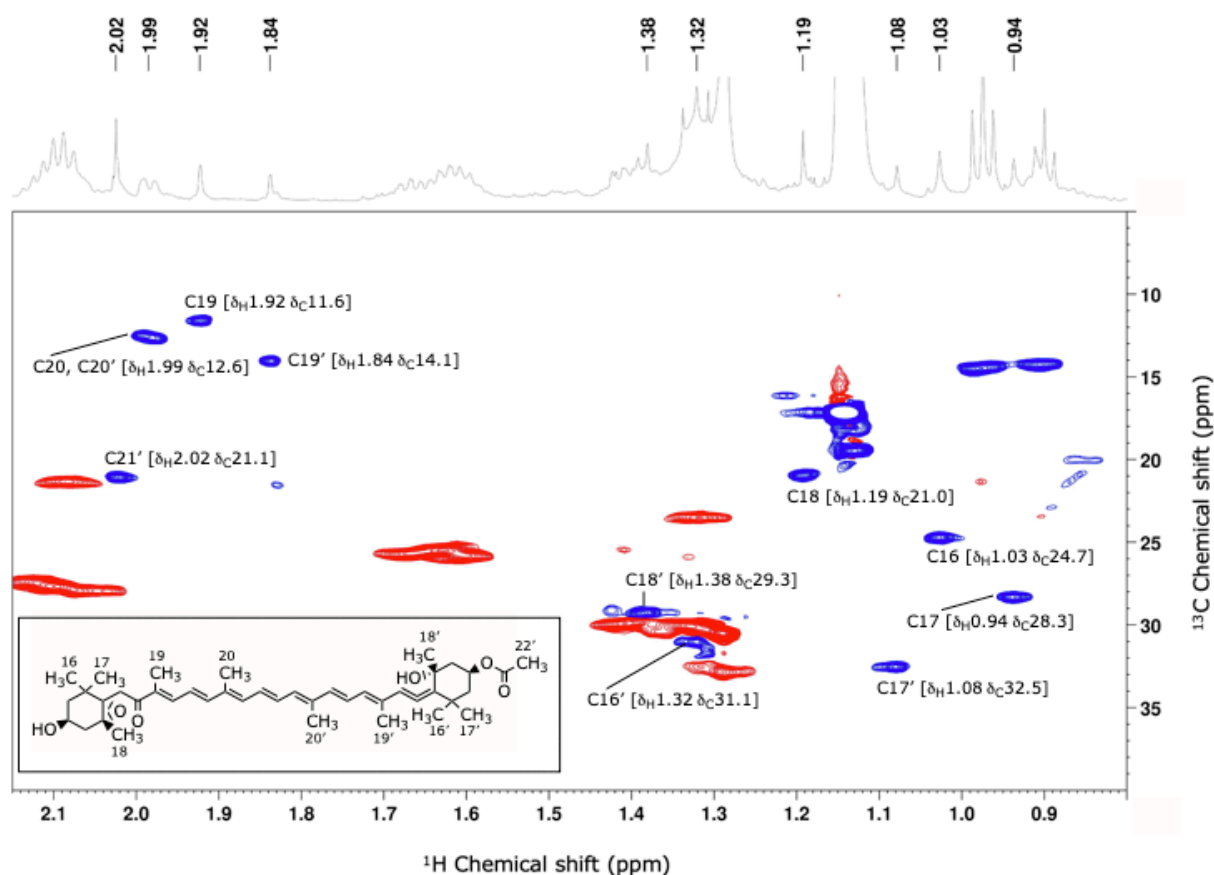


**Figure 3.19:**  $^1\text{H}$ - $^{13}\text{C}$  HSQC spectrum of SL-Ac100 fraction of *Saccharina latissima*. The annotated signals show the proton-carbon spin pairs consistent with the methyl groups found in fucoxanthin (structure in bottom left corner). The sample were dissolved in deuterated methanol ( $\text{CD}_3\text{OD}$ ) and run at 298.1 K on 600 MHz.

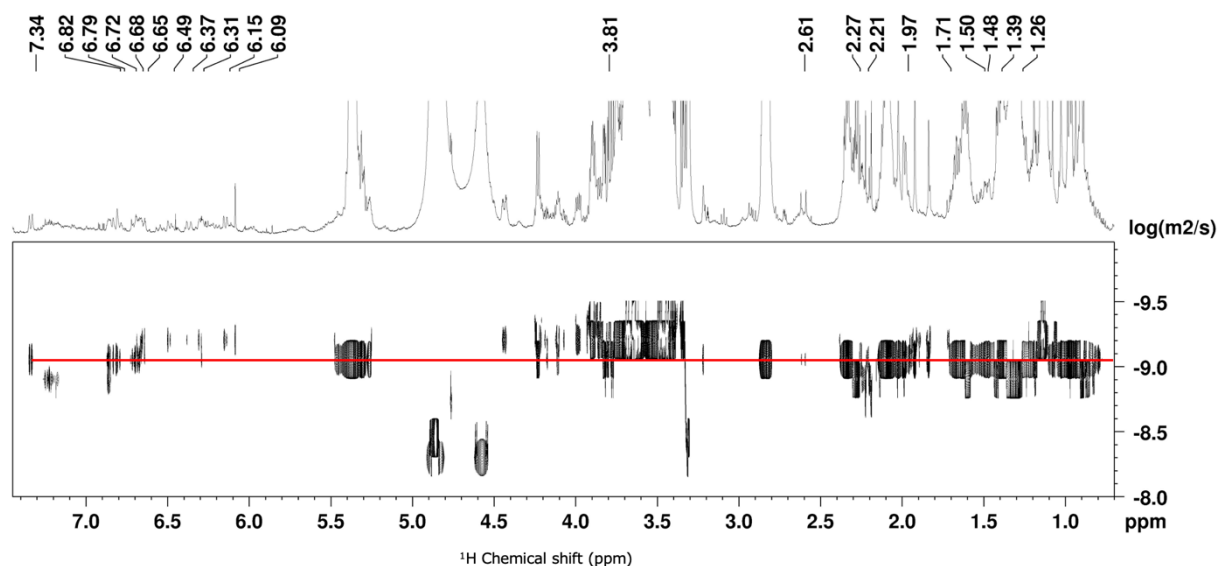


**Figure 3.20:**  $^1\text{H}$  DOSY spectrum of SL-Ac100 fraction of *Saccharina latissima*. The red line shows the fucoxanthin-like signals (these chemical shifts are annotated in the  $^1\text{H}$  NMR spectrum and can be seen in at the top of the DOSY spectrum). The sample was dissolved in deuterated methanol ( $\text{CD}_3\text{OD}$ ) and run at 298.1 K on 800 MHz.

The second elution scheme was further used for the purifying of both *Alaria esculenta* and *Saccharina latissima*. The  $^1\text{H}$  NMR spectra of R0 and R2 fractions of *A. esculenta* between 0.7 and 4.2 ppm (figure 3.21) show clearly how the R2 fraction is purified of mannitol. The R2 fraction (3.21b) show signals that are consistent with fatty acids, indicating that some lipids are still retained. The same spectra between 5.0 and 8.0 ppm (figure 3.22) show signals consistent with aromatic or phenolic compounds. These are more intense in the R0-fraction than the R2 fraction, indicating that the resin also purifies the R2 from some aromatic compounds.

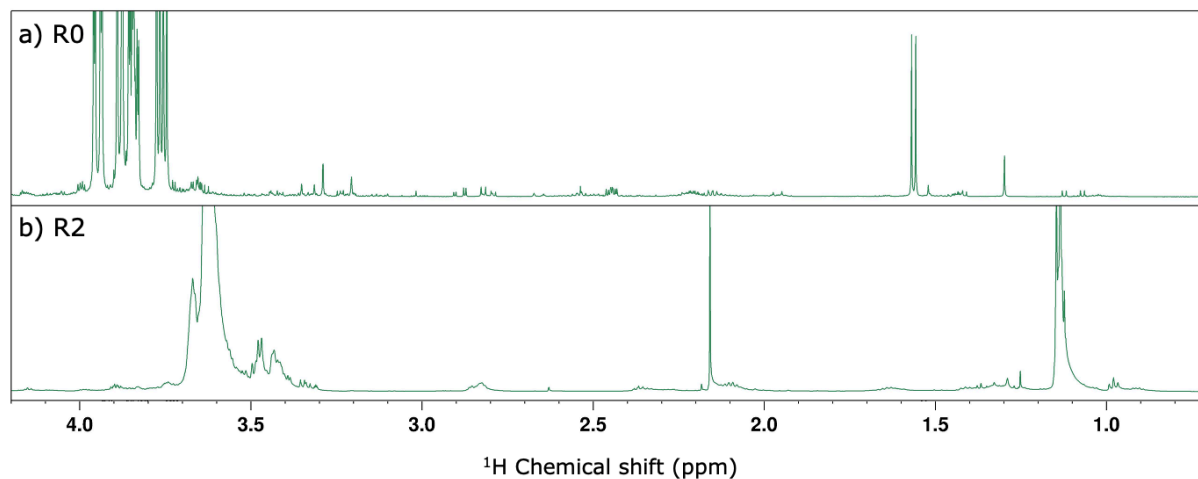


**Figure 3.21:  $^1\text{H}$  NMR spectra (0.7-4.2 ppm) of *A. esculenta* R0 and R2 fraction from purification with XAD-16 resin.** a) R0 fraction, the flow through from the sample loading (unbonded extract still suspended in RO-water). The sample was dissolved in deuterium oxide ( $\text{D}_2\text{O}$ ). b) R2 fraction, eluted with 100 % acetone. The sample was dissolved in deuterated methanol ( $\text{CD}_3\text{OD}$ ). Both spectra were run at 298.1 K on 600 MHz.

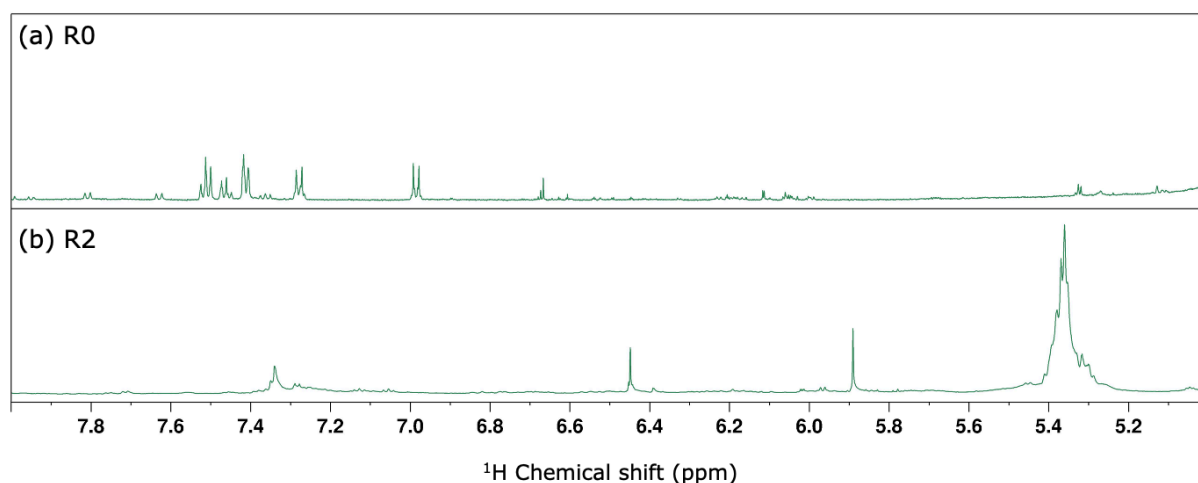


**Figure 3.22:  $^1\text{H}$  NMR spectra (5.0-8.0 ppm) of *A. esculenta* R0 and R2 fraction from purification with XAD-16 resin.** a) R0 fraction, the flow through from the sample loading (unbonded extract still suspended in RO-water). The sample was dissolved in deuterium oxide ( $\text{D}_2\text{O}$ ). b) R2 fraction, eluted with 100 % acetone. The sample was dissolved in deuterated methanol ( $\text{CD}_3\text{OD}$ ). Both spectra were run at 298.1 K on 600 MHz.

The LC-MS chromatograms of the R2-fractions (figure 3.23) show various components with  $m/z$  values between approximately 130–710 Da. The chromatograms show approximately similar  $m/z$  values between the two species. Compared to the crude extract, the chromatograms for the R2 samples show more clear signals higher  $m/z$  values between 3-8 minutes of retention time.

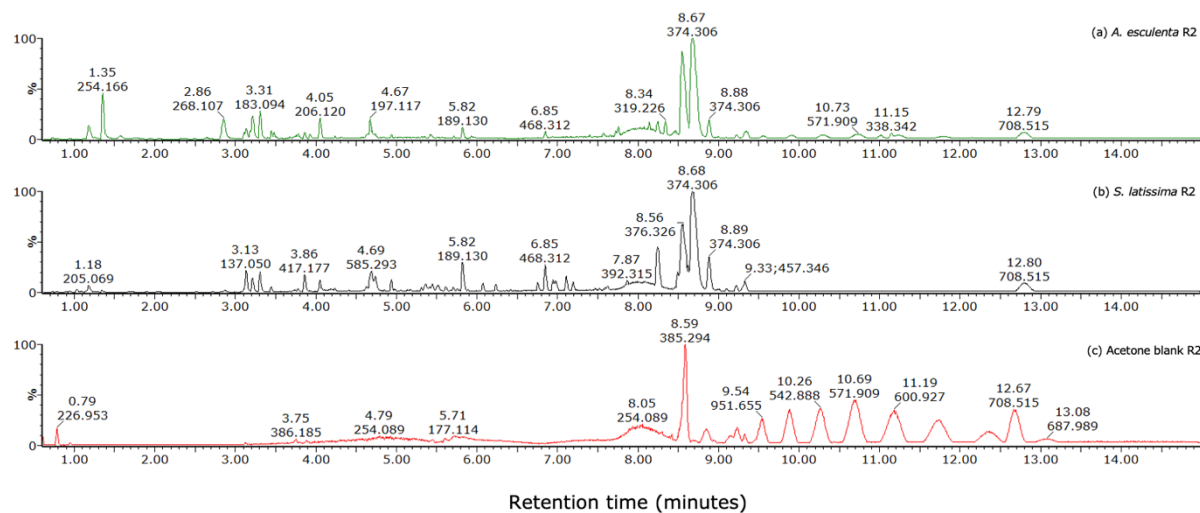


**Figure 3.23: Base peak chromatograms of AE-R2 and SL-R2 from the purification with resin.** a) *Alaria esculenta*. b) *Saccharina latissima*. c) Acetone blank from the resin procedure. The x-axis is showing the retention time in minutes. The y-axis is showing the base peak intensity in percentage (%). The chromatogram was recorded in positive ion mode.

### 3.4 Column chromatography with Sephadex LH-20

R2 fractions were resuspended in methanol and run chromatographically on the column packed with Sephadex LH-20. The full chromatograms can be seen in appendix E, figure E-1 and E-2. Based on the UV-peaks in the chromatograms selected fractions were analyzed by NMR and LC-MS.

The chromatogram produced from running *Alaria esculenta* R2 on the column packed with Sephadex LH-20 showed seven UV-peaks and one conductivity peak. From this, fraction F-15 (at ~200 mL), F-29 (at ~340 mL), F-35 (at ~400 mL), F-40 (at ~450 mL), F-53 (at ~500 mL), and W (at ~650 mL) were analyzed by NMR and LC-MS. The chromatogram produced from running *Saccharina latissima* R2 on the column showed five UV-peaks, no clear conductivity peaks. From this F-11 (at ~160 mL), F24 (at ~300 mL), F30 (at ~350 mL), F35 (at ~400 mL), and F39 (at ~440 mL) were analyzed by NMR and LC-MS.

Fraction 53 and W were the only fractions with high enough concentration to reveal any specific compounds by NMR. The spectral data, including chemical shift ( $\delta_H$ ,  $\delta_C$ ), multiplicity ( $J$  in Hz), and type of hydrocarbon for the peaks detected is displayed in table 2 below. By comparing the proton-carbon spin pairs in the  $^1\text{H}$ - $^{13}\text{C}$  HSQC spectrum (3.24) with values described in the literature, the amino acid tryptophan was identified. The full NMR spectra of fraction 53 can be seen in appendix E, figure E-3 and E-4.

**Table 2: Spectral data of *A. esculenta* F-53**, including  $\delta_H$  (multiplicity,  $J$  in Hz), integral of proton,  $\delta_H$ , and the type of hydrocarbon. The sample was dissolved in methanol- $d_4$  and run at 298 K. The em dash (-) is used where data from the conducted experiments,  $^1\text{H}$ -NMR and  $^1\text{H}$ - $^{13}\text{C}$  HSQC, is not obtained.

Nr	$\delta_H$ multiplicity, $J$ (Hz)	Integral-H	$\delta_C$	C-H
$\alpha$	3.86 (dd, $J=4.7, 4.1$ )	1	56.6	CH
$\beta$	3.15 (dd, $J=15.3, 9.4$ ) 3.52 (ddd, $J=15.3, 4.0, 0.7$ )	1	28.2	CH <sub>2</sub>
1	-	-	-	-
2	7.19 (s)	1	125.0	CH
3	-	-	-	-
3 $\alpha$	-	-	-	-
4	7.70 (d, $J=8.0$ )	1	119.2	CH
5	7.05 (dd, $J=7.5, 0.9$ )	1	120.0	CH
6	7.12 (dd/t* $J=7.5, 1.1$ )	1	122.7	CH
7	7.36 (d, $J=8.1$ )	1	112.3	CH
7 $\alpha$	-	-	-	-

The proton-carbon spin pairs in the aromatic region (~7.0–7.75 ppm, figure 3.25a), was found to be the resonance of C2-C7. The one methine group (3.85 ppm, figure 3.25b) and the two correlations in the methylene region (~3.1–3.6, figure b) was found to be the resonance of  $\alpha$ -C and  $\beta$ -C, respectively.

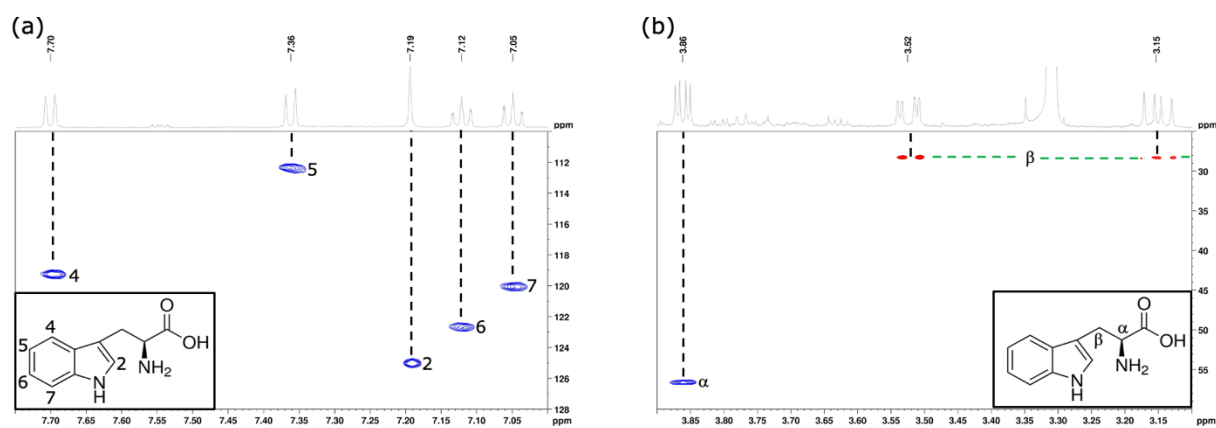


**Figure 3.24:**  $^1\text{H}$ - $^{13}\text{C}$  HSQC spectra of tryptophan in F-53 *A. esculenta* collected from column at  $\sim 500$  mL. (a) Five proton-carbon correlations in the aromatic region (7.0-7.75 ppm). (b) One methine group (3.85 ppm) and two methylene correlations ( $\sim 3.1$  and 3.5 ppm). The structure of tryptophan is given in the spectra.

### 3.4.1 Combined fractions

Only a few fractions from the column were of high enough concentration to detect signals by NMR, and it was therefore decided to combine some of the fractions to increase the concentrations. Fractions to be combined was based on LC-MS base peak (BP) chromatograms of neighboring fractions. The criteria for combination of fractions were 1) subsequential retention times and 2) similar peaks and m/z values in the BP chromatograms. The chromatograms of the selected fractions to combine (appendix E, figure E-5 to E-12) resulted in four new fractions for each species (P1-P8, table 3). These samples were dried and analyzed by NMR.

**Table 3: List of fractions combined from the column chromatography with Sephadex LH-20, based on NMR and LC-MS analyzes.** The weight in mg is the weight of the dried samples prepared for NMR.

<i>Alaria esculenta</i>			<i>Saccharina latissima</i>		
Nr.	Fractions	Weight (mg)	Nr.	Fractions	Weight (mg)
P1	19, 20, 21	7.6	P5	15, 16, 17	3.2
P2	28, 29, 30	4.1	P6	23, 24, 25	2.8
P3	37, 38, 39	4.5	P7	29, 30, 31	2.5
P4	W	30.0	P8	35, 36, 37, 38	2.4

$^1\text{H}$ ,  $^1\text{H}$ - $^{13}\text{C}$  HSQC, and  $^1\text{H}$ -DOSY spectra were acquired for samples P1–P8 (table 1) to check the complexity of the fractions and to check for carotenoids and polyphenolic moieties. The  $^1\text{H}$  NMR spectra of sample P1–P4 (figure 3.25) and P5–P8 (figure 3.26) show several signals between 4.5 and 9.0 ppm. These signals indicate the presence of aromatic or heteroaromatic moieties (typically ~7.0–8.5 ppm) and phenolic moieties or olefinic methine protons (~6.0–6.5 ppm). Based on the number and intensity of the peaks,  $^1\text{H}$ - $^{13}\text{C}$  HSQC and  $^1\text{H}$  DOSY spectra of sample P4 and P8 will be discussed further. HSQC and DOSY spectra of other fractions can be found in appendix E, figure E13 to E-28.

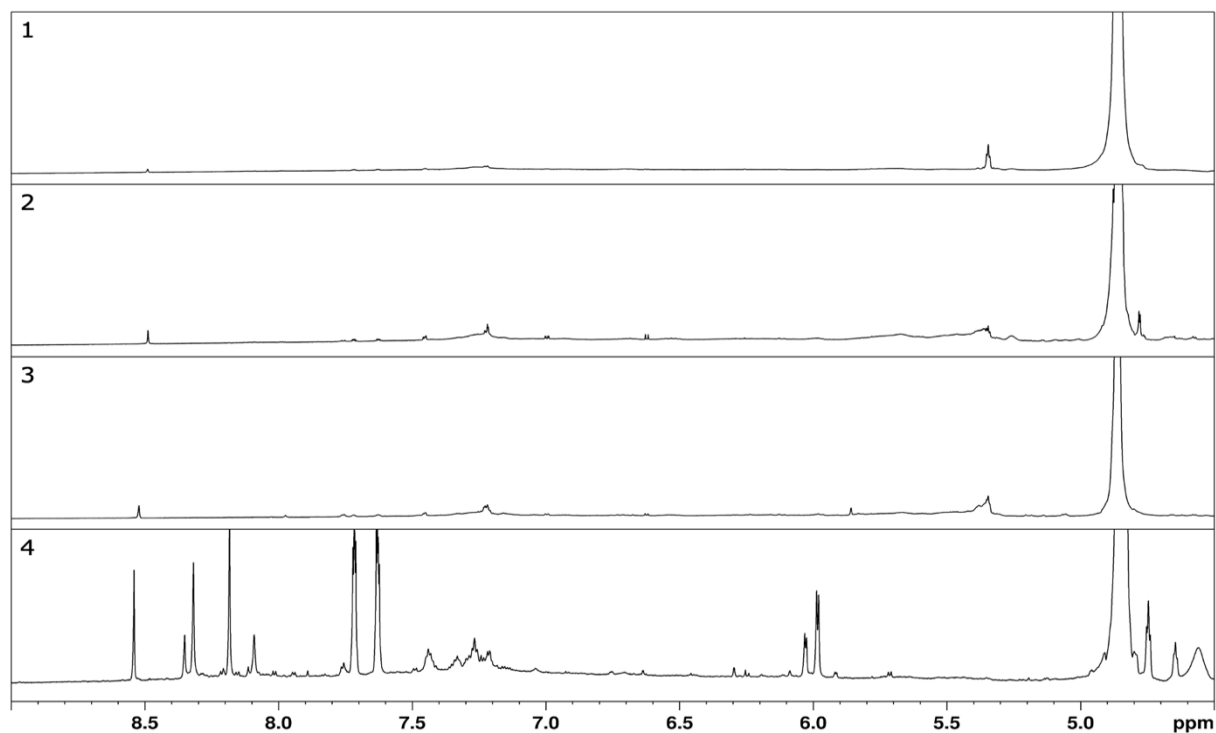


**Figure 3.25: <sup>1</sup>H NMR spectra of *Alaria esculenta*, sample P1-P4.** From top to bottom: P1 (fraction 21, 22, 23 combined), P2 (fraction 30, 31, 32 combined), P 3 (fraction 39, 40, 41 combined), and P4-(waste). Samples were dissolved in deuterated methanol (CD<sub>3</sub>OD) and run at 298.1 K at 800 MHz.

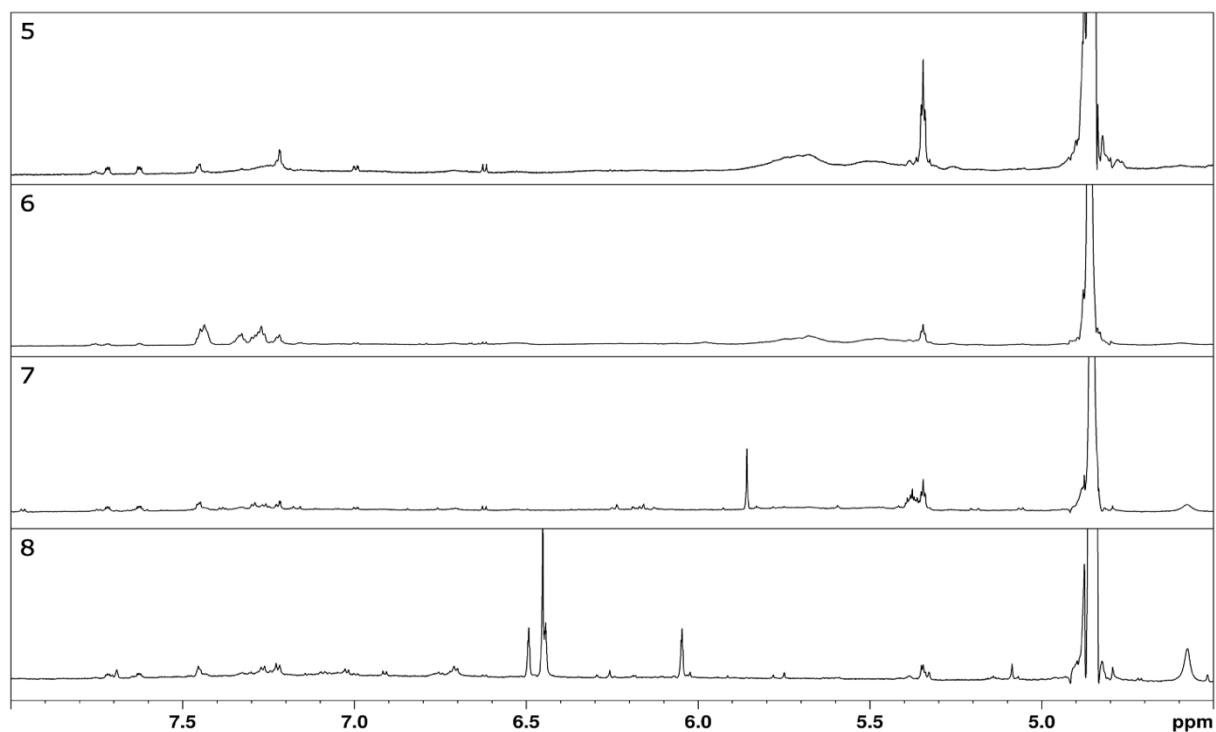


**Figure 3.26: <sup>1</sup>H NMR spectra of *Saccharina latissima*, sample P5-P8.** From top to bottom: P 5 (fraction 17, 18, 19 combined), P 6 (fraction 25, 26, 27 combined), P7 (fraction 31, 32, 33 combined), and P8 (fraction 36, 37, 38, 39 combined). Samples were dissolved in deuterated methanol (CD<sub>3</sub>OD) and run at 298.1 K at 800 MHz.

The  $^1\text{H}$ - $^{13}\text{C}$  HSQC and  $^1\text{H}$  DOSY of P4 (figure 3.27) and P8 (figure 3.28) show signals consistent with polyphenol-like moieties and carotenoid moieties. The  $^1\text{H}$ - $^{13}\text{C}$  HSQC show spectrum show some defined signals in the proton spectrum indicating the presence of small molecules, and some broader signals indicating the presence of either bigger molecules or molecules very similar in structure. The carbon chemical shifts correlates well with the protons. The molecules present in the two samples are clearly different between the two species. The DOSY indicates that the compounds are of approximately the same size, but that there is possibly two to three different compounds present. Either of the samples are pure, which can be seen in both DOSY spectra where the signals have slightly different rate of diffusion. The full spectra can be seen in appendix E.

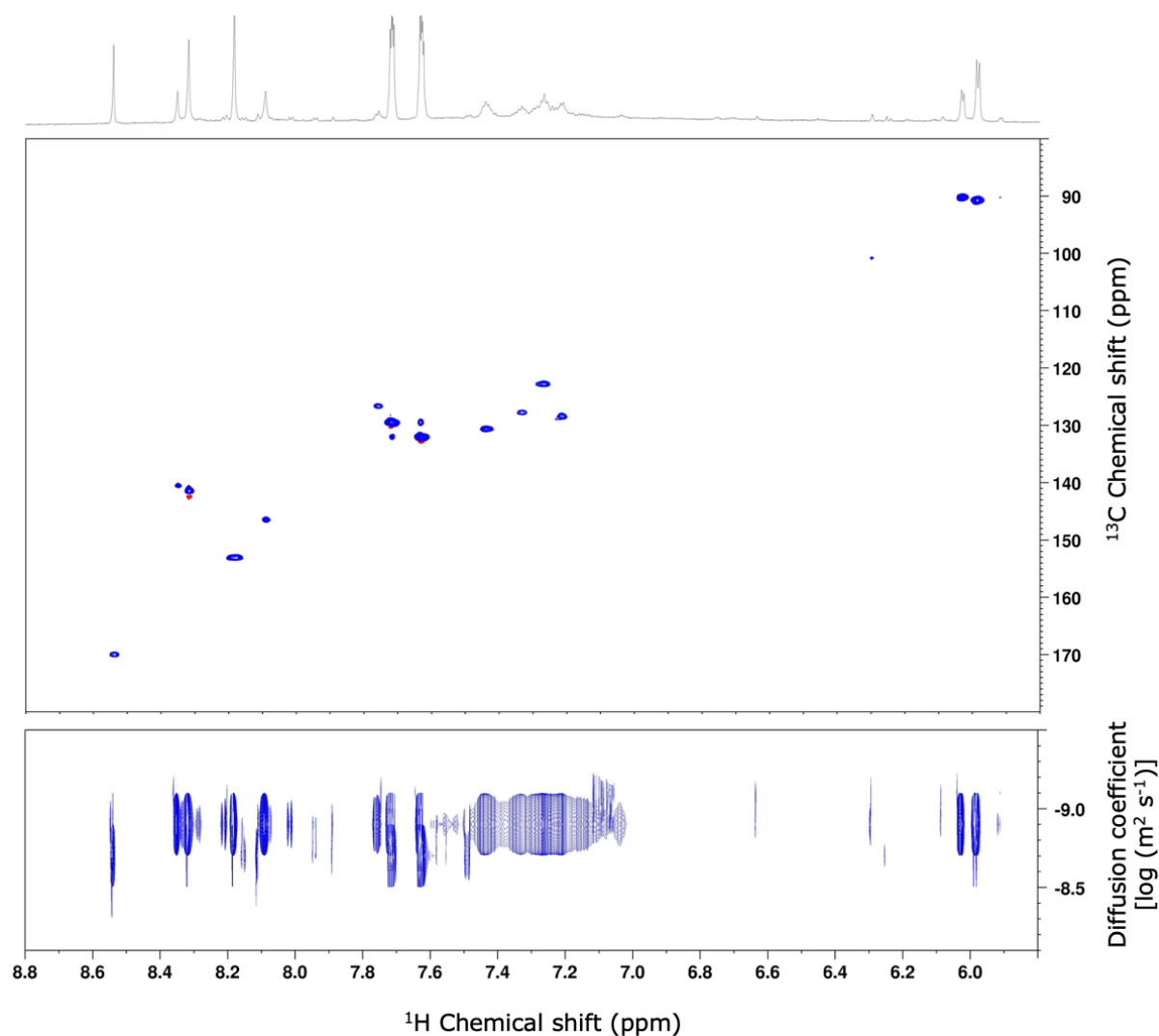


**Figure 3.27:  $^1\text{H}$ - $^{13}\text{C}$  HSQC and DOSY spectrum (5.8-8.8 ppm) of *Alaria esculenta*, P4.** HSQC spectrum in top, DOSY spectrum in bottom. Signals consistent with polyphenol-like moieties. The sample was dissolved in deuterated methanol ( $\text{CD}_3\text{OD}$ ) and run at 298.1 K at 800 MHz.



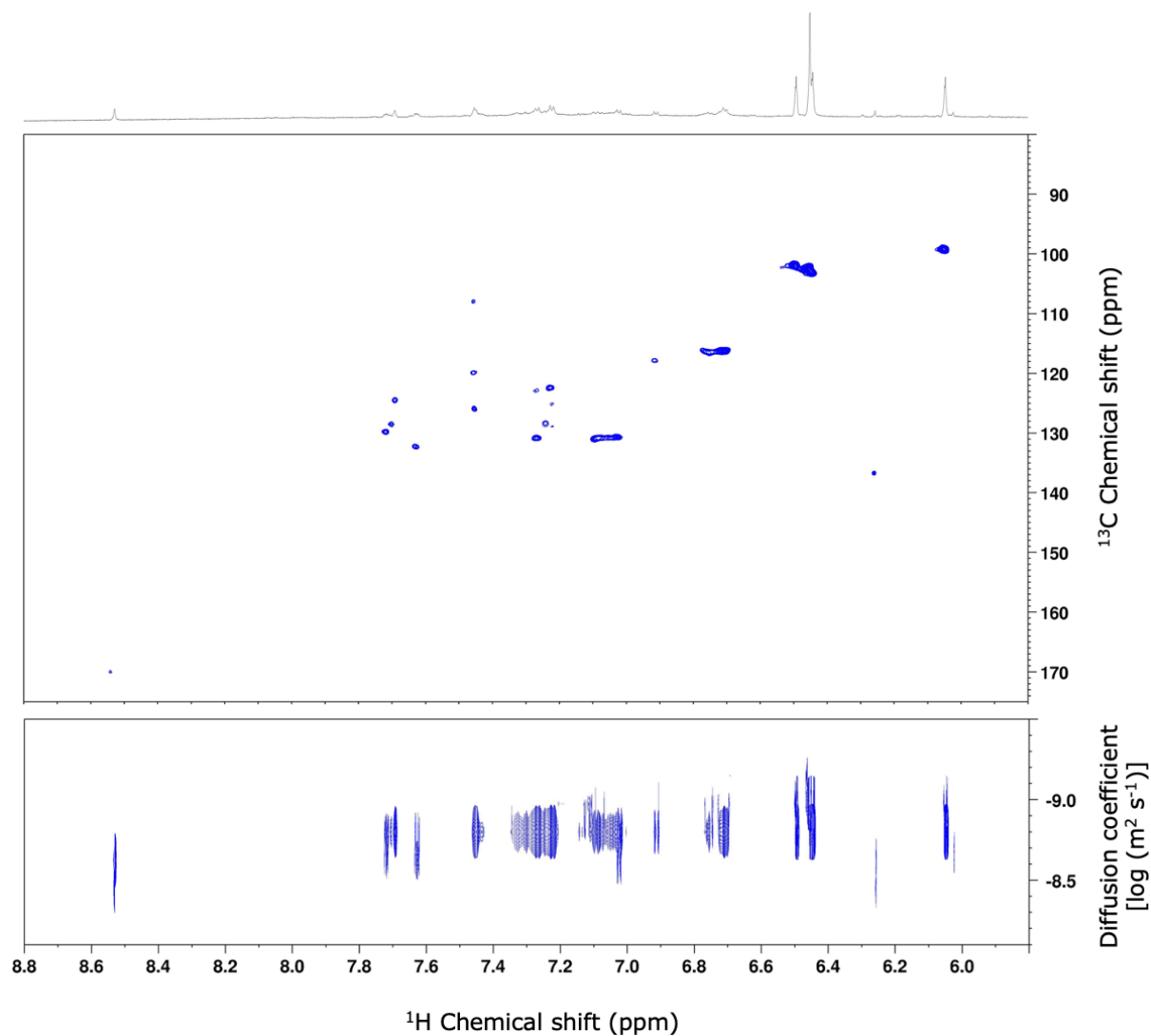


**Figure 3.28:  $^1\text{H}$ - $^{13}\text{C}$  and DOSY spectra (5.8-8.8 ppm) of *Saccharina latissima*, P8.** HSQC spectrum in top, DOSY spectrum in bottom. Signals consistent with polyphenol-like moieties or carotenoid-like moieties. The sample was dissolved in deuterated methanol ( $\text{CD}_3\text{OD}$ ) and run at 298.1 K at 800 MHz.

### 3.5 Freeze-dried material

Freeze-dried material was extracted with acetone in the bulk extraction and purified with XAD-16 resin. The samples were further sent to Aalborg University (Denmark) for further processing. The NMR data in this section were acquired from Aalborg University, and the full spectra can be seen in appendix F.

The NMR data showed signals consistent with carotenoid moieties and some lipid moieties. The spectra were further analyzed to look for the presence of fucoxanthin. The  $^1\text{H}$  NMR spectra (figure 3.29) show eleven signals consistent with methine protons. Some of the signals are overlapping and thus hard to measure their integral value. The chemical shift of the proton-carbon spin pairs of the methine groups (table 4) were established by correlations in the  $^1\text{H}$ - $^{13}\text{C}$  HSQC spectrum (appendix F).

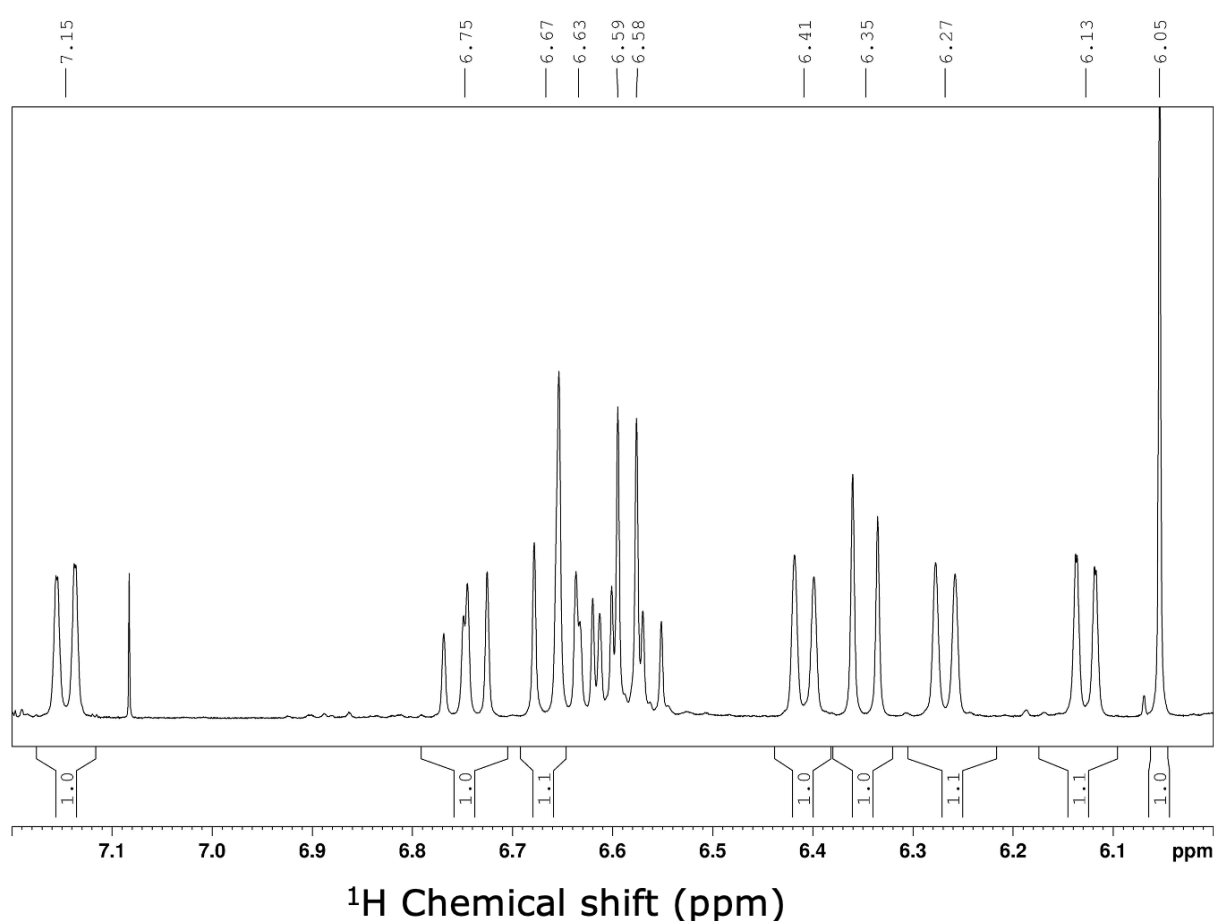
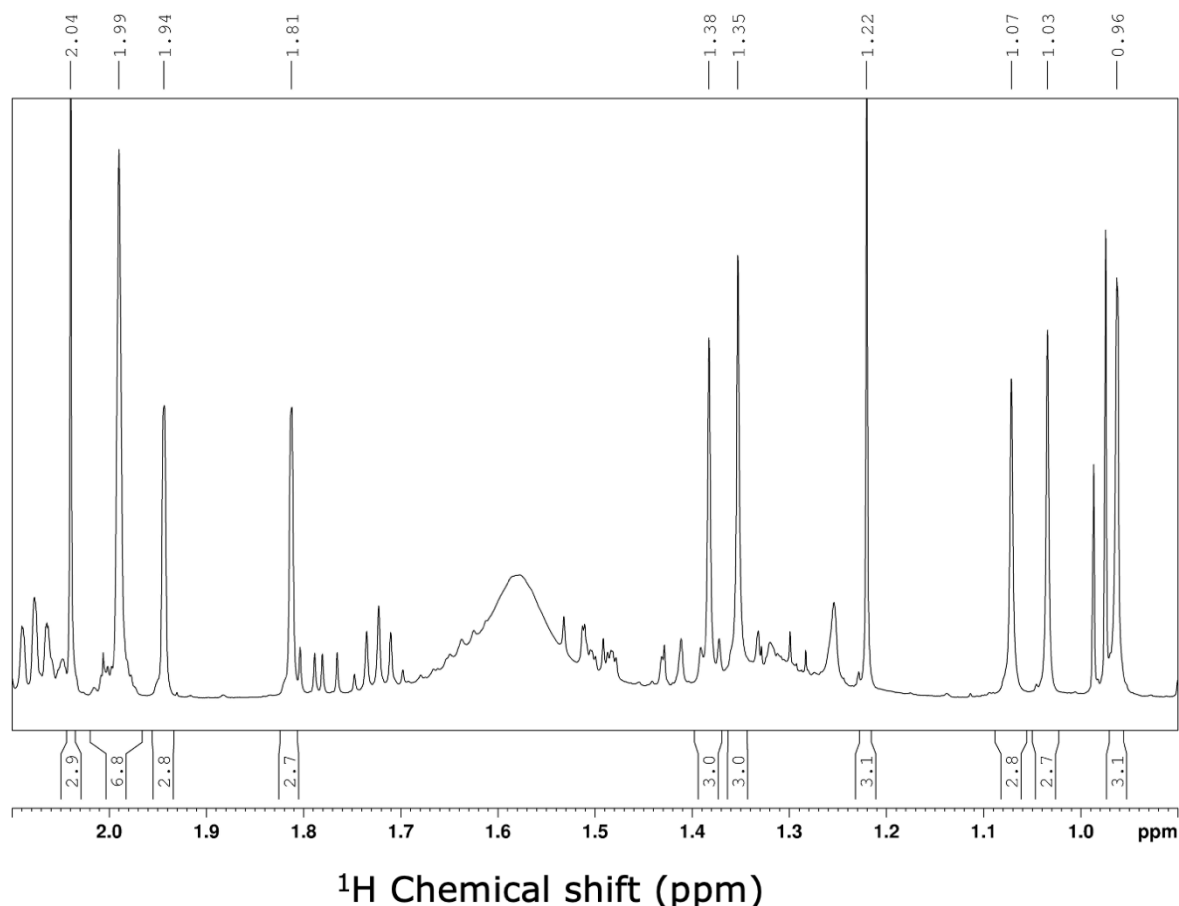


**Figure 3.29:  $^1\text{H}$  spectrum (6.0–7.2 ppm) of acetone extracted material from *Alaria esculenta* FD.** The eleven annotated peaks represent the methines. The sample were dissolved in deuterated chloroform ( $\text{CDCl}_3$ ) and run at 298.1 K at 600 MHz.

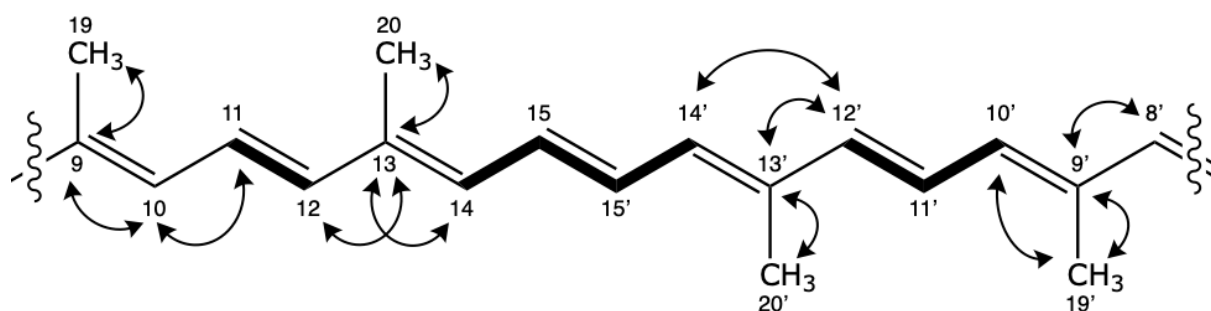
The  $^1\text{H}$  NMR spectra (figure 3.30) show ten signals consistent with the methyl protons. Seven protons give rise to the peak at 1.99 ppm which integrate to a value of approximately seven (6.8). Three protons give rise to the rest of the signals which integrate to a value of approximately three. The fact that all the signals are singlets indicates that there are no protons on the neighboring carbons. The chemical shifts of the

proton-carbon spin pairs of the methyl groups (table 4) were established by correlations in  $^1\text{H}$ - $^{13}\text{C}$  HSQC spectrum (appendix F).

The central acyclic region of carotenoids (C11 – C11') was partially established by COSY correlations, showing scalar couplings between adjacent hydrogen atoms (figure 3.32). The rest of the conjugated chain (figure 3.31) with methyl groups (C9 – C8') was confirmed by correlations in the  $^1\text{H}$ - $^{13}\text{C}$  HMBC spectrum (table 4).

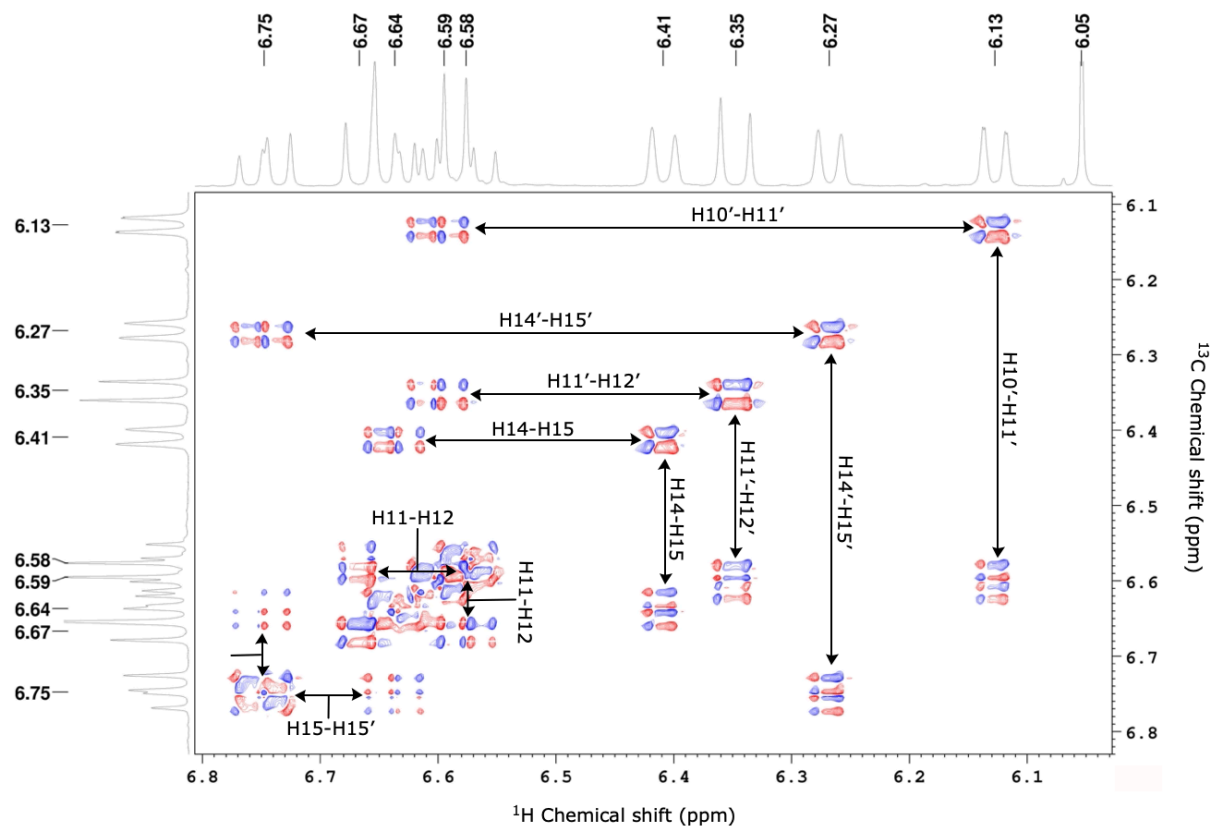


**Figure 3.30:  $^1\text{H}$  spectrum (0.7–2.2 ppm) of FD *Alaria esculenta* extracted with acetone.** The ten annotated peaks represent the methyl protons in fucoxanthin. The peak at 1.99 arise from 7 protons (two methyl groups + one proton). The sample were dissolved in deuterated chloroform ( $\text{CDCl}_3$ ) and run at 298.1 K at 600 MHz. The spectrum is referenced to the residual solvent peak at 7.26 ppm (not displayed) and the peak seen at  $\sim 7.08$  ppm belong to the residual solvent peak.



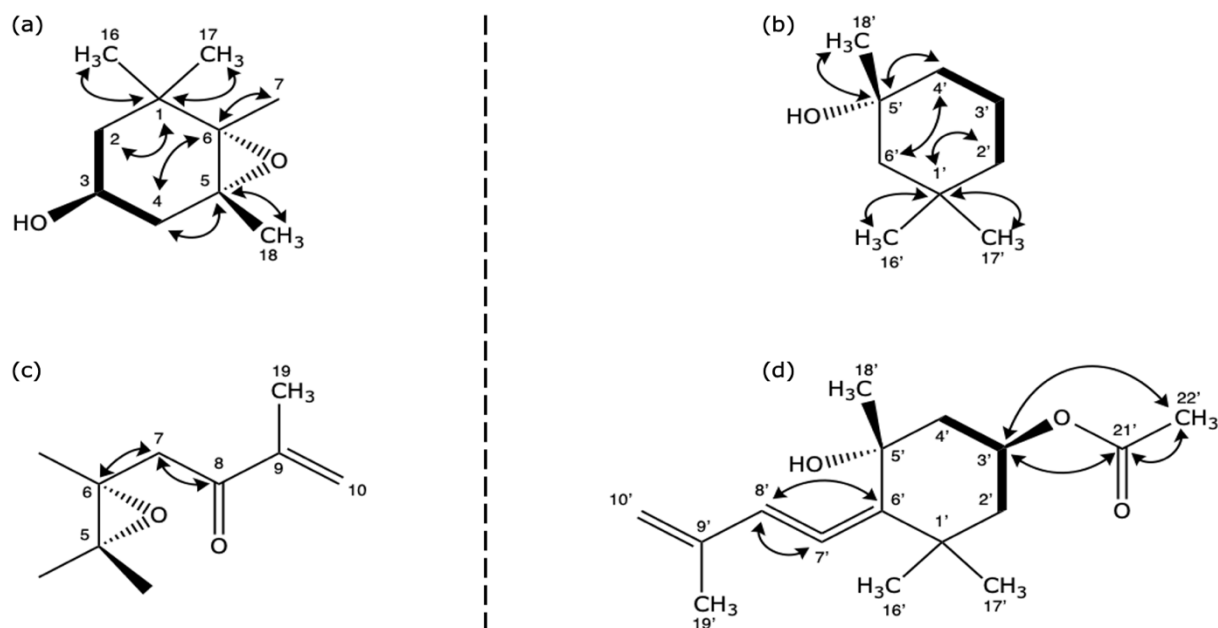
**Figure 3.31: Partial structure of C9–C8' showing the typical acyclic conjugated chain in carotenoids.** COSY correlations represented by bold linkages, HMBC correlations represented by arrows. The

figure is not comprehensive, only some of the HMBC correlations are shown in the figure, see full spectrum (appendix F) for all correlations.



**Figure 3.32: Part of  $^1\text{H}$ - $^1\text{H}$  COSY spectrum of FD *Alaria esculenta* extracted with acetone.** The arrows show couplings between the protons in the structure in figure 3.31 above. The sample were dissolved in deuterated chloroform ( $\text{CDCl}_3$ ) and run at 298.1 K at 600 MHz.

The aromatic ring structures on each side of the chain was partially determined (C2-C4 and C2'-C4') by correlations in the  $^1\text{H}$ - $^1\text{H}$  COSY spectrum (figure 3.33 a and b). The final assignment of both rings (figure 3.34 a and b) and the connection between the rings and the chain (figure c and d) was established by correlations in the  $^1\text{H}$ - $^{13}\text{C}$  HMBC spectrum.



**Figure 3.33: Partial structures and how they are connected to the conjugated chain.** (a) Ring structure at "keto-end" and its connection to C-7. (b) Ring structure at "allenic-end". (c) HMBC correlations showing the connection of ring at "keto-end" to the chain. (d) HMBC correlations proving the connection of ring at "allenic-end" to the chain and the acetyl group (C21-C22') to the ring. COSY correlations represented by bold linkages, HMBC correlations represented by arrows.

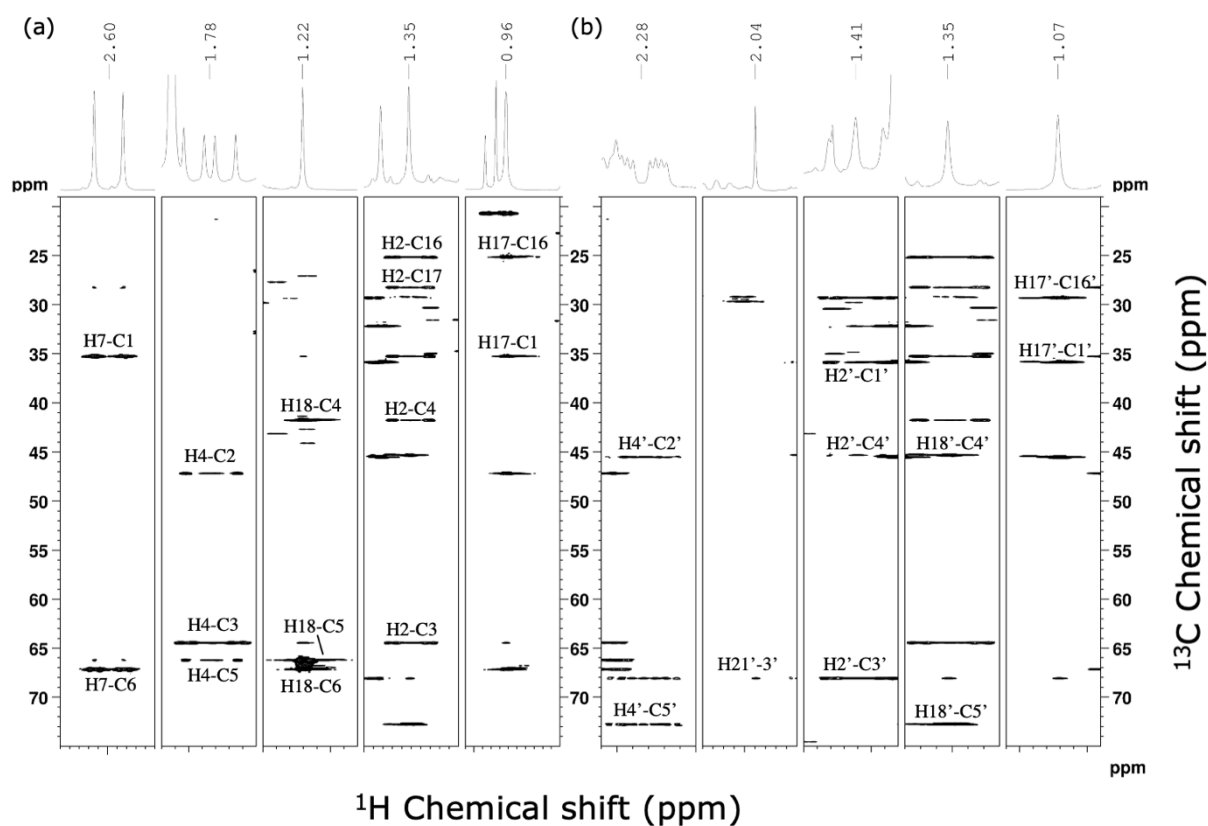


**Figure 3.34: Panel with "slices" of <sup>1</sup>H-<sup>13</sup>C HMBC spectrum of *A. esculenta* FD.** The spectra show some of the key correlations for establish the two cyclic ends (figure 3.33). (a) Correlations in ring at "keto-end". (b) Correlations in the ring at "allenic-end". The sample was dissolved in deuterated chloroform (CDCl<sub>3</sub>) and run at 298.1 K at 600 MHz.

The  $^1\text{H}$ - $^{13}\text{C}$  HMBC spectrum was also used to determine the placement and chemical shift of quaternary carbons in positions C1, C1', C8, and C21'. C1 ( $\delta_{\text{C}}35.1$ ) show correlations (figure 3.35) to the methyl groups H16 ( $\delta_{\text{H}}0.96$ ), H17 ( $\delta_{\text{H}}1.04$ ), and H-18 ( $\delta_{\text{H}}1.22$ ), and the methylene group H-2 ( $\delta_{\text{H}}1.35$  and  $\delta_{\text{H}}1.49$ ). C-1' ( $\delta_{\text{C}}35.8$ ) show correlations to the methine proton H8 ( $\delta_{\text{H}}6.06$ ), the methylene group H2' ( $\delta_{\text{H}}1.41$  and  $\delta_{\text{H}}1.99$ ), and the methylene groups H16' ( $\delta_{\text{H}}1.38$ ) and H17' ( $\delta_{\text{H}}1.07$ ).

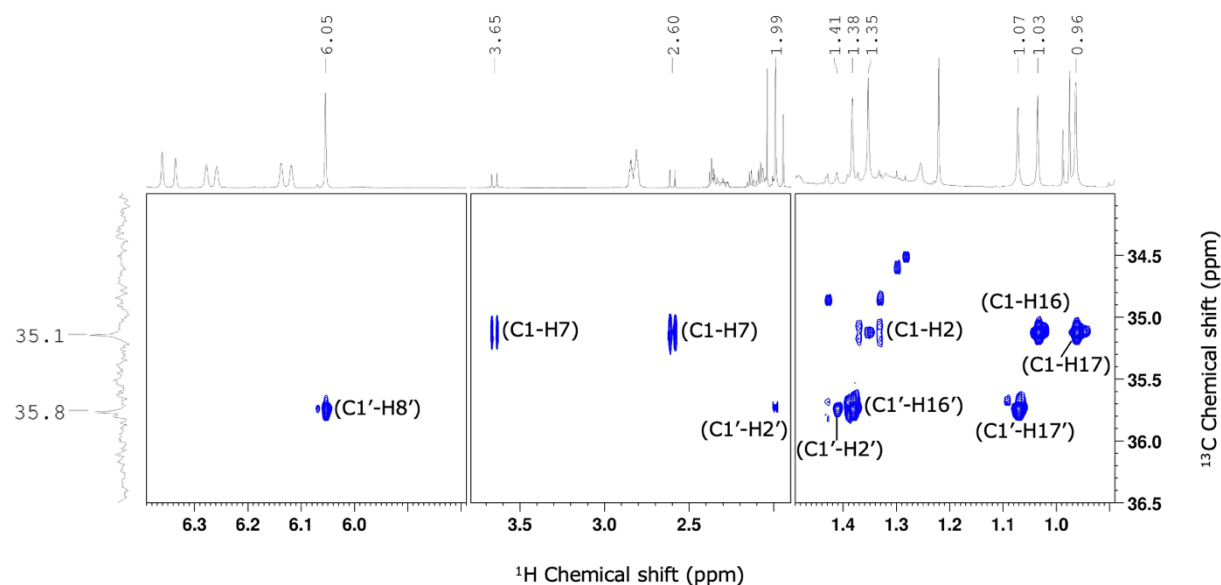


**Figure 3.35:  $^1\text{H}$ - $^{13}\text{C}$  HMBC of C-1 and C-1' in compound from *Alaria esculenta* FD.** The spectrum shows the correlations proving the chemical shift of C1 ( $\delta_{\text{C}}35.1$ ) and C1' ( $\delta_{\text{C}}35.8$ ). The proton-carbon spin pairs are given at each correlation. The sample was dissolved in deuterated chloroform ( $\text{CDCl}_3$ ) and run at 298.1 K at 600 MHz.

C8 ( $\delta_{\text{C}}197.8$ ) show correlations (figure 3.36) to correlations to H-10 ( $\delta_{\text{H}}7.15$ ), H-7 ( $\delta_{\text{H}}2.60$  and  $\delta_{\text{H}}3.65$ ), and H-19 ( $\delta_{\text{H}}1.94$ ).

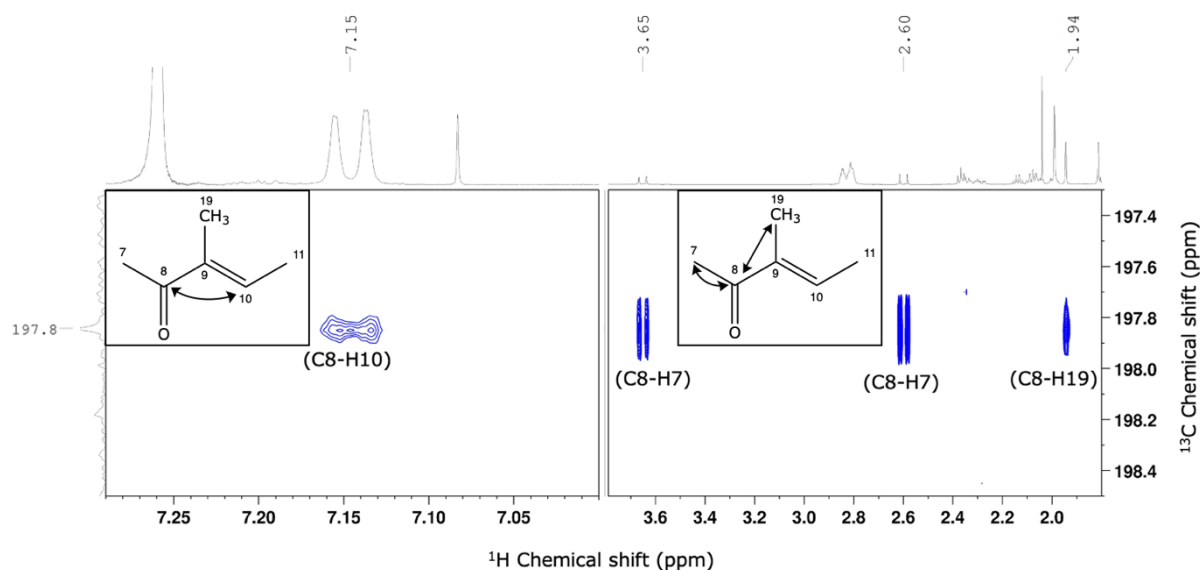


**Figure 3.36:  $^1\text{H}$ - $^{13}\text{C}$  HMBC spectra of correlations from C8 ( $\delta_{\text{C}}197.9$ ).** The spectra show correlations to H-10 ( $\delta_{\text{H}}7.15$ ), H-7 ( $\delta_{\text{H}}2.60$  and  $\delta_{\text{H}}3.65$ ), and H-19 ( $\delta_{\text{H}}1.94$ ) (partial structures with arrows). The sample was dissolved in deuterated chloroform ( $\text{CDCl}_3$ ) and run at 298.1 K at 600 MHz.

C21' ( $\delta_c 170.4$ ) correlations to the methyl group H22' ( $\delta_H 2.04$ ) and the methine proton H3' ( $\delta_H 5.38$ ). The spectral data, including chemical shift ( $\delta_H$ ,  $\delta_C$ ), multiplicity (J in Hz), and type of hydrocarbon is displayed in table 4.

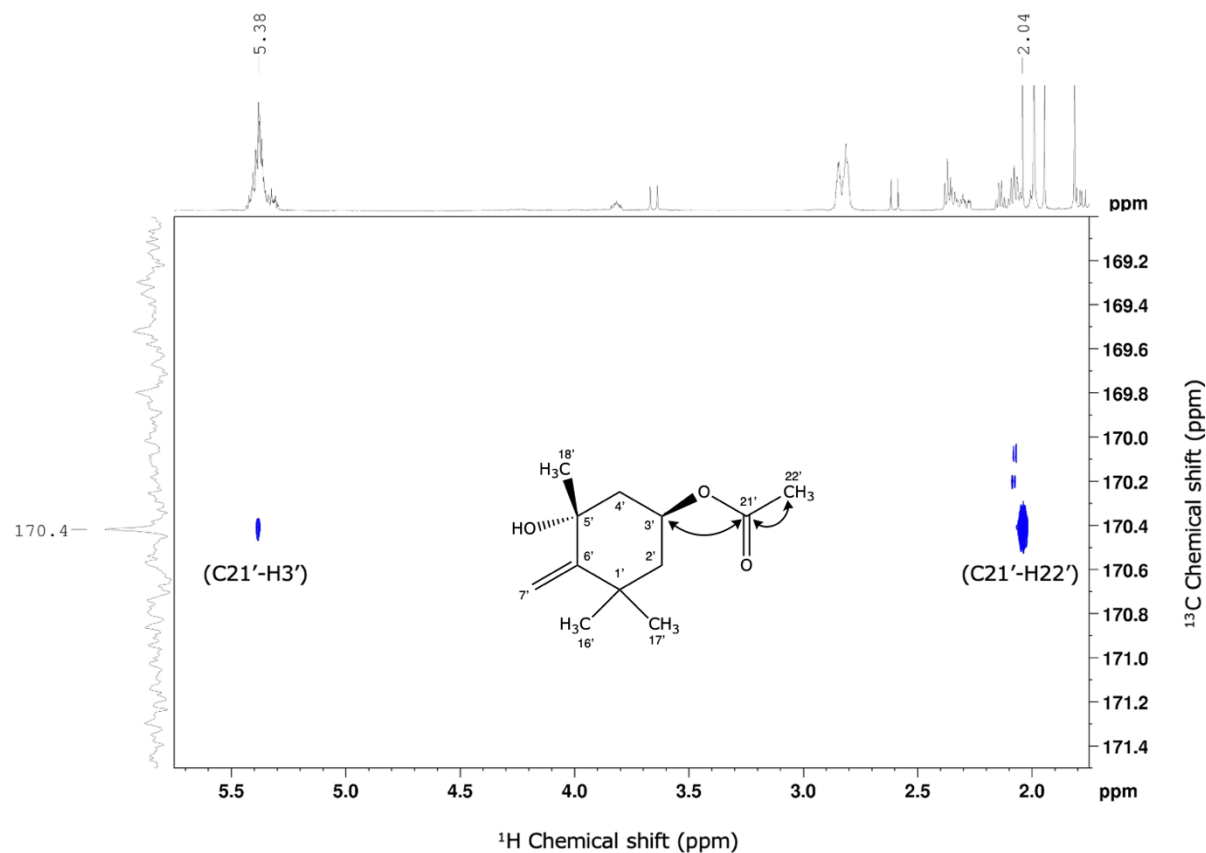


**Figure 3.37:**  $^1\text{H}$ - $^{13}\text{C}$  HMBC of C-21' in compound from *Alaria esculenta* FD. Correlation between  $\delta_c 170.4$  and  $\delta_H 1.94$  and  $\delta_H 5.38$  at C-3'. The sample was dissolved in deuterated chloroform ( $\text{CDCl}_3$ ) and run at 298.1 K at 600 MHz.

By piecing all the partial structures together, it was possible to determine the full structure of fucoxanthin. The full table with the spectral data of the elucidation of fucoxanthin can be seen below (table 2). The complete structure with atom numbers, COSY-correlations, and some of the HMBC correlations used to define the structure of the compounds can be seen in figure 3.38. As the NMR also indicated lipids, further analyzes of the NMR data should be done to see if the fucoxanthin may be esterified with any fatty acids.

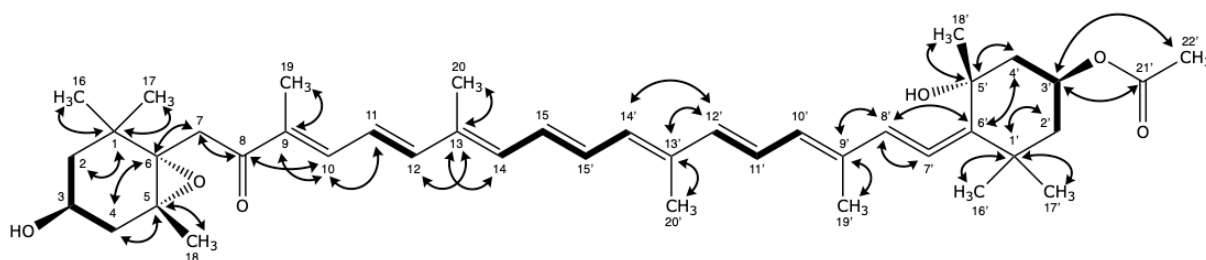


**Figure 3.38:** Fucoxanthin structure with atom numbers, COSY correlations, and HMBC correlations. The COSY correlations are marked in bold, the HMBC correlations with arrows. The figure is not comprehensive, only some of the HMBC correlations are shown in the figure, see full spectrum (appendix F) for all correlations.

**Table 4: Spectral data of fucoxanthin from *A. esculenta***, including  $\delta_H$  (multiplicity, J in Hz), integral of protons,  $\delta_C$ , integral of carbons, and the type of hydrocarbon. The sample was dissolved in chloroform-d6 (CDCl3) and run at 298 K. The em dash (-) is used where data from the conducted experiments,  $^1H$ -NMR and  $^1H$ - $^{13}C$  HSQC, are not obtained, a blank space is used when there is no proton. s=singlet, d=doublet, t=triplet, m=multiplet, dd=doublet of doublets, ddd=doublet of doublets. The full spectra used to obtain these correlations can be seen in appendix F.

Nr	$\delta_H$ multiplicity, J (Hz)	Integral H	$\delta_C$	Hydrocarbon
1			35.1	C
2	1.35 (t, J=11.9) 1.49 (t, J=11.7)	3.0 -	47.1	CH <sub>2</sub>
3	3.82 (m)	1.2	64.3	CH-O
4	1.78 (dd, J=9.2, 4.7) 2.32 (ddd, J=9.1, 4.7)	- -	41.7	CH <sub>2</sub>
5			66.1	C-O
6			67.1	C-O
7	2.60 (d, J=18.3) 3.65 (d, J=18.2)	1.1 1.2	40.8	CH <sub>2</sub>
8			197.8	C=O
9			134.5	C
10	7.15 (dd, J=11.0, 0.99)	1.0	139.1	CH
11	6.58 (t, J=14.9)	-	123.4	CH
12	6.67 (d, J=14.8)	1.2	145.0	CH
13			135.4	C
14	6.41 (d, J=11.7)	1.0	136.6	CH
15	6.64 (t, J=13.5)	-	129.4	CH
16	1.04 (s)	2.7	25.0	CH <sub>3</sub>
17	0.96 (s)	-	28.1	CH <sub>3</sub>
18	1.22 (s)	3.1	21.2	CH <sub>3</sub>
19	1.94 (s)	2.8	11.8	CH <sub>3</sub>
20	1.99 (s)	-	12.8	CH <sub>3</sub>



1'			35.8	C
2'	1.41 (t, $J=12.0$ ) 1.99 (d, $J=13.5$ )	- -	45.4	CH <sub>2</sub>
3'	5.38 <sup>1</sup>	-	68.0	CH
4'	1.51 (dd, $J=13.6, 11.5$ ) 2.28 (ddd, $J=12.8, 4.4, 2.2$ )	- -	45.2	CH <sub>2</sub>
5'			72.7	C
6'			117.5	C
7'			202.3	=C=
8'	6.06 (s)	1.0	103.4	CH
9'			132.51	C
10'	6.13 (dd, $J=11.4, 0.92$ )	1.1	128.5	CH
11'	6.59 (t, $J=15.1$ )	-	125.7	CH
12'	6.35 (d, $J=15.0$ )	1.0	137.1	CH
13'			138.1	C
14'	6.27 (d, $J=11.6$ )	1.0	132.2	CH
15'	6.75 (dd, $J=14.6, 11.9$ )	1.0	132.49	CH
16'	1.38 (s)	3.0	29.2	CH <sub>3</sub>
17'	1.07 (s)	2.8	32.1	CH <sub>3</sub>
18'	1.35 (s)	3.0	31.3	CH <sub>3</sub>
19'	1.81 (s)	2.6	14.0	CH <sub>3</sub>
20'	1.99 (s)	-	12.9	CH <sub>3</sub>
21'			170.4	C
22'	2.04 (s)	2.8	21.4	CH <sub>3</sub>

<sup>1</sup> Overlapping signals with protons from another molecule.

## 4 DISCUSSION

The aim of this thesis was to investigate the presence of carotenoids and polyphenols in brown seaweed, purify the samples through a set of purification steps, and extract the carotenoid fucoxanthin.

Investigation of the presence of carotenoids and polyphenols was done by solvent extraction on seaweed material from the two species *Alaria esculenta* and *Saccharina latissima*. A small-scale experiment was conducted to compare extractions with methanol and acetone of the species with different pretreatments. A bulk extraction was conducted on wet material and freeze-dried material. Purification of the extracts included defatting with *n*-hexane, adsorption chromatography with macroporous resin (XAD-16), and column chromatography with liquid chromatography medium (LH-20). A gradient elution with ratios of 1:0, 4:1, 3:2, 2:3, 1:4, and 0:1 water:acetone was used to purify the crude acetone extract of *Saccharina latissima* with XAD-16. Based on the result from this, a standardized elution scheme with only two steps, first an elution with RO-water then with acetone (100 %) was developed. The fraction eluted with 100 % acetone was further separated on a column packed with LH-20 medium and eluted off the column with methanol.

To examine if fucoxanthin was present in any of the purified samples, subsamples were analyzed by NMR and LC-MS throughout the process. The characterization was done by NMR analysis and by comparison of obtained data with previously reported data in the literature.

### 4.1 Investigation of the presence of polyphenols and carotenoids

Comparing the different extracts from solvent extractions on freeze-dried and enzyme treated material in the small-scale experiment, extraction with methanol on freeze-dried material gave the highest yield from both species. The yield was approximately the same for *Alaria esculenta* and *Saccharina latissima*, 146.4 mg and 144.8 mg respectively. In regard of polyphenol-like and carotenoid-like molecules, the NMR data indicate that these compounds are extracted from both freeze-dried and enzyme treated material and with both methanol and acetone as solvents. <sup>1</sup>H NMR spectrum of *Alaria esculenta* extracted with acetone have the most intense signal, especially in the region to expect protons from phenolic compounds. This agrees with previously reported findings of polyphenols concentrations in brown seaweed by Roleda *et al.* (2019), being higher in *A. esculenta* than *S. latissima* regardless of collection site and season.

The chemical and structural complexity of the seaweed cell walls, containing sulphated polysaccharides, limit the efficiency of general extraction procedures of bioactive compounds (Wijesinghe and Jeon, 2012). Enzyme assisted extraction (EAE) with cellulases, enzymes that break down insoluble plant polymer cellulosic substrates into soluble sugars (Merck KGaA, s.a.), is widely used to enhance the extraction of polyphenols and other metabolites from plant material (Mourtzinou and Goula, 2019;

Wijesinghe and Jeon, 2012). In this work extracts from enzyme treated material show more diverse and intense polyphenol-like signals, especially from *Alaria esculenta* extracted with acetone. This indicates that the enzyme treatment prior to extraction can be useful when targeting polyphenols. Enzyme treated material was however not proceeded with due to the time frame of this work. Although, when targeting polyphenols from seaweed, EAE looks like a promising extraction method before further purification and isolation steps. As enzymatic hydrolysis of polysaccharides in the plant cell wall, drying at low temperatures and mechanical grinding also have shown to potentially yield the same carotenoid concentration compared to extraction with organic solvents (Shannon and Abu-Ghannam, 2018), future research on isolation of polyphenols and carotenoids should include EAE methods and further purifying of these extracts.

The chemical composition of brown seaweed varies between species, seasons, and location (Holdt and Kraan, 2011; Schiener *et al.*, 2015). The fact that the content differs is important when targeting specific components and comparing species. The seaweed used in this work was two different species of brown seaweed, *Alaria esculenta* and *Saccharina latissima*, cultivated and harvested at Frøya between 06.01.2020 to 11.05.2020 and from 17.01.2020 to 19.05.2020, respectively. The difference in the period of cultivation is so small that seasonal variations is not considered a critical factor. In other words, the climatic conditions and location is the same for both species.

## 4.2 Purification steps

### 4.2.1 Defatting

The NMR spectra from the small-scale experiment show that lipids were removed by first extracting the seaweed material with *n*-hexane. This is consistent with the literature, where *n*-hexane has shown to be the most efficient solvent for defatting biomolecules from natural products (Kim *et al.*, 2021). Besides this, the hexane fraction also shows signals indicating aldehydes, aromatic, and phenolic moieties. This indicates compounds with carotenoid-like and polyphenol-like moieties are also extracted with *n*-hexane. Carotenoids are lipophilic, fat-soluble compounds (Mezzomo and Ferreira, 2016) and these properties explain why these chemical moieties are present in the hexane fractions. Still, the results from the defatting step in this work indicates that defatting with *n*-hexane does remove lipids from seaweed material, even though complete separation was not achieved.

Even though the defatting step does remove lipids, some lipids remain in the samples. This can be due to the presence of lipids with polar functional groups or that the defatting step is not efficient enough. Although, as the hexane also extract compounds with polyphenol or carotenoid moieties, a more exhaustively extraction with hexane will most likely also extract more of the targeted compounds. An alternative method for removal of lipids could be freezing-lipid filtration. Ahn *et al.* (2007) used this method successfully on fish material for the removal of 90 % of the lipids without any significant loss of phenolic compounds. In addition, this same method is described in HarvestPlus Handbook for Carotenoid Analysis (Rodríguez-Amaya and Kimura, 2004) where the samples are dissolved in acetone and left in the freezer for 4-5 hours to solidify the lipids before separating by filtration. They carry out the whole process under low temperatures and state that about 90 % of the lipids are removed. Further research on defatting of seaweed material, when targeting carotenoids and polyphenols, is still needed and should focus on the most efficient way to achieve a complete separation of lipids from the targeted compounds.

Aldehyde signals were observed in NMR spectra of *Alaria esculenta*, both in the hexane-fraction of freeze-dried material and the acetone fraction of enzyme treated material. It is worth noting that dissolving carotenoids in organic solutions make them less stable than naturally occurring in tissues (Lu *et al.*, 2020), and these aldehyde signals could indicate that some carotenoids starts degrading already at this stage. Fucoxanthin, like other carotenoids, is highly susceptible to isomerization and degradation due to its functional groups and extended conjugated system (Mortensen and Skibsted, 2000). During oxidative attacks carotenoids may break down to highly reactive aldehydes and epoxides (Kalariya *et al.*, 2008). The aldehyde signals present in the  $^1\text{H}$ - $^{13}\text{C}$  HSQC (observed as folded signals) could be degradation products of carotenoids. The time between maceration and extraction and the time the extracted molecules are kept in solution should thus be as short as possible to avoid degradation of carotenoids. Quick freezing, and storage of the sample in a frozen condition could be a way to preserve the carotenoids in between purification steps, but as described by Rodríguez-Amaya and Kimura (2004), slow thawing of the samples must then be avoided.

#### 4.2.2 XAD-16 resin

The first purification step after defatting was separation with the macroporous resin XAD-16. Fucoxanthin-like signals were characterized by NMR from the sample eluted with 100 % acetone (Ac100). From this result, it was decided to make a standardized elution scheme with only two steps, first an elution with RO-water then with acetone (100 %). The NMR data show how hydrophilic storage carbohydrates like mannitol are separated from more hydrophobic compounds like carotenoids by the resin. Mannitol which is clearly present in the crude extract is found both in the flow through of the sample loading (R0) and the fraction collected from washing the resin with water (R1), but not in the fraction collected from the elution with acetone (R2). The R2, which is equivalent to the Ac100 fraction from the first elution scheme, are thus more purified than the crude extract. In regard of making a what could be a fucoxanthin-rich fraction, the purification step with XAD-16 resin was successful. However, in regard of polyphenols, the NMR data reveals that signals consistent with polyphenols are not as observed in the R2 as the crude fraction (R0). The solubility of polyphenols is dependent on the polarity of each polyphenol (Kim and Lee, 2002). Phlorotannins, which comprise most of the polyphenols found in seaweed, are often water-soluble and would thus be eluted in the R1 fraction along with mannitol and other compounds with similar properties. This would explain why the signals indicating polyphenols in the crude extract (R0) is practically not visible in the elution with acetone (R2).

Overall, the purification with XAD-16 resin was an efficient way of separating hydrophilic and hydrophobic compounds. Even though it looks like polyphenolic compounds are separated from the R2 fraction, polyphenol-like signals were localized in NMR data of additionally purified R2-fractions, indicating that some polyphenols were purified in the R2 fraction.

#### 4.2.3 Sephadex LH-20

The next step of purification after adsorption with XAD-16 resin was column chromatography with LH-20. From the collected fractions it was no longer possible to locate or identify fucoxanthin. The column chromatography with LH-20 resin was a time-consuming operation, where the sample was dissolved in methanol over a period for 11-12 hours in the column and up to 24 hours before dried. This is a step in the purification procedure where further oxidation might take place. To minimize the risk of isomerization and degradation, the column should be kept in a dark room to avoid light exposure. The samples eluted off the column should be dried as quickly as possible to avoid oxidate degradation.

Carotenoids possessing hydroxyl groups, such as fucoxanthin, can be found as both free xanthophyll acylated with fatty acids and exist as carotenoid esters (Mariutti and Mercadante, 2018). Analysis of such carotenoid esters can be challenging because these are usually present in a mixture of esters with a variety of fatty acids and thus hard to separate (Rodriguez-Amaya and Kimura, 2004). As fatty acids are seen in the fucoxanthin-rich fraction from the XAD-16 resin and fucoxanthin is not identified in the sample after the column chromatography, this could indicate the presence of such carotenoid esters. To simplify chromatographic separation, saponification of the sample could be useful as this can hydrolyze carotenoid esters, making it possible to analyze the free carotenoids.

### 4.3 Extraction and elucidation of fucoxanthin

NMR data of *Saccharina latissima* wet material extracted with acetone and purified by XAD-16 resin, showed proton-carbon correlations in agreement with previously reported data for fucoxanthin in the literature (Englert *et al.*, 1990). However, the sample was not completely purified, and further purification is needed to isolate and verify the presence of fucoxanthin.

NMR data of the freeze-dried material extracted with acetone and purified by XAD-16 resin also showed correlations consistent with fucoxanthin. By using both various NMR experiments including  $^1\text{H}$ - $^1\text{H}$  COSY and  $^1\text{H}$ - $^{13}\text{C}$  HMBC, the structure of fucoxanthin could be elucidated. The carbons at position C8 and C21' has previously been described with various chemical shifts. Imbs *et al.* (2013) and Mori *et al.* (2004) reports the chemical shift of C8 to be  $\delta_{\text{C}}170.4$  and C21' to be  $\delta_{\text{C}}197.8$ . Using  $^1\text{H}$ - $^{13}\text{C}$ -HMBC correlations the chemical shift of C8 is  $\delta_{\text{C}}197.8$  and the chemical shift for C21' is  $\delta_{\text{C}}170.4$ . The HMBC spectrum show a correlation between  $\delta_{\text{C}}197.8$  (C-8) the methylene group,  $\delta_{\text{H}}2.60$  and  $\delta_{\text{H}}3.65$ , at C-7, and the methyl group,  $\delta_{\text{H}}1.94$ , at C19, but not to the methyl group,  $\delta_{\text{H}}2.04$ , at C-22'. The opposite is true for  $\delta_{\text{C}}170.4$ . However, this data also showed signals consistent with fatty acids. The fucoxanthin could be acylated with fatty acids and consist in the carotenoid ester form. To confirm the presence of fucoxanthin in the free xanthophyll form, further purification is needed.

In order to detect the presence of carotenoids or polyphenols a  $^1\text{H}$ - $^{13}\text{C}$  HSQC overview (appendix G) was made from previously reported chemical shifts in the literature, of proton and carbons in polyphenols and carotenoids. The map allowed evaluation of the NMR spectra in a more efficient matter, in regard of investigating the presence of these molecules. The map could hopefully be a useful contribution as a guide for future investigation and chemical characterization of carotenoids and polyphenols by NMR.

### 4.4 Future perspectives

No specific actions were taken in regard of protecting the carotenoids from degradation in this work. Due to the indications of degradation seen in the samples, such as the presence of aldehydes, and the loss of carotenoid-like signals in the data obtained after the column, a protocol with protective measures should be developed. This would help to minimize the oxidation and degradation of carotenoids throughout the extraction and purification process and simplify the analysis and identification of these structures. It would be advantageous to minimize the duration of extraction procedures, to reduce the time that samples are kept in solution. As exposure to oxygen, light, and high temperatures are highly destructive, these factors should be avoided as much as possible. In addition to this, avoiding contact with acids would help prevent the carotenoids from decomposing, dehydration, and isomerization (Rodríguez-Amaya and Kimura, 2004). As carotenoids and polyphenols exhibit antioxidation activity, a possibility could be to add other antioxidants, *e.g.* vitamin C or vitamin E, to the samples to prevent the oxidation of these targeted molecules. This has previously been done

As the chemical composition of seaweeds varies between species, seasons, and locations, a more efficient utilization of the seaweed plant assumes harvesting of the right specie, in the right location and at the right time to ensure peak yield of the targeting compounds. To establish protocols for the right harvest, further research on specific compounds and the content of these in seaweed are still needed. The research should

also focus on further understanding carotenoids and polyphenols from seaweed and how they can be purified, isolated, preserved in the best manner.

## 5 CONCLUSION

The presence of carotenoids and polyphenols in the brown seaweed species *Alaria esculenta* and *Saccharina latissima* has been investigated. A small-scale experiment was conducted to compare the species, differences between extraction solvents and material pretreatments. Both freeze-dried and enzyme treated material from both species showed indications of polyphenols and carotenoids, when extracted with methanol and acetone. Extraction with acetone showed most signals in regard of polyphenol-like and carotenoid-like signals, even though methanol gave the highest yield of extract. Based on the NMR data, *Alaria esculenta* seems to have a higher content of these types of molecules compared to *Saccharina latissima*.

In a bulk extraction, wet seaweed material was extracted with 62.5 % aqueous acetone and subsequently extracted with 100 % methanol. Freeze-dried material was extracted with 100 % acetone. These extracts were purified through a set of purification steps. Defatting was to a certain degree achieved with *n*-hexane, but not completely as lipids were still associated with the targeted compounds after defatting. NMR data also indicated the presence of carotenoids and polyphenols in the hexane-fraction. Signals consistent with aldehydes indicates oxidation and degradation of carotenoids.

Purification with XAD-16 resin could be an effective way of producing a fucoxanthin-rich extract. NMR data of wet material from *Saccharina latissima* and freeze-dried material from *Alaria esculenta*, eluted with 100 % acetone off the resin, indicated the presence of fucoxanthin. Fucoxanthin could not be seen after the purification with LH-20 column chromatography. It is suspected that this is due to oxidation and degradation of carotenoids or the presence of carotenoid esters.

The complete structure of fucoxanthin was characterized by correlations in  $^1\text{H}$ - $^{13}\text{C}$  HSQC,  $^1\text{H}$ - $^1\text{H}$  COSY, and  $^1\text{H}$ - $^{13}\text{C}$  HMBC spectra of a purified sample from the freeze-dried material. As these fractions still contained lipids, fucoxanthin could be acetylated with fatty acids, and further purification steps are needed to isolate the compound. As the complete structure of fucoxanthin was established by NMR it is clearly evident that fucoxanthin was present.

No protective measures were taken during these investigations, most likely leading to oxidation and degradation of any carotenoids present. In any prospective research on carotenoids and polyphenols from seaweed, protective measures should be considered. These could include protection from oxygen, light, and high temperatures, in addition to time efficient extractions, preferable storage conditions, and addition of other antioxidants. Further research is still needed to develop efficient and preservative purification and isolation methods for carotenoids and polyphenols from seaweed.



# REFERENCES

- AHN, Y. G., SHIN, J. H., KIM, H.-Y., KHIM, J., LEE, M.-K. & HONG, J. 2007. Application of solid-phase extraction coupled with freezing-lipid filtration clean-up for the determination of endocrine-disrupting phenols in fish. *Analytica Chimica Acta*, 603, 67-75.
- ALSAUD, N. & FARID, M. 2020. Insight into the Influence of Grinding on the Extraction Efficiency of Selected Bioactive Compounds from Various Plant Leaves. *Applied Sciences*, 10.
- AMAGATA, T. 2010. 2.18 - Missassigned Structures: Case Examples from the Past Decade. *In: LIU, H.-W. & MANDER, L. (eds.) Comprehensive Natural Products II*. Oxford: Elsevier.
- AMERICAN CHEMICAL SOCIETY. s.a. *NMR and MRI: Applications in Chemistry and Medicine* [Online]. Available: <https://www.acs.org/content/acs/en/education/whatischemistry/landmarks/mri.html> [Accessed July 19 2021].
- AMORIM-CARRILHO, K. T., CEPEDA, A., FENTE, C. & REGAL, P. 2014. Review of methods for analysis of carotenoids. *TrAC Trends in Analytical Chemistry*, 56, 49-73.
- BARRIOS-GONZÁLEZ, J. 2018. Chapter 13 - Secondary Metabolites Production: Physiological Advantages in Solid-State Fermentation. *In: PANDEY, A., LARROCHE, C. & SOCCOL, C. R. (eds.) Current Developments in Biotechnology and Bioengineering*. Elsevier.
- BLÜMICH, B. 2005. *Essential NMR*, Springer.
- BOROS, B., JAKABOVÁ, S., DÖRNYEI, Á., HORVÁTH, G., PLUHÁR, Z., KILÁR, F. & FELINGER, A. 2010. Determination of polyphenolic compounds by liquid chromatography–mass spectrometry in *Thymus* species. *Journal of Chromatography A*, 1217, 7972-7980.
- BRANDSLET, S. 2019. *Seaweed and kelp are more than food* [Online]. Norwegian SciTech News. Available: <https://norwegianscitechnews.com/2019/08/seaweed-and-kelp-are-more-than-food/> [Accessed July 15 2021].
- BRITTON, G., LIAAEN-JENSEN, S. & PFANDER, H. 2008. Special Molecules, Special Properties. *In: G. BRITTON, S. LIAAEN-JENSEN & PFANDER, H. (eds.) Carotenoids* Basel, Switzerland: Birkhäuser Verlag.
- BRUKER 2018. Basic NMR Experiments User Manual. TopSpin.
- CHEDEA, V. S. & POP, R. M. 2019. Total Polyphenol Content and Antioxidant DPPH Analysis on Biological Samples. *In: WATSON, R. R. (ed.) Polyphenols in Plants Isolation, Purification and Extract Preparation*. 2nd ed.: Academic Press.
- CHEMISTRY LIBRETEXT. 2020. *Nuclear Magnetic Resonance (NMR) of Alkenes* [Online]. Available: <https://chem.libretexts.org/@go/page/873> [Accessed].
- CHRISTENSEN, B. E. 2015. *Biopolymers*, Trondheim, NTNU.
- CLARIDGE, T. D. W. 2016a. Chapter 2 - Introducing High-Resolution NMR. *In: CLARIDGE, T. D. W. (ed.) High-Resolution NMR Techniques in Organic Chemistry (Third Edition)*. Boston: Elsevier.
- CLARIDGE, T. D. W. 2016b. Chapter 3 - Practical Aspects of High-Resolution NMR. *In: CLARIDGE, T. D. W. (ed.) High-Resolution NMR Techniques in Organic Chemistry (Third Edition)*. Boston: Elsevier.
- CLARIDGE, T. D. W. 2016c. Chapter 5 - Introducing Two-Dimensional and Pulsed Field Gradient NMR. *In: CLARIDGE, T. D. W. (ed.) High-Resolution NMR Techniques in Organic Chemistry (Third Edition)*. Boston: Elsevier.
- CLARIDGE, T. D. W. 2016d. Chapter 10 - Diffusion NMR Spectroscopy. *In: CLARIDGE, T. D. W. (ed.) High-Resolution NMR Techniques in Organic Chemistry (Third Edition)*. Boston: Elsevier.
- CONNAN, S., GOULARD, F., STIGER, V., DESLANDES, E. & AR GALL, E. 2004. Interspecific and temporal variation in phlorotannin levels in an assemblage of brown algae. 47, 410-416.

- COTAS, J., LEANDRO, A., MONTEIRO, P., PACHECO, D., FIGUEIRINHA, A., GONÇALVES, A. M. M., DA SILVA, G. J. & PEREIRA, L. 2020. Seaweed Phenolics: From Extraction to Applications. *Marine Drugs*, 18.
- COULTATE, T. 2016. *Food The Chemistry of its Components*, The Royal Society of Chemistry.
- DAWES, C. 2016. Chapter 4 - Macroalgae Systematics. In: FLEURENCE, J. & LEVINE, I. (eds.) *Seaweed in Health and Disease Prevention*. San Diego: Academic Press.
- DE ROSSO, V. V. & MERCADANTE, A. Z. 2007. Identification and quantification of carotenoids, by HPLC-PDA-MS/MS, from Amazonian fruits. *J Agric Food Chem*, 55, 5062-72.
- DOMÍNGUEZ, H. 2013. 1 - Algae as a source of biologically active ingredients for the formulation of functional foods and nutraceuticals. In: DOMÍNGUEZ, H. (ed.) *Functional Ingredients from Algae for Foods and Nutraceuticals*. Woodhead Publishing.
- DRAGET, K. I., SMIDSRØD, O. & SKJÅK-BRÆK, G. 2005. Alginates from Algae. *Biopolymers Online*.
- ENGLERT, G. 1985. NMR of carotenoids - new experimental techniques. *Pure and Applied Chemistry*, 57, 801-821.
- ENGLERT, G., BJØRNLAND, T. & LIAAEN-JENSEN, S. 1990. 1D and 2D NMR study of some allenic carotenoids of the fucoxanthin series. *Magnetic Resonance in Chemistry*, 28, 519-528.
- FLEURENCE, J. 2004. 9 - Seaweed proteins. In: YADA, R. Y. (ed.) *Proteins in Food Processing*. Woodhead Publishing.
- FORD, L., THEODORIDOU, K., SHELDRAKE, G. N. & WALSH, P. J. 2019. A critical review of analytical methods used for the chemical characterisation and quantification of phlorotannin compounds in brown seaweeds. *Phytochemical Analysis*, 30, 587-599.
- FREILE-PELEGRIN, Y. & ROBLEDO, D. 2014. Bioactive phenolic compounds from algae. *Bioactive Compounds from Marine Foods: Plant and Animal Sources*, 113-129.
- GLOMBITZA, K. W. & ZIEPRATH, G. 1989. Phlorotannins from the Brown Alga *Analipus japonicus* 1. *Planta Med*, 55, 171-5.
- GÜNTHER, H. 2013. *NMR spectroscopy. Basic principles, Concepts, and Application in Chemistry*. , Wiley VCH.
- HAUGAN, J. A. & LIAAEN-JENSEN, S. 1994a. Isolation and characterisation of four allenic (6'S)-isomers of fucoxanthin. *Tetrahedron Letters*, 35, 2245-2248.
- HAUGAN, J. A. & LIAAEN-JENSEN, S. V. 1994b. Algal carotenoids 54. Carotenoids of brown algae (Phaeophyceae). *Biochemical Systematics and Ecology*, 22, 31-41.
- HEO, S.-J., KO, S.-C., KANG, S.-M., KANG, H.-S., KIM, J.-P., KIM, S.-H., LEE, K.-W., CHO, M.-G. & JEON, Y.-J. 2008. Cytoprotective effect of fucoxanthin isolated from brown algae *Sargassum siliquastrum* against H<sub>2</sub>O<sub>2</sub>-induced cell damage. *European Food Research and Technology*, 228, 145-151.
- HERBERT, C. G. & JOHNSTONE, R. A. W. 2003. *MASS SPECTROMETRY BASICS*, CRC Press.
- HOLDT, S. L. & KRAAN, S. 2011. Bioactive compounds in seaweed: functional food applications and legislation. *Journal of Applied Phycology*, 23, 543-597.
- HOSOKAWA, M., KUDO, M., MAEDA, H., KOHNO, H., TANAKA, T. & MIYASHITA, K. 2004. Fucoxanthin induces apoptosis and enhances the antiproliferative effect of the PPAR $\gamma$  ligand, troglitazone, on colon cancer cells. *Biochimica et Biophysica Acta (BBA) - General Subjects*, 1675, 113-119.
- HUMAN METABOLOME DATABASE. s.a.-a. *1H NMR Spectrum (HMDB0000765)* [Online]. Available: [https://hmdb.ca/spectra/nmr\\_one\\_d/1531](https://hmdb.ca/spectra/nmr_one_d/1531) [Accessed June 30 2021].
- HUMAN METABOLOME DATABASE. s.a.-b. *HMDB* [Online]. Available: <https://hmdb.ca/> [Accessed June 10 2021].
- IMBS, T. I., ERMAKOVA, S. P., FEDOREYEV, S. A., ANASTYUK, S. D. & ZVYAGINTSEVA, T. N. 2013. Isolation of Fucoxanthin and Highly Unsaturated Monogalactosyldiacylglycerol from Brown Alga *Fucus evanescens* C Agardh and In

- Vitro Investigation of Their Antitumor Activity. *Marine Biotechnology*, 15, 606-612.
- IMBS, T. I. & ZVYAGINTSEVA, T. N. 2018. Phlorotannins are Polyphenolic Metabolites of Brown Algae. *Russian Journal of Marine Biology*, 44, 263-273.
- JACOBSEN, N. E. 2007. *NMR Spectroscopy Explained: Simplified Theory, Applications and Examples for Organic Chemistry and Structural Biology* John Wiley & Sons, Inc. .
- KALARIYA, N. M., RAMANA, K. V., SRIVASTAVA, S. K. & VAN KUIJK, F. J. G. M. 2008. Carotenoid derived aldehydes-induced oxidative stress causes apoptotic cell death in human retinal pigment epithelial cells. *Experimental eye research*, 86, 70-80.
- KEUSGEN, M. & GLOMBITZA, K.-W. 1995. Phlorethols, fuhalols and their derivatives from the brown alga *Sargassum spinuligerum*. *Phytochemistry*, 38, 975-985.
- KIM, D.-O. & LEE, C. Y. 2002. Extraction and Isolation of Polyphenolics. *Current Protocols in Food Analytical Chemistry*, 6, 11.2.1-11.2.12.
- KIM, K.-N., HEO, S.-J., YOON, W.-J., KANG, S.-M., AHN, G., YI, T.-H. & JEON, Y.-J. 2010. Fucoxanthin inhibits the inflammatory response by suppressing the activation of NF- $\kappa$ B and MAPKs in lipopolysaccharide-induced RAW 264.7 macrophages. *European Journal of Pharmacology*, 649, 369-375.
- KIM, T.-K., YONG, H. I., KIM, Y.-B., JUNG, S., KIM, H.-W. & CHOI, Y.-S. 2021. Effects of organic solvent on functional properties of defatted proteins extracted from *Protaetia brevitarsis* larvae. *Food Chemistry*, 336, 127679.
- KOIVIKKO, R., LOPONEN, J., HONKANEN, T. & JORMALAINEN, V. 2005. Contents of soluble, cell-wall-bound and exuded phlorotannins in the brown alga *Fucus vesiculosus*, with implications on their ecological functions. *Journal of chemical ecology*, 31, 195-212.
- LI, J. & CHASE, H. A. 2010. Development of adsorptive (non-ionic) macroporous resins and their uses in the purification of pharmacologically-active natural products from plant sources. *Natural Product Reports*, 27, 1493-1510.
- LI, Y.-X., WIJESEKARA, I., LI, Y. & KIM, S.-K. 2011. Phlorotannins as bioactive agents from brown algae. *Process Biochemistry*, 46, 2219-2224.
- LU, W., MAIDANNYK, V. A. & LIM, A. S. L. 2020. 7 - Carotenoids degradation and precautions during processing. In: GALANAKIS, C. M. (ed.) *Carotenoids: Properties, Processing and Applications*. Academic Press.
- MA, J., YANG, H., BASILE, M. J. & KENNELLY, E. J. 2004. Analysis of polyphenolic antioxidants from the fruits of three pouteria species by selected ion monitoring liquid chromatography-mass spectrometry. *J Agric Food Chem*, 52, 5873-8.
- MAEDA, H., HOSOKAWA, M., SASHIMA, T., FUNAYAMA, K. & MIYASHITA, K. 2005. Fucoxanthin from edible seaweed, *Undaria pinnatifida*, shows antiobesity effect through UCP1 expression in white adipose tissues. *Biochemical and Biophysical Research Communications*, 332, 392-397.
- MAKKAR, H. P. S., TRAN, G., HEUZÉ, V., GIGER-REVERDIN, S., LESSIRE, M., LEBAS, F. & ANKERS, P. 2016. Seaweeds for livestock diets: A review. *Animal Feed Science and Technology*, 212, 1-17.
- MARIUTTI, L. & MERCADANTE, A. 2018. Carotenoid esters analysis and occurrence: What do we know so far? *Archives of Biochemistry and Biophysics*, 648.
- MATSUMOTO, H., IKOMA, Y., KATO, M., KUNIGA, T., NAKAJIMA, N. & YOSHIDA, T. 2007. Quantification of Carotenoids in Citrus Fruit by LC-MS and Comparison of Patterns of Seasonal Changes for Carotenoids among Citrus Varieties. *Journal of Agricultural and Food Chemistry*, 55, 2356-2368.
- MCHUGH, D. J. 2003. A guide to the seaweed industry. *FAO Fisheries Technical Paper*, 441.
- MELLON, F. A. 2003. MASS SPECTROMETRY | Principles and Instrumentation. In: CABALLERO, B. (ed.) *Encyclopedia of Food Sciences and Nutrition (Second Edition)*. Oxford: Academic Press.
- MERCK KGAA. s.a. *Cellulase, enzyme blend* [Online]. sigmaaldrich.com. Available: <https://www.sigmaaldrich.com/NO/en/product/sigma/sae0020?gclid=Cj0KCQjwraqHBhDsARIsAKuGZeEnXKxakxA->

- SwDGx\_AAuXW6EFF8GCSbV8qJEZjsgLt3YpimxcOs68waArRoEALw\_wcB [Accessed June 11 2021].
- MEZZOMO, N. & FERREIRA, S. R. S. 2016. Carotenoids Functionality, Sources, and Processing by Supercritical Technology: A Review. *Journal of Chemistry*, 2016, 3164312.
- MISURCOVA, L. 2011. Chemical Composition of Seaweeds.
- MOLDOVEANU, S. C. 2021. 4 - Analytical pyrolysis of polymeric carbohydrates. In: MOLDOVEANU, S. C. (ed.) *Analytical Pyrolysis of Natural Organic Polymers (Second Edition)*. Elsevier.
- MORI, K., OOI, T., HIRAOKA, M., OKA, N., HAMADA, H., TAMURA, M. & KUSUMI, T. 2004. Fucoxanthin and Its Metabolites in Edible Brown Algae Cultivated in Deep Seawater. *Marine Drugs*, 2, 63-72.
- MORTENSEN, A. & SKIBSTED, L. H. 2000. Kinetics and Mechanism of the Primary Steps of Degradation of Carotenoids by Acid in Homogeneous Solution. *Journal of Agricultural and Food Chemistry*, 48, 279-286.
- MOSS, G. P. 1976. Carbon-13 NMR Spectra of Carotenoids. *Pure and Applied Chemistry*, 47, 97-102.
- MOTTAGHIPISHEH, J. & IRITI, M. 2020. Sephadex® LH-20, Isolation, and Purification of Flavonoids from Plant Species: A Comprehensive Review. *Molecules*, 25.
- MOURTZINOS, I. & GOULA, A. 2019. Polyphenols in Agricultural Byproducts and Food Waste. In: WATSON, R. R. (ed.) *Polyphenols in Plants Isolation, Purification and Extract Preparation*. 2nd ed.: Academic Press.
- MURRAY, K. K., BOYD, R. K., EBERLIN, M. N., LANGLEY, G. J., LI, L. & NAITO, Y. 2013. Definitions of terms relating to mass spectrometry (IUPAC Recommendations 2013). *Pure and Applied Chemistry*, 85, 1515-1609.
- NARAYAN, B., MIYASHITA, K. & HOSAKAWA, M. 2006. Physiological Effects of Eicosapentaenoic Acid (EPA) and Docosahexaenoic Acid (DHA)—A Review. *Food Reviews International*, 22, 291-307.
- NATURE PORTFOLIO. s.a. *Structure elucidation* [Online]. nature.com: Springer Nature. Available: <https://www.nature.com/subjects/structure-elucidation> [Accessed June 14 2021].
- NELSON, D. L. & COX, M. M. 2013. *Principles of Biochemistry*, United States of USA, Freeman, W. H. & Company.
- NIESSEN, W. M. A. & HONING, M. 2015. Mass Spectrometry Strategies in the Assignment of Molecular Structure: Breaking Chemical Bonds before Bringing the Pieces of the Puzzle Together. *Structure Elucidation in Organic Chemistry*, 105-144.
- OREOPOULOU, A., TSIMOGIANNIS, D. & OREOPOULOU, V. 2019. Extractions of Polyphenols From Aromatic and Medicinal Plants: An overview of the Methods and the Effect of Extraction Parameters. In: WATSON, R. R. (ed.) *Polyphenols in Plants Isolation, Purification and Extract Preparation*. 2nd ed.: Academic Press.
- ORGANIC CHEMISTRY DATA. 2005a. *NMR Spectroscopy* [Online]. Available: [https://organicchemistrydata.org/hansreich/resources/nmr/?index=nmr\\_index%2F13C\\_shift](https://organicchemistrydata.org/hansreich/resources/nmr/?index=nmr_index%2F13C_shift) [Accessed June 15 2021].
- ORGANIC CHEMISTRY DATA. 2005b. *NMR Spectroscopy* [Online]. Available: [https://organicchemistrydata.org/hansreich/resources/nmr/?index=nmr\\_index%2F1H\\_shift](https://organicchemistrydata.org/hansreich/resources/nmr/?index=nmr_index%2F1H_shift) [Accessed June 15 2021].
- PAULI, G. F., JAKI, B. U. & LANKIN, D. C. 2005. Quantitative 1H NMR: Development and Potential of a Method for Natural Products Analysis. *Journal of Natural Products*, 68, 133-149.
- PAVLUK, T. & BIJ DE VAATE, A. 2017. Trophic Index and Efficiency☆. In: FATH, B. (ed.) *Encyclopedia of Ecology (Second Edition)*. Oxford: Elsevier.
- PENG, J., YUAN, J.-P., WU, C.-F. & WANG, J.-H. 2011. Fucoxanthin, a marine carotenoid present in brown seaweeds and diatoms: metabolism and bioactivities relevant to human health. *Marine drugs*, 9, 1806-1828.
- PINELO, M., RUBILAR, M., JEREZ, M., SINEIRO, J. & NÚÑEZ, M. J. 2005. Effect of Solvent, Temperature, and Solvent-to-Solid Ratio on the Total Phenolic Content

- and Antiradical Activity of Extracts from Different Components of Grape Pomace. *Journal of Agricultural and Food Chemistry*, 53, 2111-2117.
- PODGORŠAK, E. B. 2016. Rutherford–Bohr Model of the Atom. *In: PODGORŠAK, E. B. (ed.) Radiation Physics for Medical Physicists*. Cham: Springer International Publishing.
- PRATT, C. W. & CORNLEY, K. 2014. *Essential Biochemistry*, WILEY.
- QUIDEAU, S., DEFFIEUX, D., DOUAT-CASASSUS, C. & POUYSÉGU, L. 2011. Plant Polyphenols: Chemical Properties, Biological Activities, and Synthesis. *Angewandte Chemie International Edition*, 50, 586-621.
- RODRIGEZ-AMAYA, D. B. & KIMURA, M. 2004. *HarvestPlus Handbook for Carotenoid Analysis*, Washington, DC & Cali: International Food Policy Research Institute (IFPRI) and International Center for Tropical Agriculture (CIAT), HarvestPlus.
- ROLEDA, M. Y., MARFAING, H., DESNICA, N., JÓNSDÓTTIR, R., SKJERMO, J., REBOURS, C. & NITSCHKE, U. 2019. Variations in polyphenol and heavy metal contents of wild-harvested and cultivated seaweed bulk biomass: Health risk assessment and implication for food applications. *Food Control*, 95, 121-134.
- RUENESS, J. 1998. *Alger i farger*, Oslo, Almater Forlag.
- SACHINDRA, N. M., SATO, E., MAEDA, H., HOSOKAWA, M., NIWANO, Y., KOHNO, M. & MIYASHITA, K. 2007. Radical Scavenging and Singlet Oxygen Quenching Activity of Marine Carotenoid Fucoxanthin and Its Metabolites. *Journal of Agricultural and Food Chemistry*, 55, 8516-8522.
- SANG, V. T., NGO, D.-H. & KIM, S.-K. 2012. Marine algae as a potential pharmaceutical source for anti-allergic therapeutics. *Process Biochemistry*, 47, 386–394.
- SANGEETHA, R. K., BHASKAR, N., DIVAKAR, S. & BASKARAN, V. 2009. Bioavailability and metabolism of fucoxanthin in rats: structural characterization of metabolites by LC-MS (APCI). *Molecular and Cellular Biochemistry*, 333, 299.
- SCHIENER, P., BLACK, K. D., STANLEY, M. S. & GREEN, D. H. 2015. The seasonal variation in the chemical composition of the kelp species *Laminaria digitata*, *Laminaria hyperborea*, *Saccharina latissima* and *Alaria esculenta*. *Journal of Applied Phycology*, 27, 363-373.
- SHANNON, E. & ABU-GHANNAM, N. 2017. Optimisation of fucoxanthin extraction from Irish seaweeds by response surface methodology. *Journal of Applied Phycology*, 29, 1027-1036.
- SHANNON, E. & ABU-GHANNAM, N. 2018. Enzymatic extraction of fucoxanthin from brown seaweeds. *International Journal of Food Science & Technology*, 53, 2195-2204.
- SILVA, E. M., POMPEU, D. R., LARONDELLE, Y. & ROGEZ, H. 2007. Optimisation of the adsorption of polyphenols from *Inga edulis* leaves on macroporous resins using an experimental design methodology. *Separation and Purification Technology*, 53, 274-280.
- SIMPSON, J. H. 2008. *Organic structure determination using 2-D NMR spectroscopy*, Canada, Academic Press.
- SINGH, I. P. & SIDANA, J. 2013. 5 - Phlorotannins. *In: DOMÍNGUEZ, H. (ed.) Functional Ingredients from Algae for Foods and Nutraceuticals*. Woodhead Publishing.
- SKJERMO, J., AASEN, I. M., ARFF, J., BROCH, O. J., CARVAJAL, A., CHRISTIE, H., FORBORD, S., OLSEN, Y., REITAN, K. I., RUSTAD, T., SANDQUIST, J., SOLBAKKEN, R., STEINHOVDEN, K. B., WITTGENS, B., WOLFF, R. & HANDÅ, A. 2014. A new Norwegian bioeconomy based on cultivation and processing of seaweeds: Opportunities and R&D needs. 2nd ed.: SINTEF.
- SKJÅK-BRÆK, G. 1988. *Biosynthesis and structure - function relationships in alginates*. Dr.tech, NTH/NTNU.
- SOTO, M. L., MOURE, A., DOMÍNGUEZ, H. & PARAJÓ, J. C. 2011. Recovery, concentration and purification of phenolic compounds by adsorption: A review. *Journal of Food Engineering*, 105, 1-27.
- STICHER, O. 2008. Natural product isolation. *Natural Product Reports*, 25, 517-554.

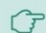
- SUGAWARA, T., BASKARAN, V., TSUZUKI, W. & NAGAO, A. 2002. Brown Algae Fucoxanthin Is Hydrolyzed to Fucoxanthinol during Absorption by Caco-2 Human Intestinal Cells and Mice. *The Journal of Nutrition*, 132, 946-951.
- SULTANA, B., ANWAR, F. & ASHRAF, M. 2009. Effect of Extraction Solvent/Technique on the Antioxidant Activity of Selected Medicinal Plant Extracts. *Molecules*, 14.
- TAN, S. P., O'SULLIVAN, L., LUZ PRIETO, M., MCLOUGHLIN, P., LAWLOR, P. G., HUGHES, H. & GARDINER, G. E. 2013. Seaweed Antimicrobials: Isolation, Characterization, and Potential Use in Functional Foods. *Bioactive Compounds from Marine Foods*, 269-312.
- THIEMAN, W. J. & PALLADINO, M. A. 2009. *Introduction to Biotechnology*, Pearson Education.
- TSIMOGIANNIS, D. & OREOPOULOU, V. 2019. Classification of Phenolic Compounds in Plants. In: WATSON, R. R. (ed.) *Polyphenols in Plants*. 2nd ed.: Academic Press.
- UIO. 2011. *Alger* [Online]. Universitet i Oslo. Available: <https://www.mn.uio.no/ibv/tjenester/kunnskap/plantefys/leksikon/a/alger.html> [Accessed July 15 2021].
- UNFCCC 1992. United Nations Framework Convention on Climate Change. United Nations.
- UNFCCC 1998. Kyoto Protocol to the United Nations Framework Convention on Climate Change. United Nations.
- UNITED NATIONS s.a. Transforming Our World: The 2030 Agenda For Sustainable Development. United Nations.
- VENKATESAN, J., KEEKAN, K. K., ANIL, S., BHATNAGAR, I. & KIM, S.-K. 2019. Phlorotannins. In: MELTON, L., SHAHIDI, F. & VARELIS, P. (eds.) *Encyclopedia of Food Chemistry*. Oxford: Academic Press.
- VO, T.-S., NGO, D.-H. & KIM, S.-K. 2012. Marine algae as a potential pharmaceutical source for anti-allergic therapeutics. *Process Biochemistry*, 47, 386-394.
- VRANKEN, W. F., BOUCHER, W., STEVENS, T. J., FOGH, R. H., PAJON, A., LLINAS, M., ULRICH, E. L., MARKLEY, J. L., IONIDES, J. & LAUE, E. D. 2005. The CCPN data model for NMR spectroscopy: Development of a software pipeline. *Proteins: Structure, Function, and Bioinformatics*, 59, 687-696.
- WIJESINGHE, W. A. J. P. & JEON, Y.-J. 2012. Enzyme-assistant extraction (EAE) of bioactive components: A useful approach for recovery of industrially important metabolites from seaweeds: A review. *Fitoterapia*, 83, 6-12.
- WU, S. 2011. *1D and 2D NMR Experiment Methods*, Atlanta, GA 30322, NMR Research Center, Emory University.
- ZHANG, Q.-W., LIN, L.-G. & YE, W.-C. 2018. Techniques for extraction and isolation of natural products: a comprehensive review. *Chinese Medicine*, 13, 20.




## Appendix A: Protocol for packing column with Sephadex LH-20

### Packing a column

#### General packing protocol

 The following packing protocol works well for packing most columns. Further guidelines can be found in the individual instructions for the resins and in the instructions for empty columns.

1. Sephadex LH-20 is supplied as a dry powder and must be swollen before use. The degree of swelling depends on the solvent used (see Table A7.2). Swell the resin for at least 3 h at room temperature in an excess of the solvent to be used for the separation. Avoid using magnetic stirrers, spatulas, or glass rods since they can damage the resin.
2. Prepare a slurry in a ratio 75% settled resin to 25% solvent. Decant any fine particles.
3. Prepare a suitable empty column for packing according to the column instructions. Make sure that the column tolerates the solvent used. Mount a bottom filter if this is not part of the end piece. Wet the bottom filter. If the slurry volume exceeds the column volume, attach a packing reservoir or packing tube.
4. Equilibrate all materials to room temperature.
5. Fill the column with the solvent to a height of approximately 2 cm.
6. Resuspend and pour the slurry down the inside of the column in one continuous step. Fill the column or column reservoir to the top with solvent. Avoid air bubbles.
7. Attach a top adapter to the column tube (or the cap on the packing reservoir). Connect to a pump, and open the column outlet. Pack at 300 cm/h until the bed has reached a constant height and stop the flow. Remove the packing reservoir or packing tube if used.
8. Fill the column with solvent and mount a wetted adapter onto the column as described in the column instructions. Also, mount a wetted filter if this is not part of the adapter. Ensure no air bubbles are trapped in the column and that no air bubbles are in the flow path.
9. Open the column outlet and continue packing until the packed bed is stable. A final adjustment of the top adapter might be necessary.

 In some solvents such as chloroform, Sephadex LH-20 is less dense than the solvent and the resin will float. In this case, a column with two adapters should be used. Pour the resin into the column and drain until the second adapter can be inserted. Lock the adapter in position at the surface of the resin and direct the flow of solvent upwards. The bed will be packed against the top adapter and the lower adapter can be pushed slowly upwards towards the lower surface of the resin. Close the column outlet when moving the adapter to avoid compressing the bed.

**Table A7.2.** Approximate values for packed bed volumes of Sephadex LH-20 swollen in different solvents

Solvent	Approx. bed volume (mL/g dry Sephadex LH-20)
Dimethyl sulfoxide	4.4 to 4.6
Pyridine	4.2 to 4.4
Water	4.0 to 4.4
Dimethylformamide	4.0 to 4.4
Methanol	3.9 to 4.3
Saline	3.8 to 4.2
Ethylene dichloride	3.8 to 4.1
Chloroform <sup>1</sup>	3.8 to 4.1
Propanol	3.7 to 4.0
Ethanol <sup>2</sup>	3.6 to 3.9
Isobutanol	3.6 to 3.9
Formamide	3.6 to 3.9
Methylene dichloride	3.6 to 3.9
Butanol	3.5 to 3.8
Isopropanol	3.3 to 3.6
Tetrahydrofuran	3.3 to 3.6
Dioxane	3.2 to 3.5
Acetone	2.4 to 2.6
Acetonitrile <sup>3</sup>	2.2 to 2.4
Carbon tetrachloride <sup>3</sup>	1.8 to 2.2
Benzene <sup>3</sup>	1.6 to 2.0
Ethyl acetate <sup>3</sup>	1.6 to 1.8
Toluene <sup>3</sup>	1.5 to 1.6

<sup>1</sup> Containing 1% ethanol.

<sup>2</sup> Containing 1% benzene.

<sup>3</sup> Bed volumes < 2.5 mL/g dry Sephadex LH-20 are generally not useful.

**Figure A-1: Protocol for packing of column with sephadex LH-20.**



## Appendix B: Small-scale experiments

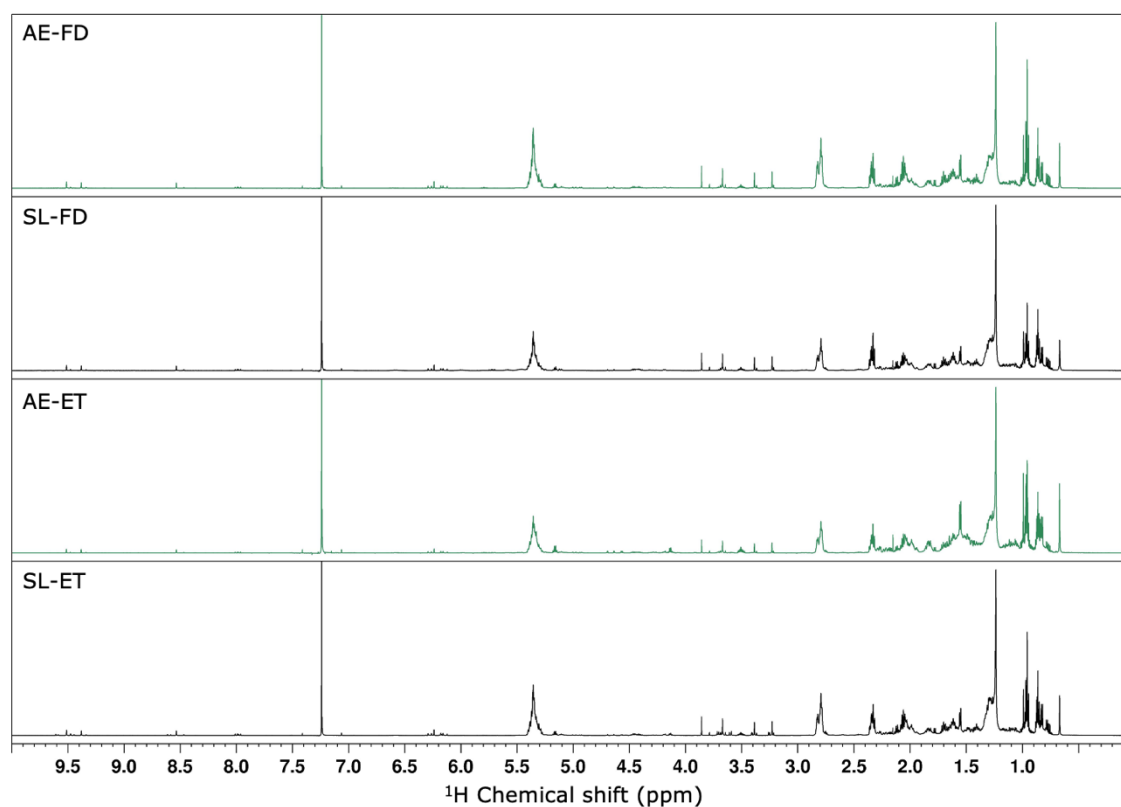


**Figure B-1:**  $^1\text{H}$  NMR spectra of hexane-phase. AE: *Alaria esculenta*, SL: *Saccharina latissima*, FD: freeze-dried, ET: enzyme treated.

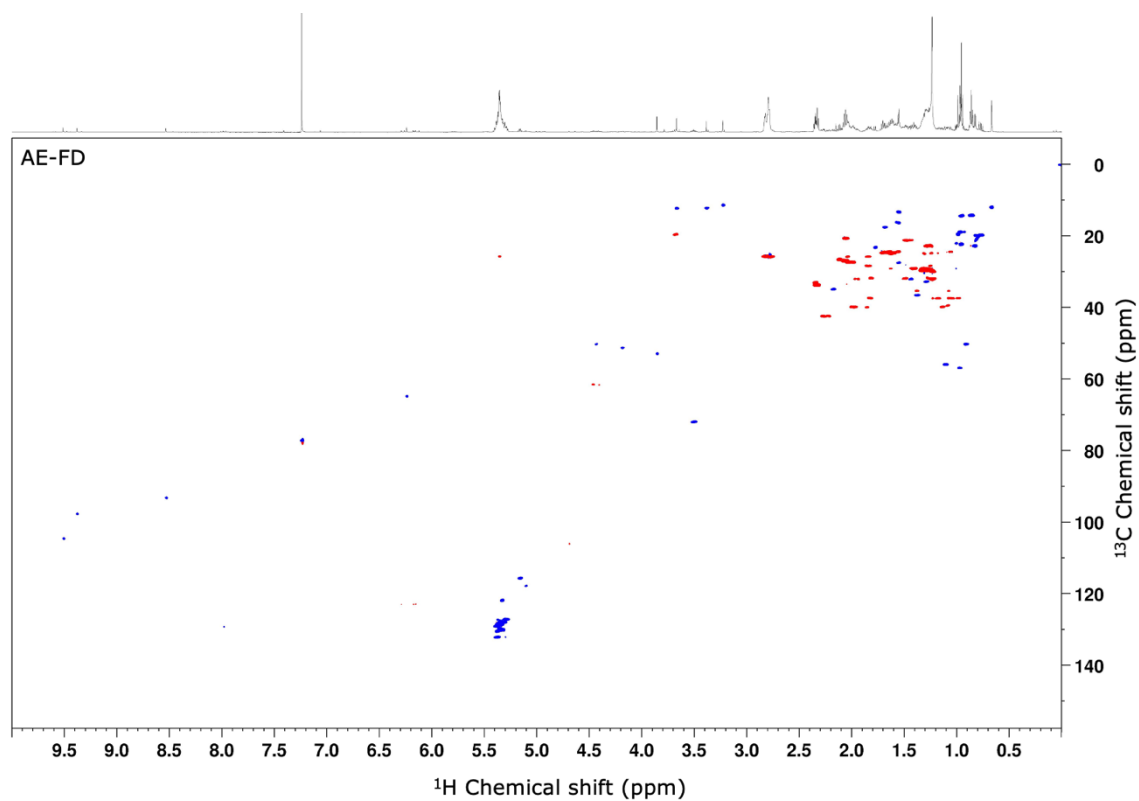


**Figure B-2:**  $^1\text{H}$ - $^{13}\text{C}$  HSQC spectrum of hexane phase from defatting *Alaria esculenta* freeze-dried. AE: *Alaria esculenta*, FD: freeze-dried.

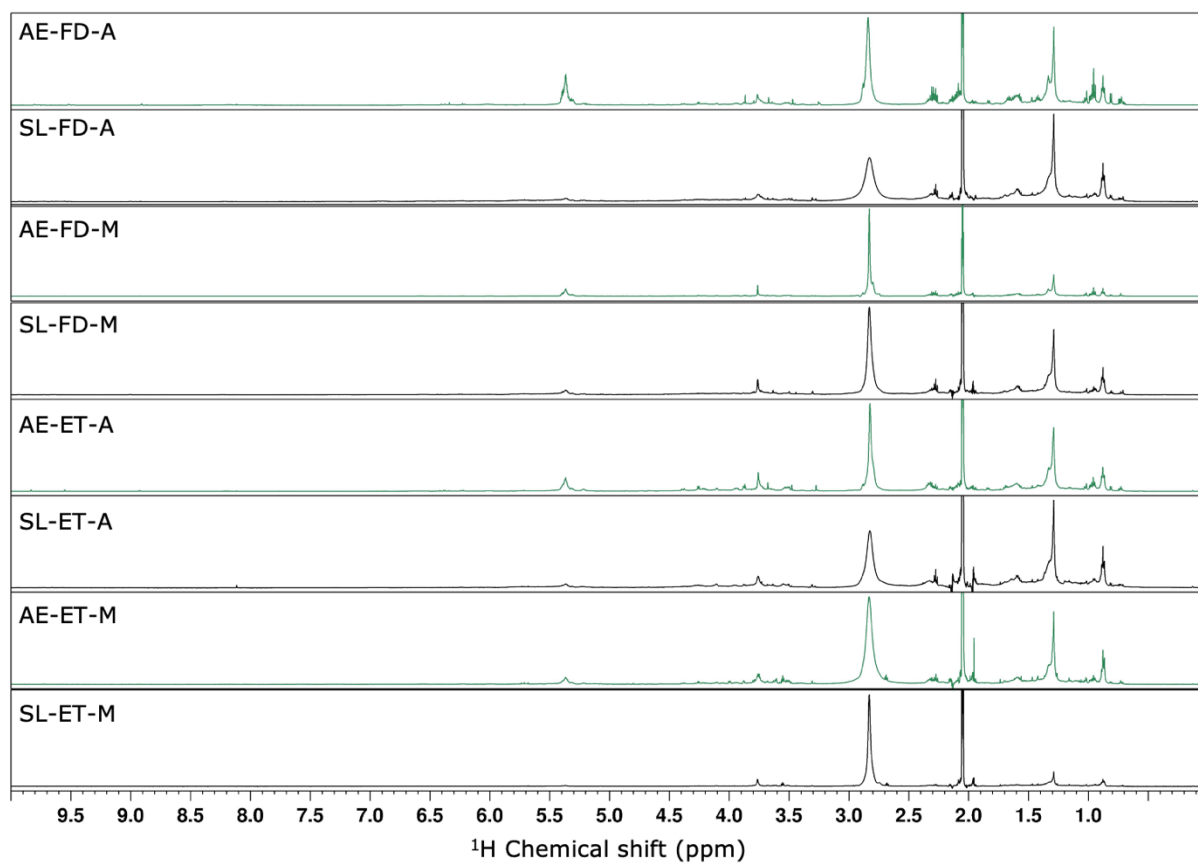


**Figure B-3: <sup>1</sup>H NMR spectra of acetone and methanol extractions.** AE: *Alaria esculenta*, SL: *Saccharina latissima*, FD: freeze-dried, ET: enzyme treated. A: acetone, M: methanol.

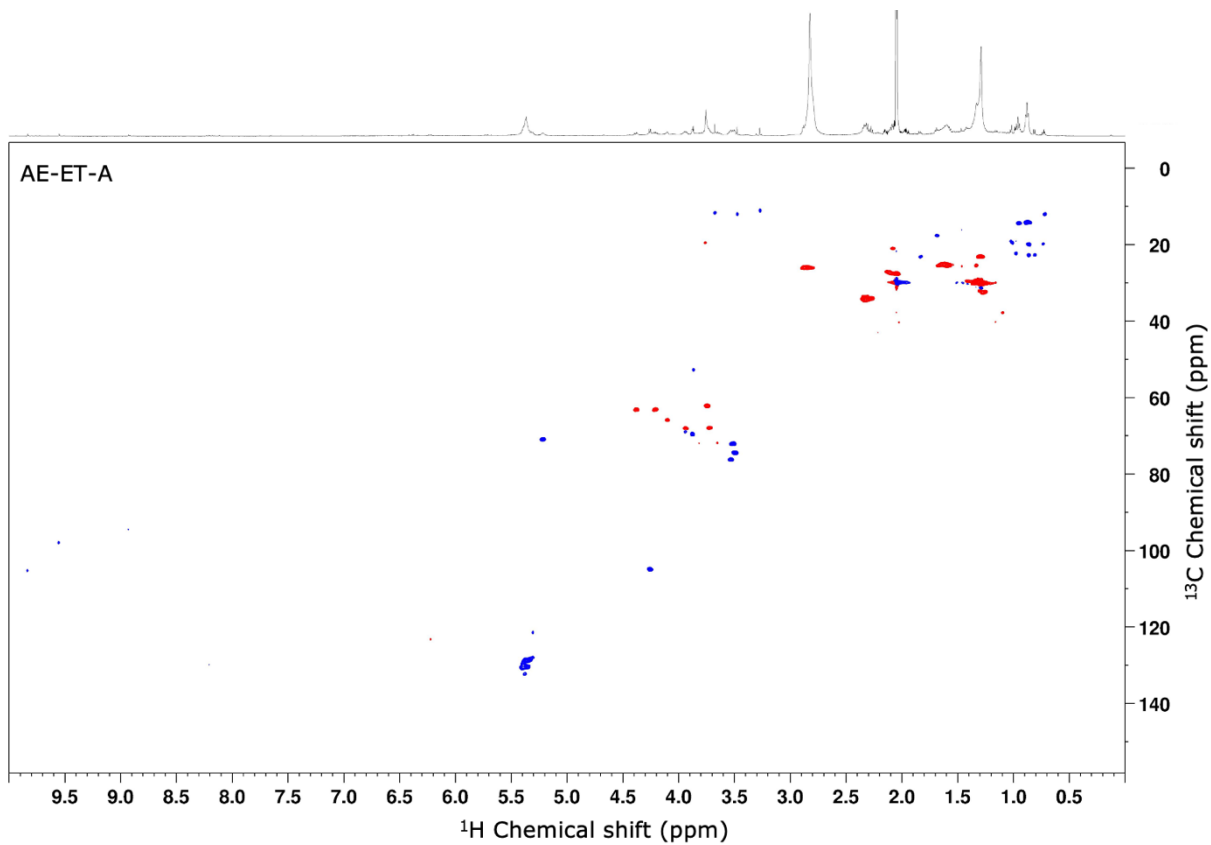


**Figure B-4:**  $^1\text{H}$ - $^{13}\text{C}$  HSQC spectrum of acetone extraction of *Alaria esculenta* enzyme treated. AE: *Alaria esculenta*, FD: freeze-dried, A: acetone.

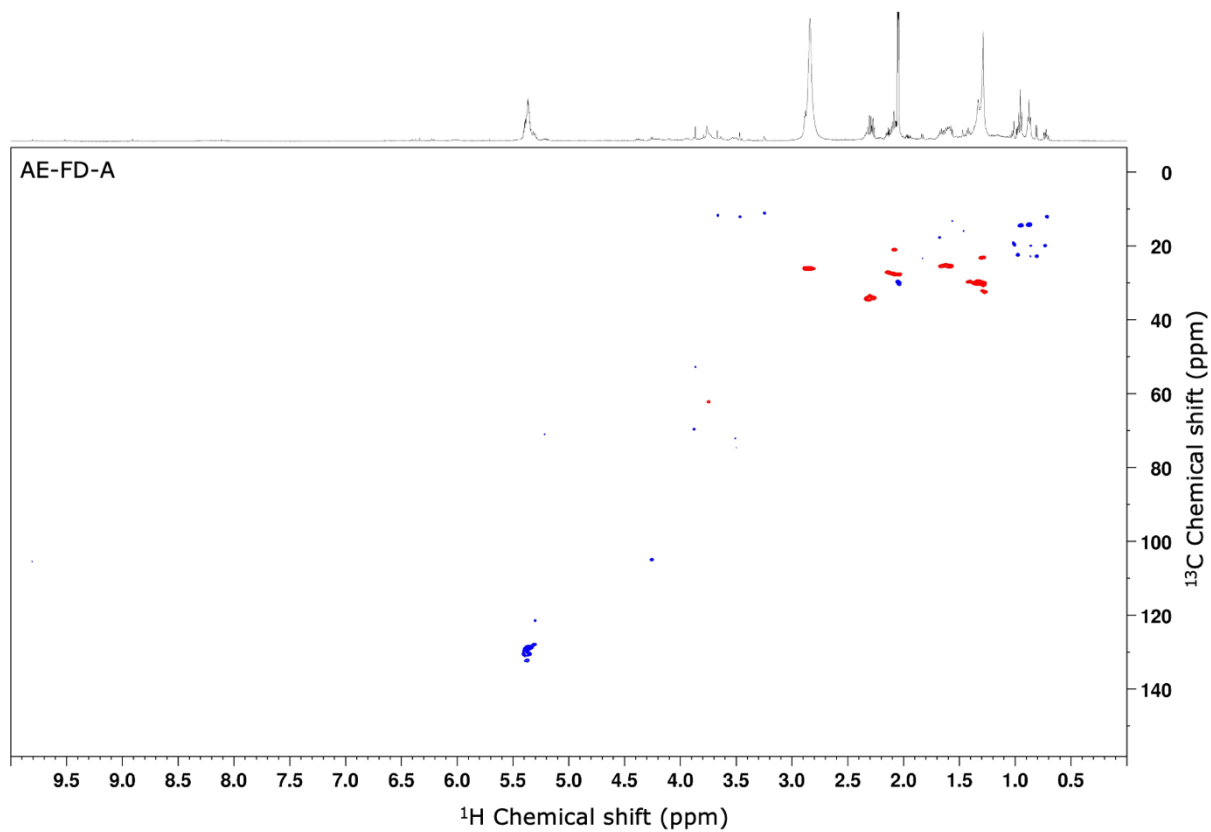


**Figure B-5:**  $^1\text{H}$ - $^{13}\text{C}$  HSQC spectrum of acetone extraction of *Alaria esculenta* freeze-dried. AE: *Alaria esculenta*, FD: freeze-dried. A: acetone.

## Appendix C: Extractions with acetone and methanol on wet material

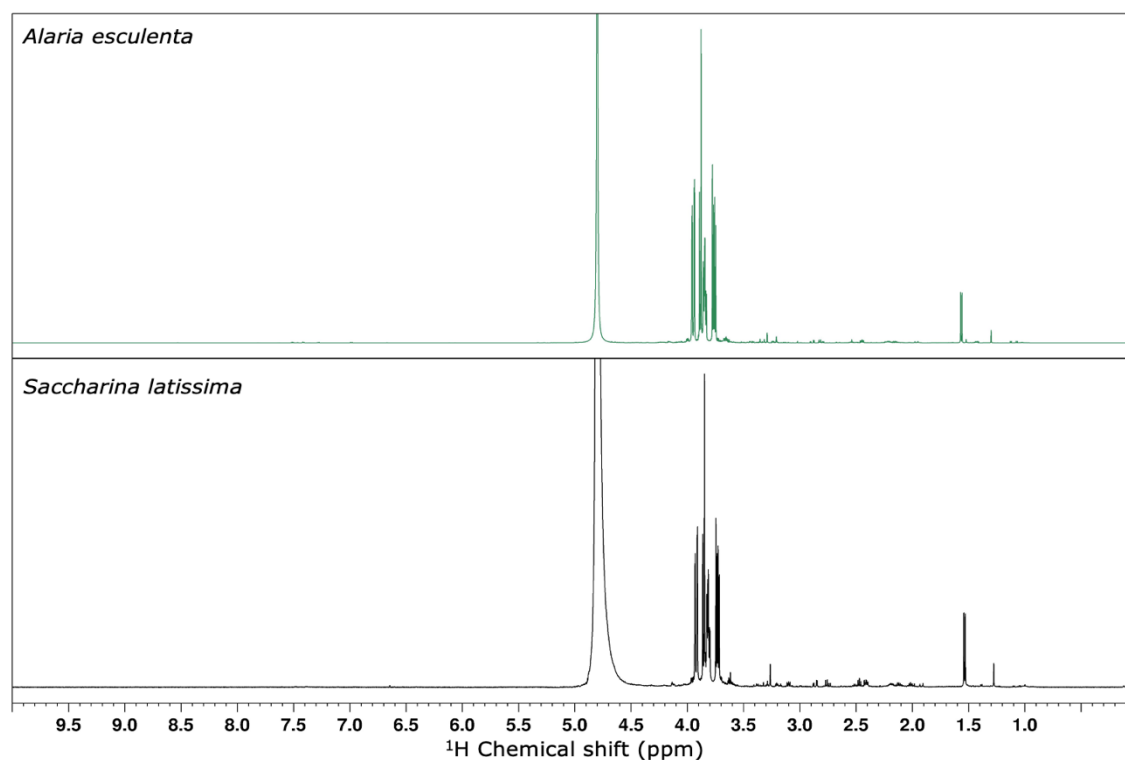


**Figure C-1:**  $^1\text{H}$  NMR spectra of aqueous fraction of defatted wet material of *Alaria esculenta* and *Saccharina latissima* extracted with acetone.

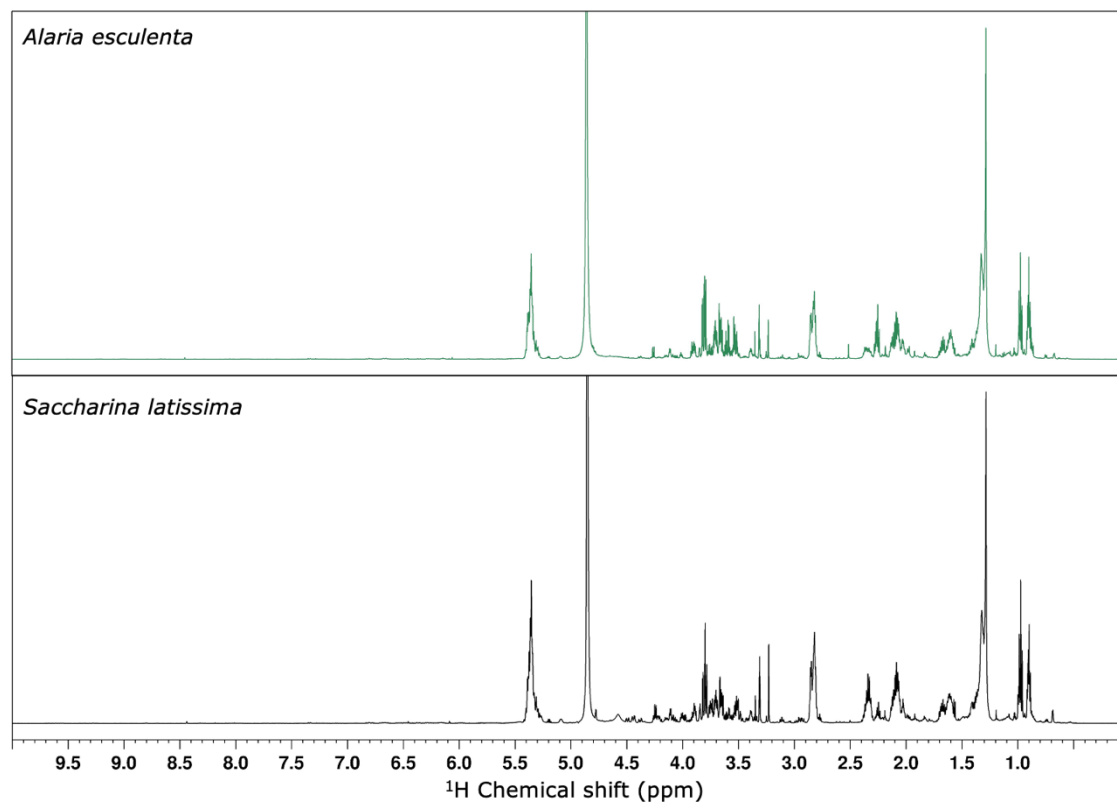


**Figure C-2:**  $^1\text{H}$  NMR spectra of aqueous fraction of defatted wet material of *Alaria esculenta* and *Saccharina latissima* extracted with methanol.

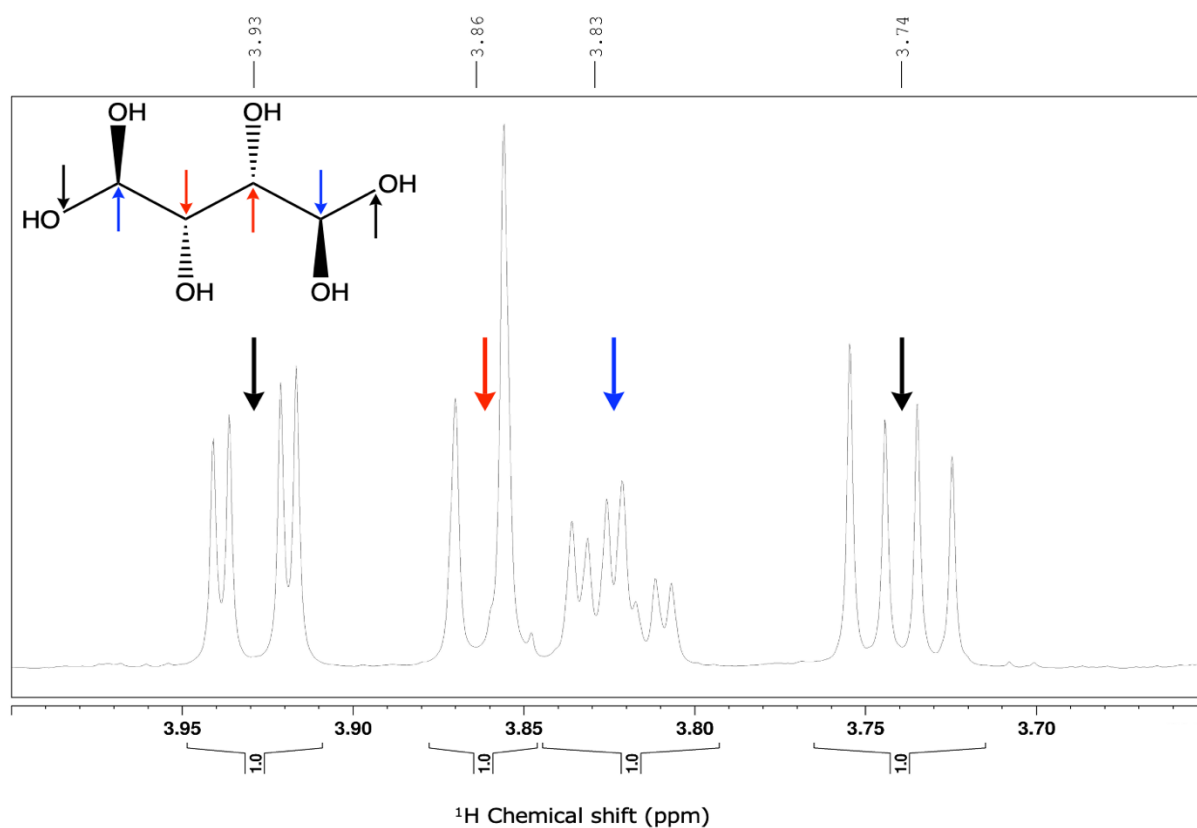


**Figure C-3:  $^1\text{H}$  NMR spectrum of mannitol in AE-W-Aq.** The structure of mannitol is given in the top left corner, and the arrows show the corresponding resonance of the protons.

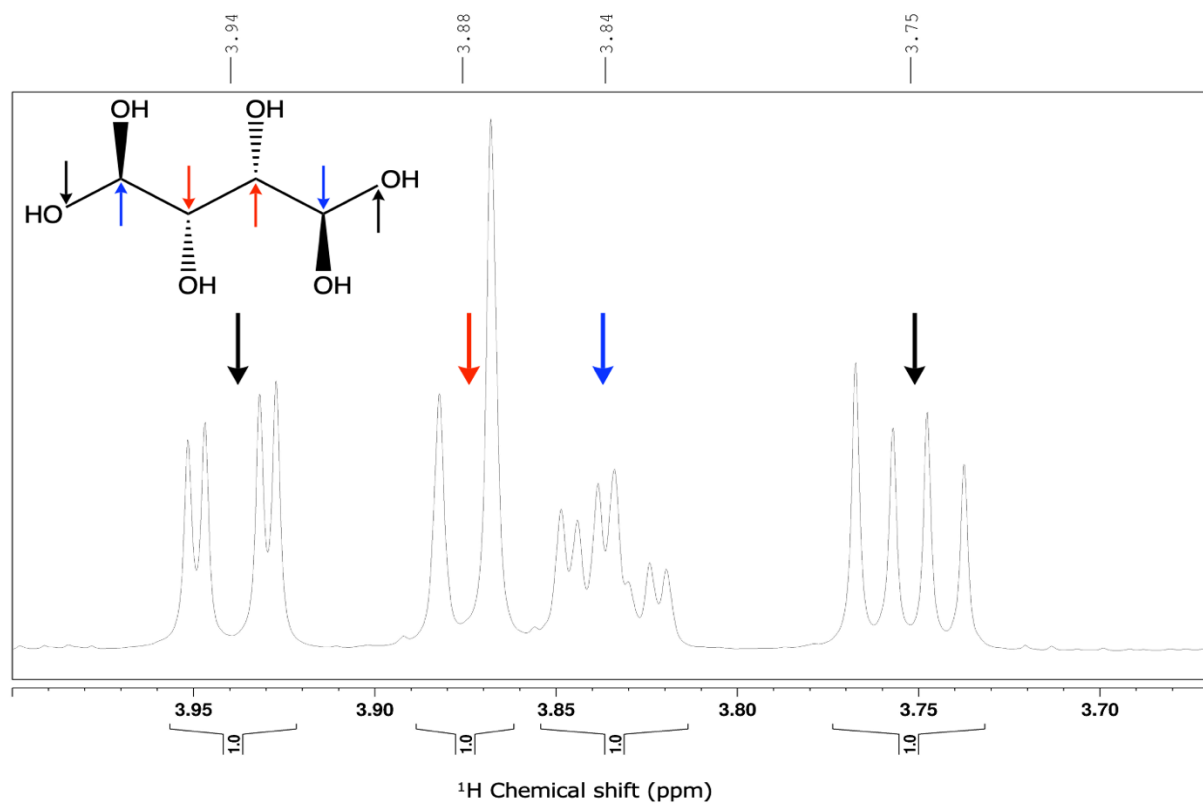


**Figure C-4:  $^1\text{H}$  NMR spectrum of mannitol in SL-W-Aq.** The structure of mannitol is given in the top left corner, and the arrows show the corresponding resonance of the protons.

## Appendix D: XAD-16 resin

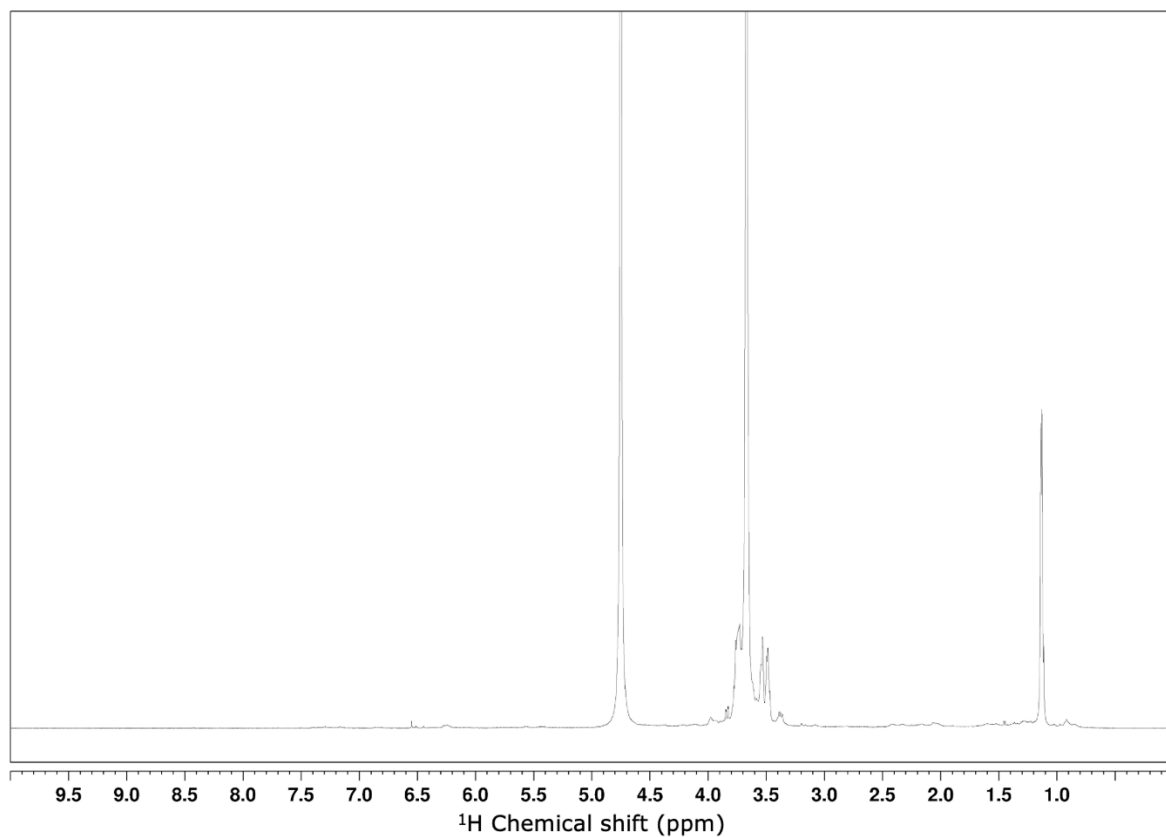


Figure D-1: <sup>1</sup>H NMR spectra of *Saccharina latissima* Ac40.

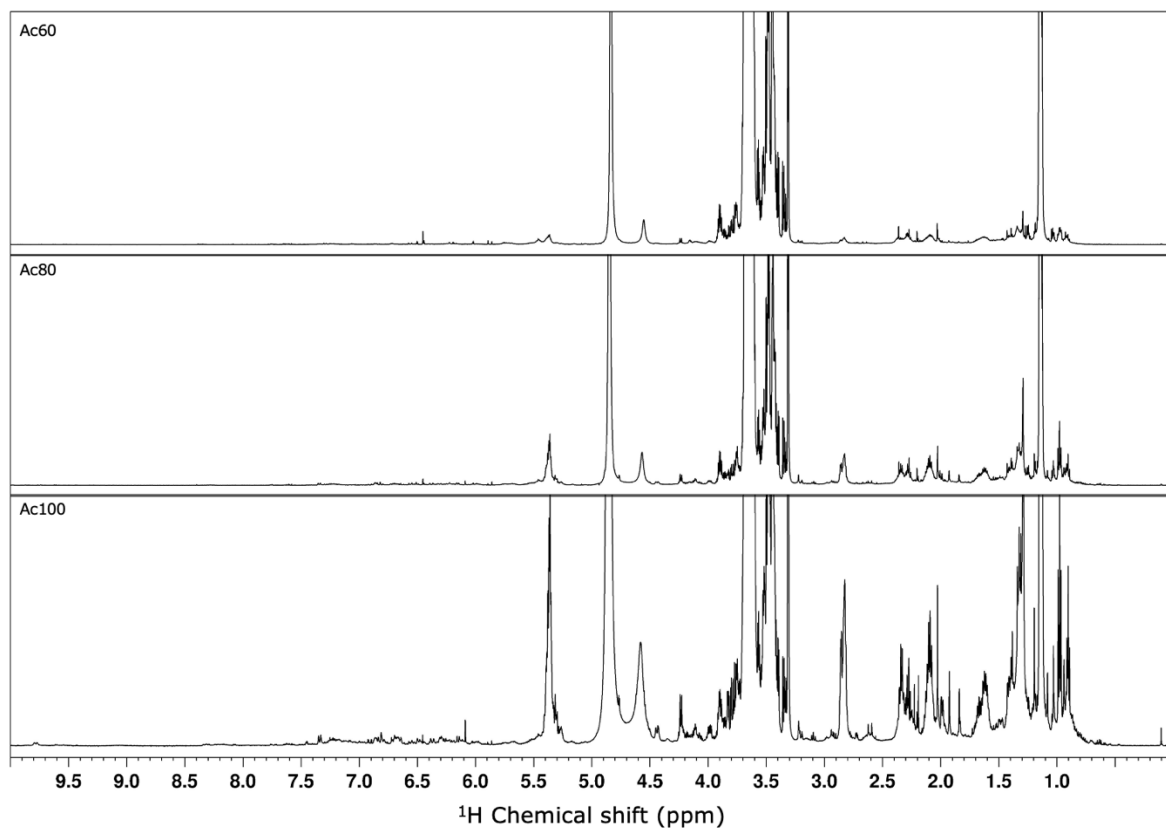
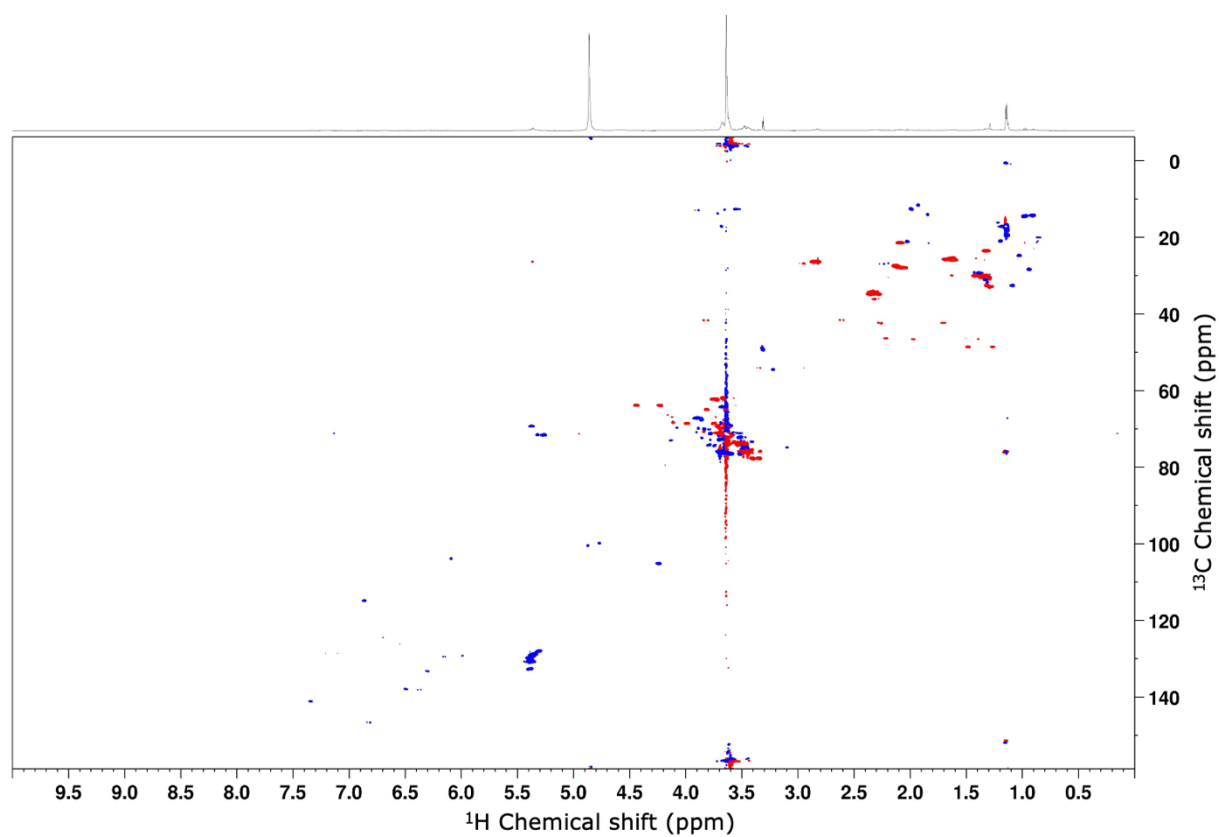


Figure D-2: <sup>1</sup>H NMR spectra of *Saccharina latissima* Ac60, Ac80, Ac100.



**Figure D-3:  $^1\text{H}$ - $^{13}\text{C}$  HSQC spectrum of *Saccharina latissima* Ac100.**

## Appendix E: Column chromatography

The column packed with Sephadex LH-20 resin was attached to a GE ÄKTA Start protein purification system (FPLC) with an UV-detector (280 nm) and chromatograms of the samples loaded onto the column were produced in UNICORN™ start 1.0 software from GE Healthcare Bio-Sciences AB. Below are the chromatograms produced for A) *Alaria esculenta* and B) *Saccharina latissima*. The red graph and the blue graph in each chromatogram, represent the conductivity signal and the UV-signal, respectively. The horizontal x-axis on the bottom shows the elution volume in ml, the vertical y-axis on the left shows the intensity of the UV-absorbance in milli-Absorbance unit (mAU), and the vertical x-axis on the right shows the intensity of the conductivity in milliSiemens per centimeter (mS/cm).

### A) *Alaria esculenta*.

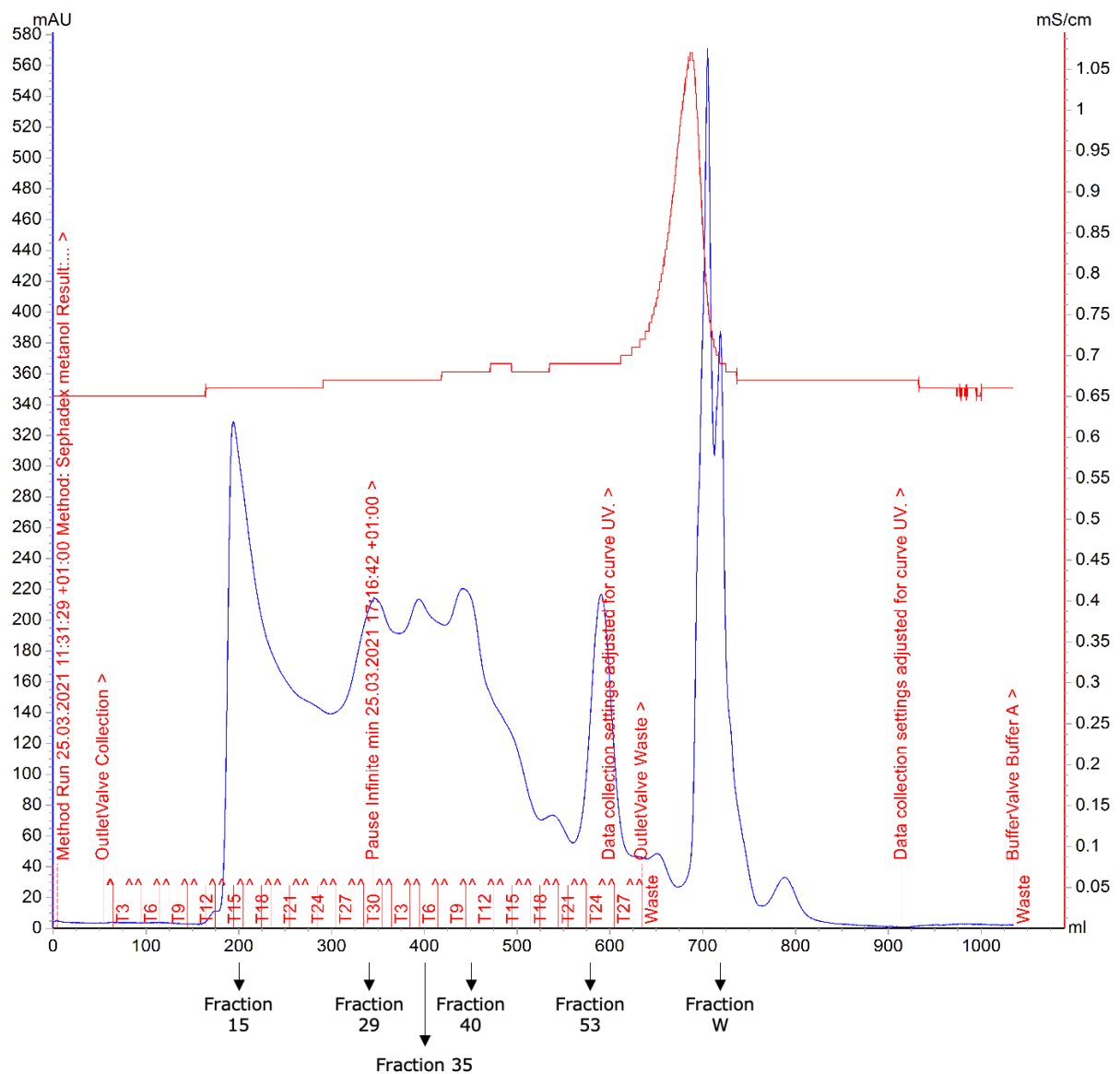
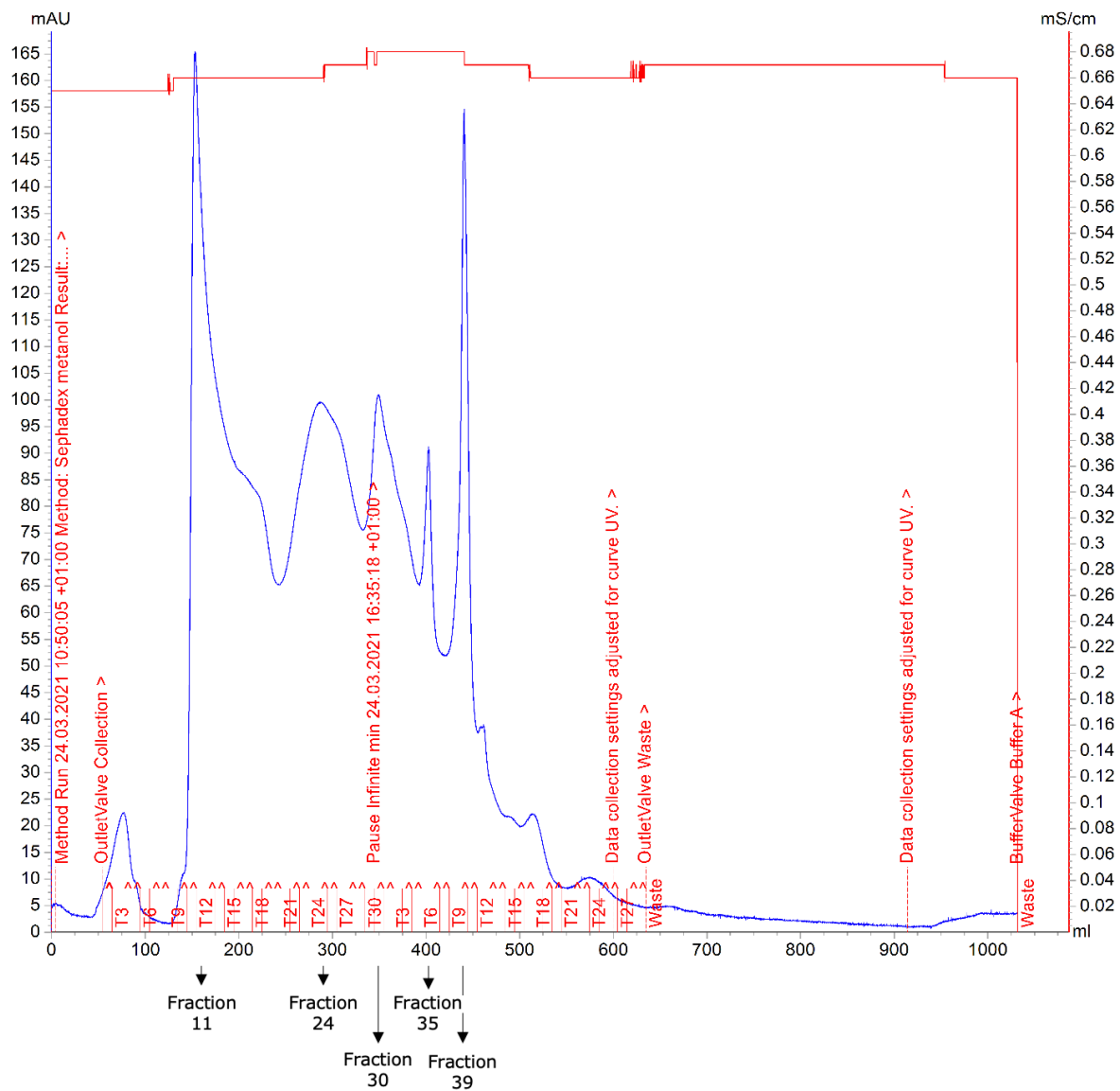


Figure E-1: Chromatogram from column of *Alaria esculenta* F2.



**Saccharina latissima**



**Figure E-2: Chromatogram from column with *Saccharina latissima* F2.**

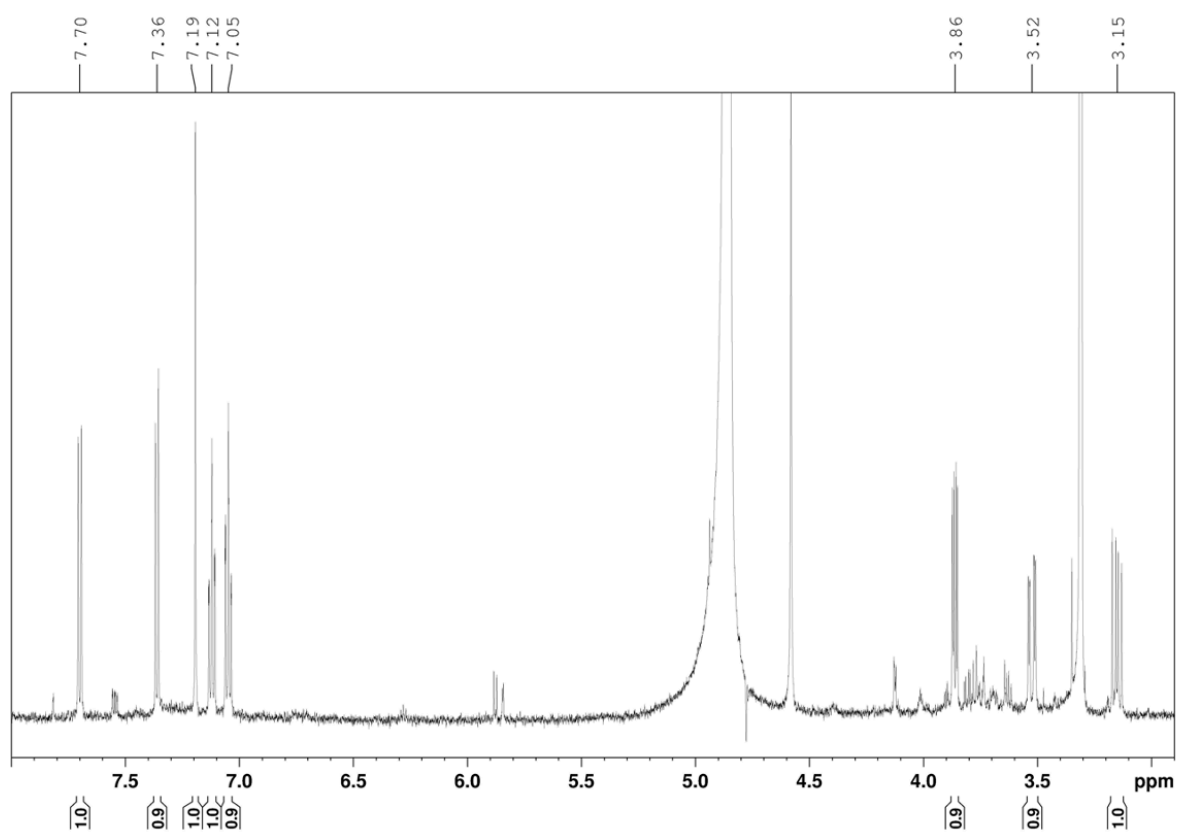


Figure E-3:  $^1\text{H}$  NMR spectrum of *Alaria esculenta* F53.

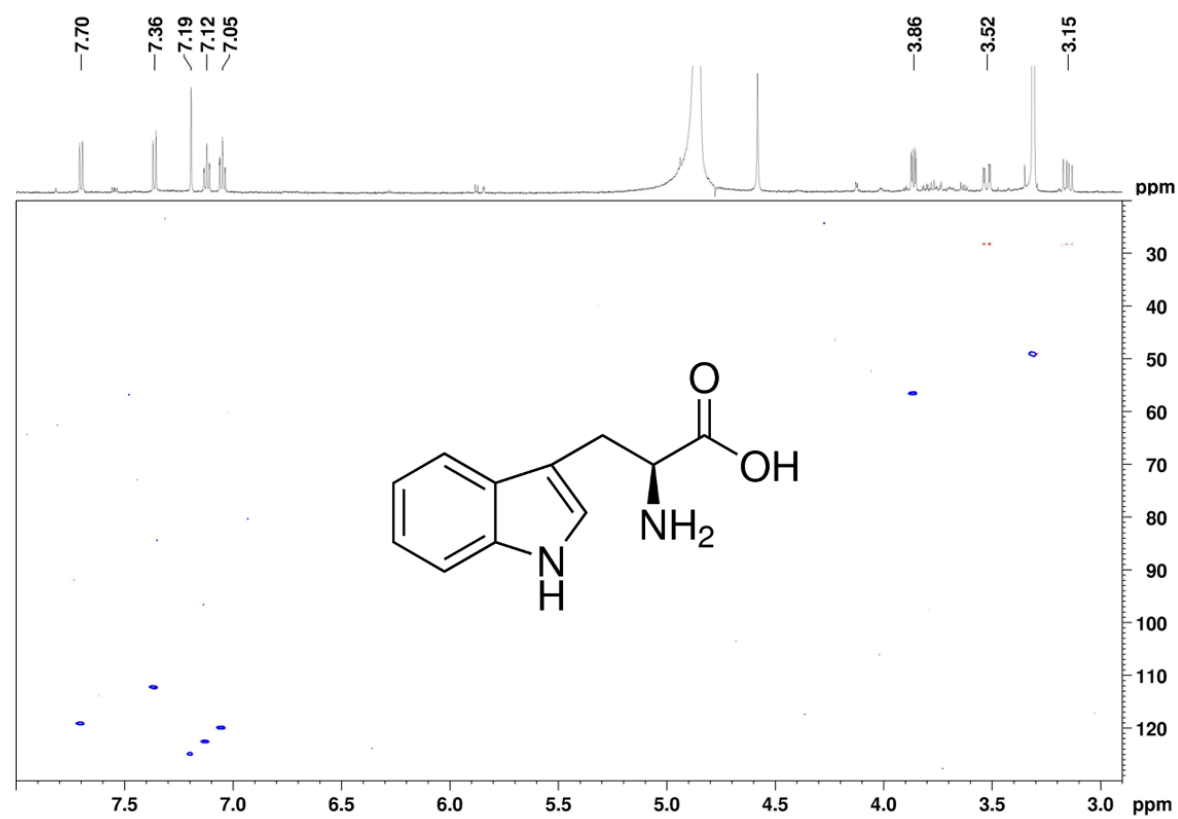


Figure E-4:  $^1\text{H}$ - $^{13}\text{C}$  HSQC spectrum of *Alaria esculenta* F53.

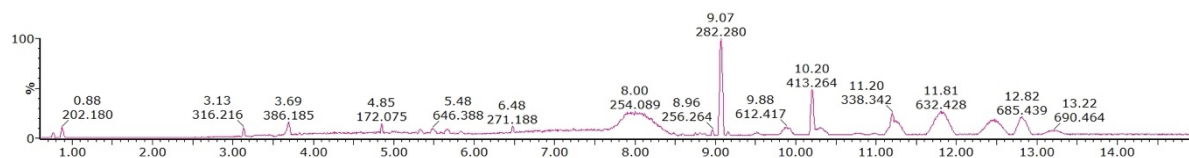


Figure E-5: Base peak chromatogram of *Alaria esculenta* F20.

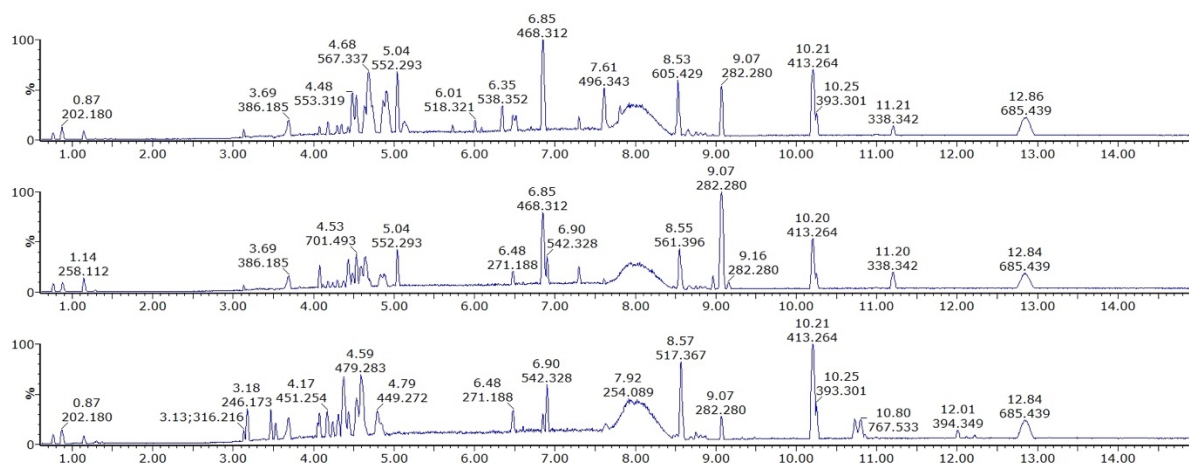


Figure E-6: Base peak chromatogram of *Alaria esculenta* F28 (top), F29, F30 (bottom).

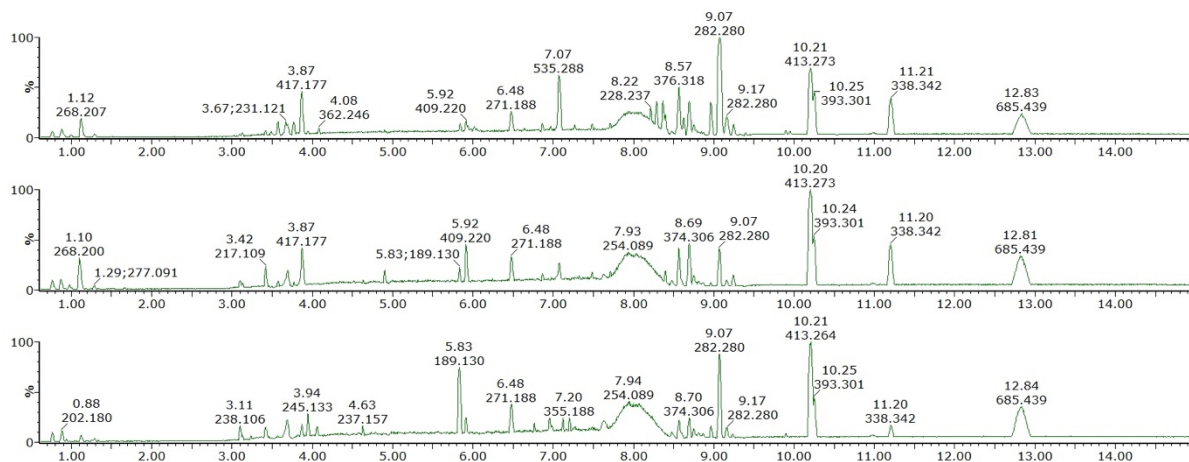


Figure E-7: Base peak chromatogram of *Alaria esculenta* F37 (top), F38, F39 (bottom).

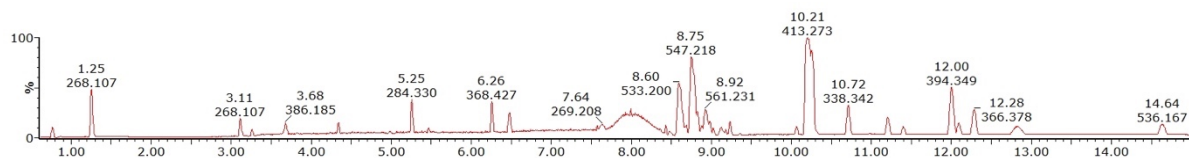
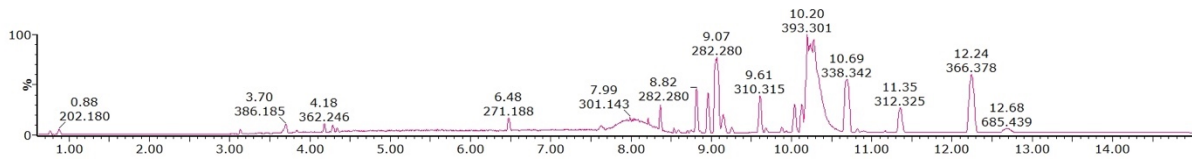
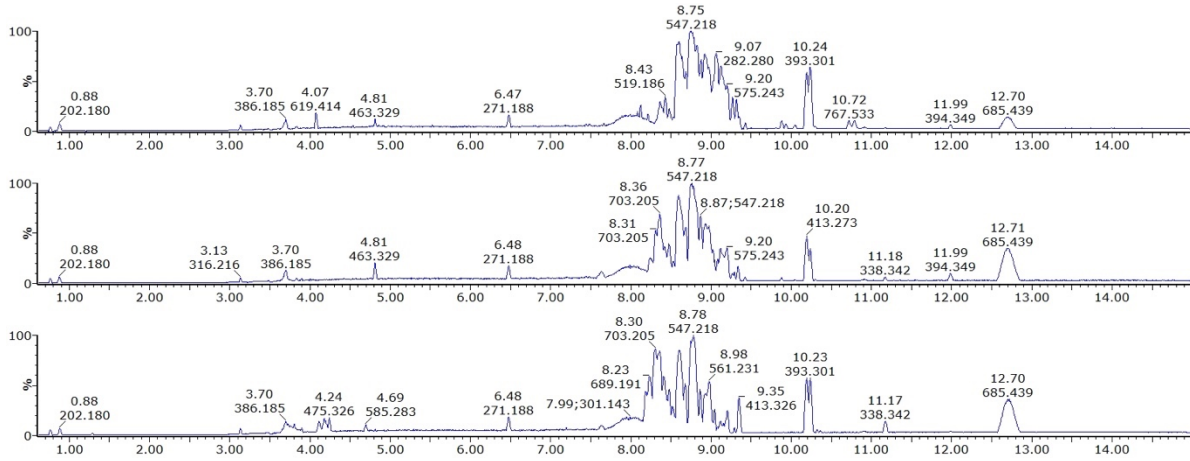


Figure E-8. Base peak chromatogram of *Alaria esculenta* W.



**Figure E-9: Base peak chromatogram of *Saccharina latissima* F16.**



**Figure E-10: Base peak chromatogram of *Saccharina latissima* F23 (top), F24, F25 (bottom).**

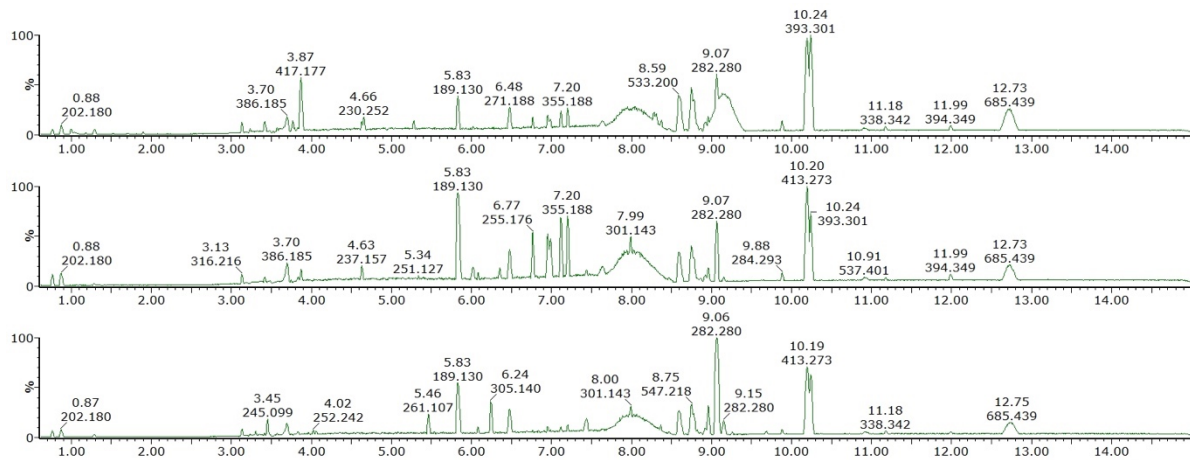


**Figure E-11: Base peak chromatogram of *Saccharina latissima* F29 (top), F30, F31 (bottom).**

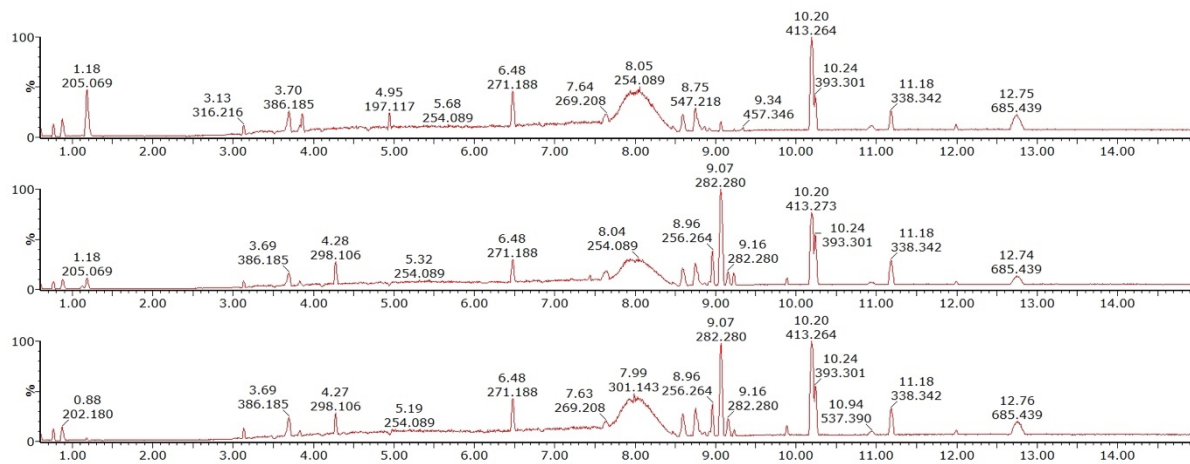


**Figure E-12: Base peak chromatogram of *Saccharina latissima* F35 (top), F36, F38 (bottom).**

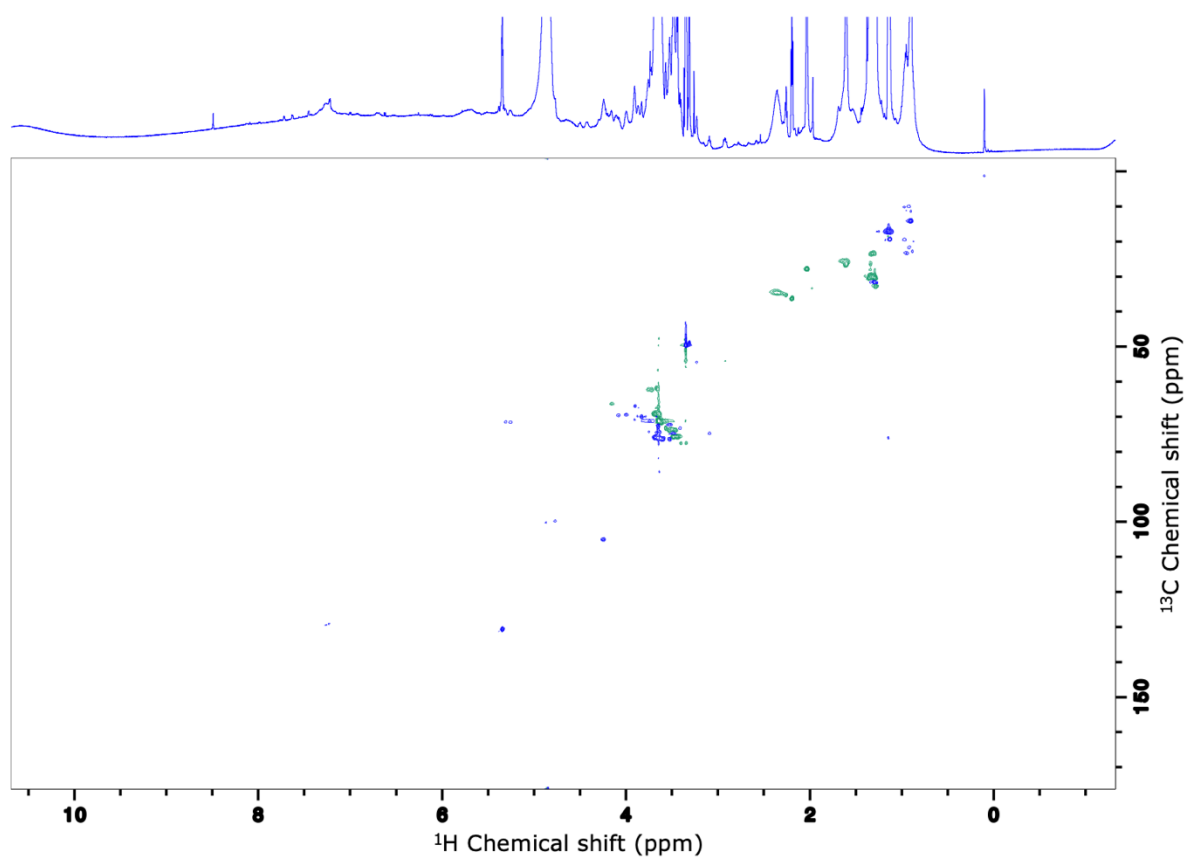


Figure E-13:  $^1\text{H}$ - $^{13}\text{C}$  HSQC of *Alaria esculenta* P1.

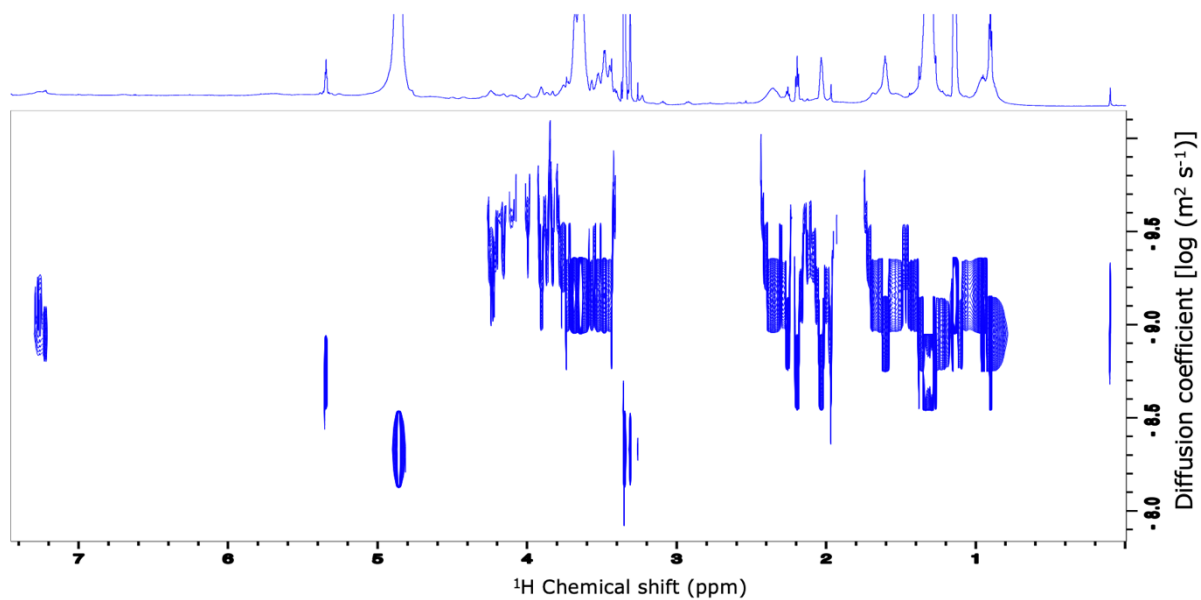
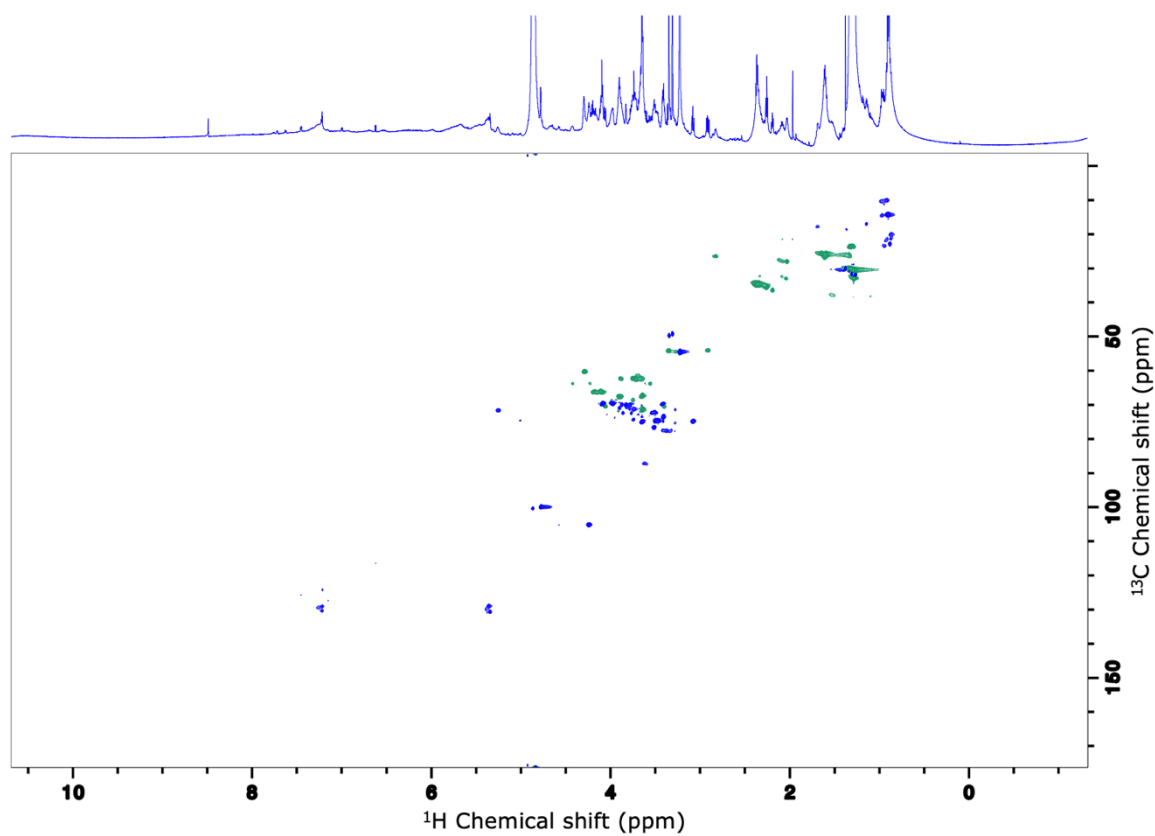
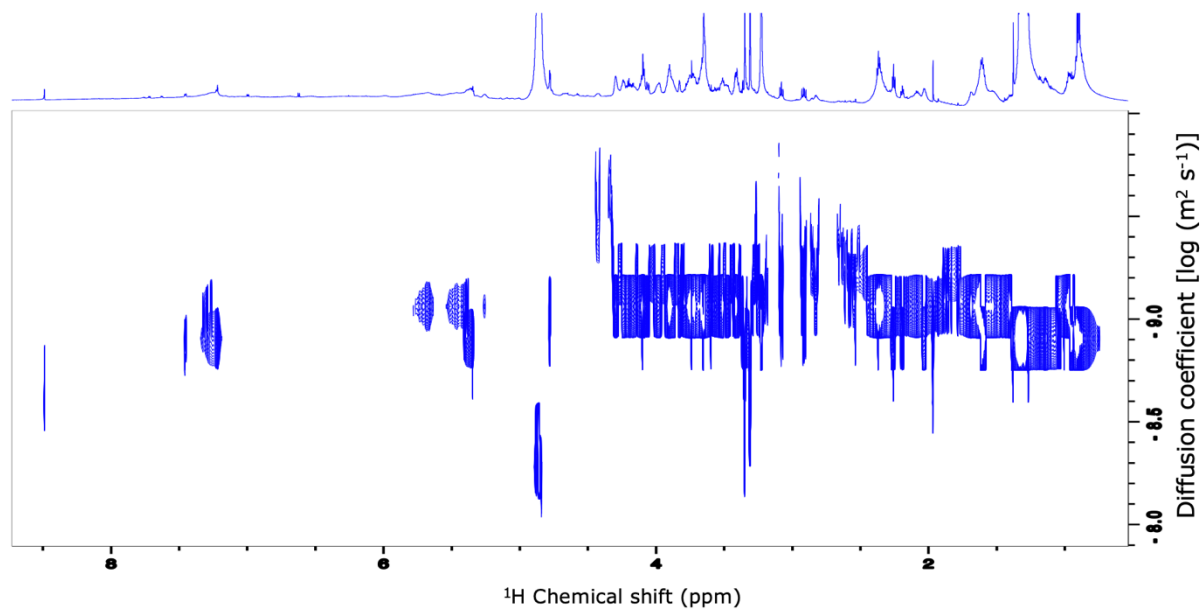


Figure E-14: DOSY spectrum of *Alaria esculenta* P1.



**Figure E-15:  $^1\text{H}$ - $^{13}\text{C}$  HSQC of *Alaria esculenta* P2.**



**Figure E-16: DOSY spectrum of *Alaria esculenta* P2.**

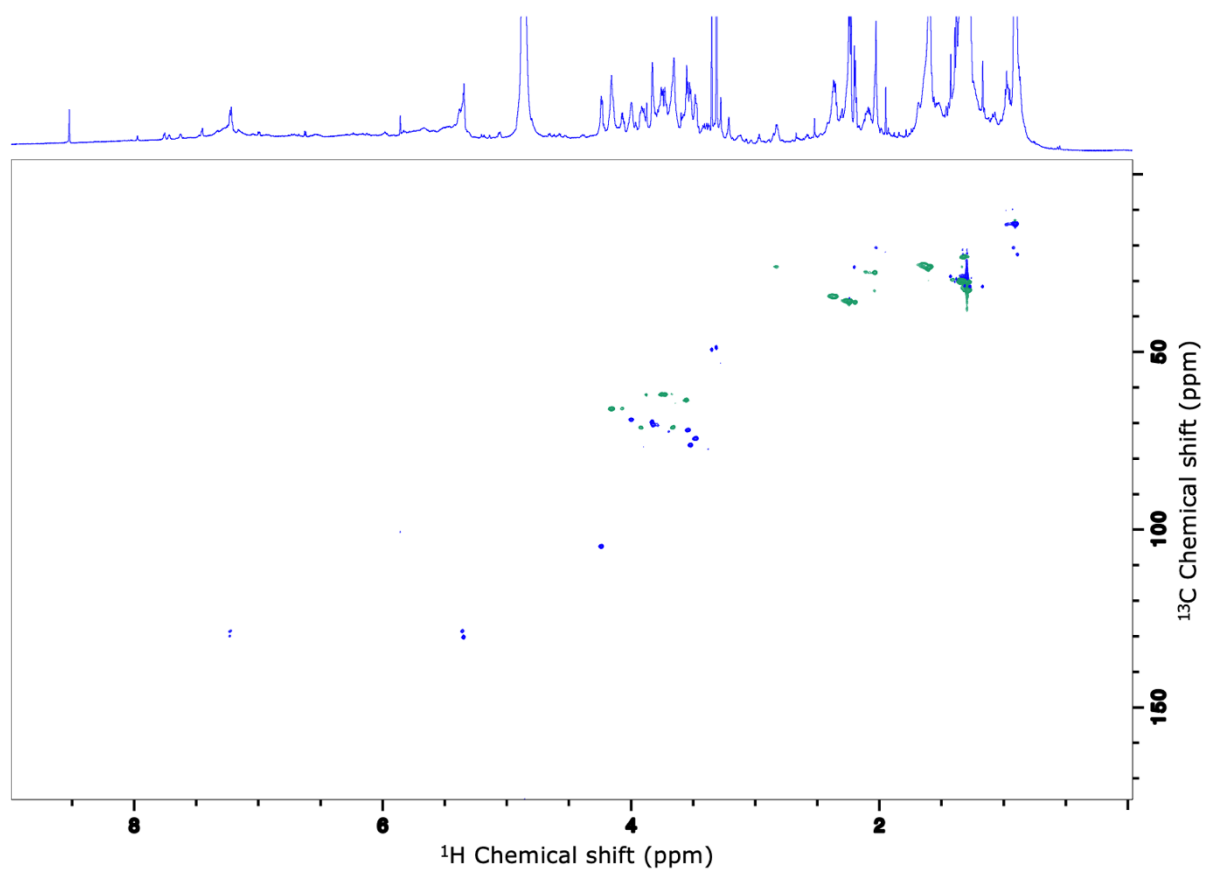


**Figure E-17:  $^1\text{H}$ - $^{13}\text{C}$  HSQC of *Alaria esculenta* P3.**

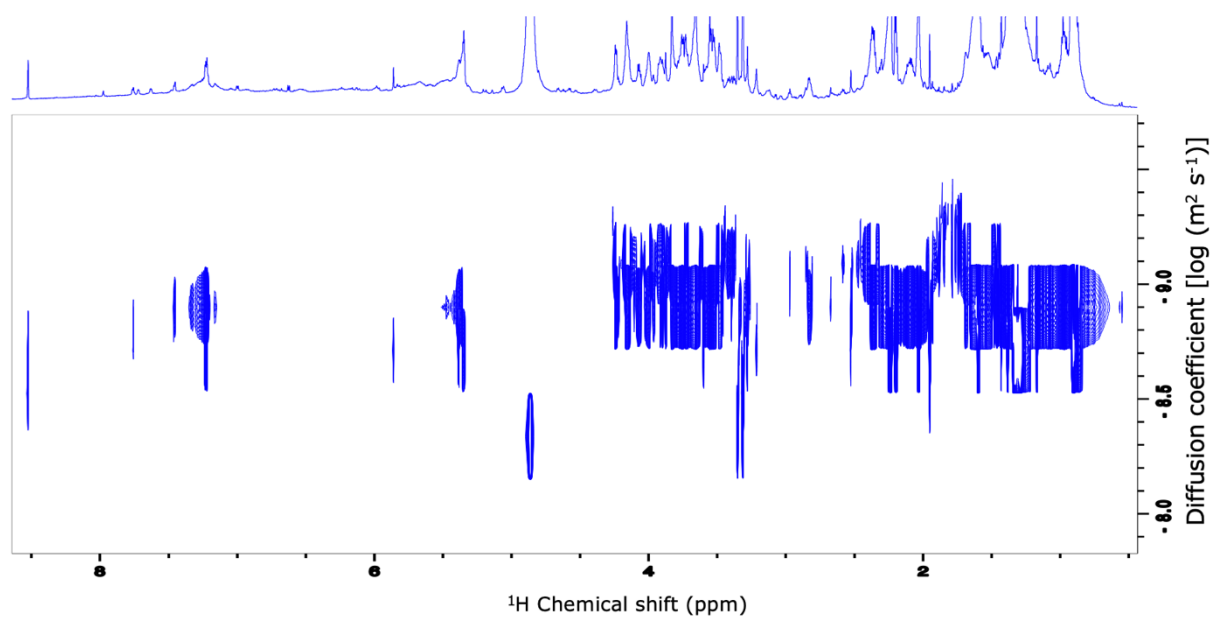


**Figure E-18: DOSY spectrum of *Alaria esculenta* P3.**



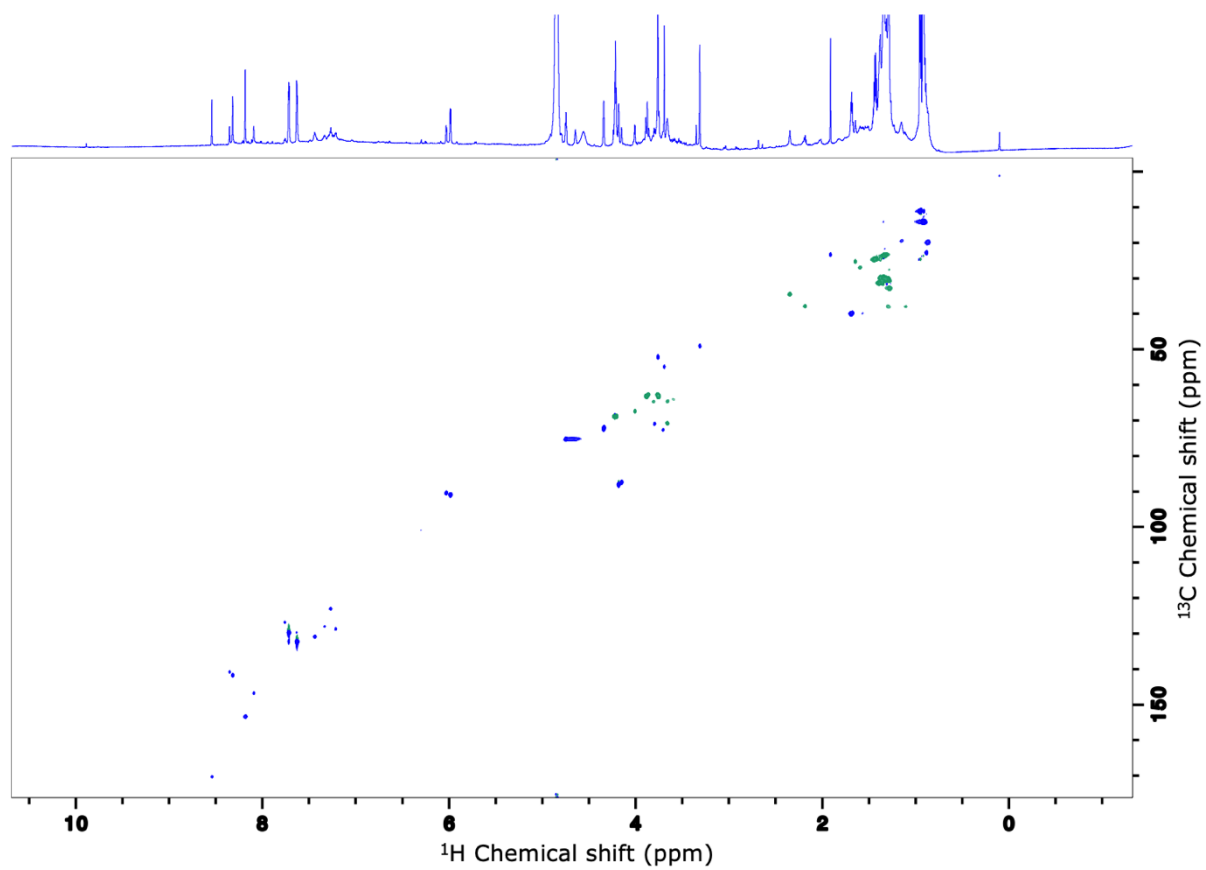


**Figure E-19:  $^1\text{H}$ - $^{13}\text{C}$  HSQC of *Alaria esculenta* P4.**

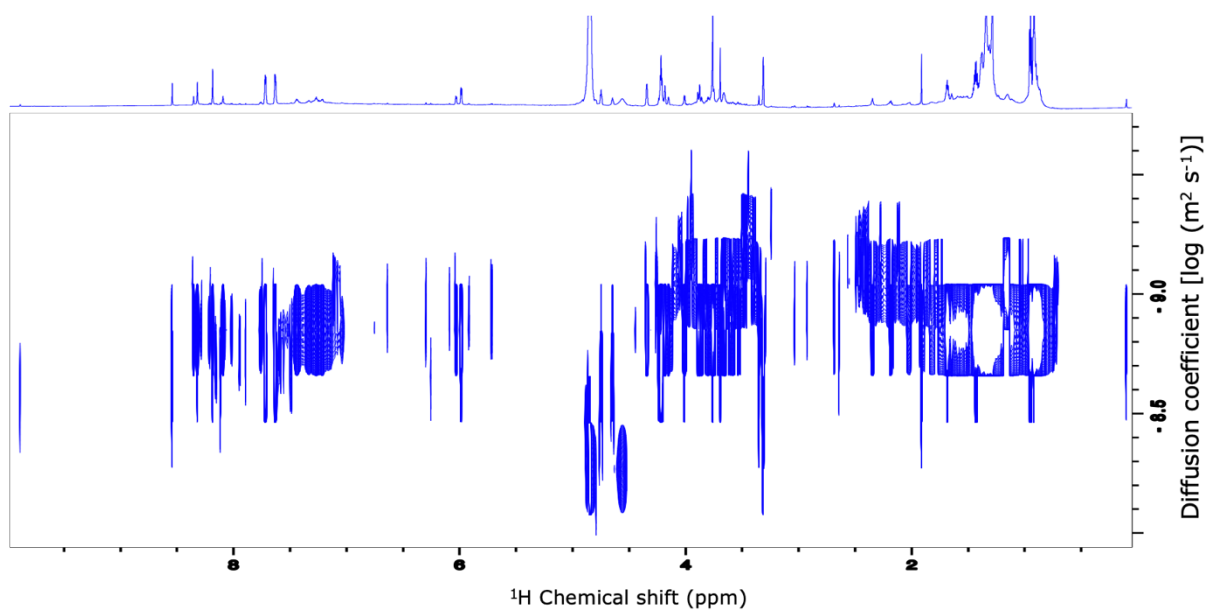


**Figure E-20: DOSY spectrum of *Alaria esculenta* P4.**

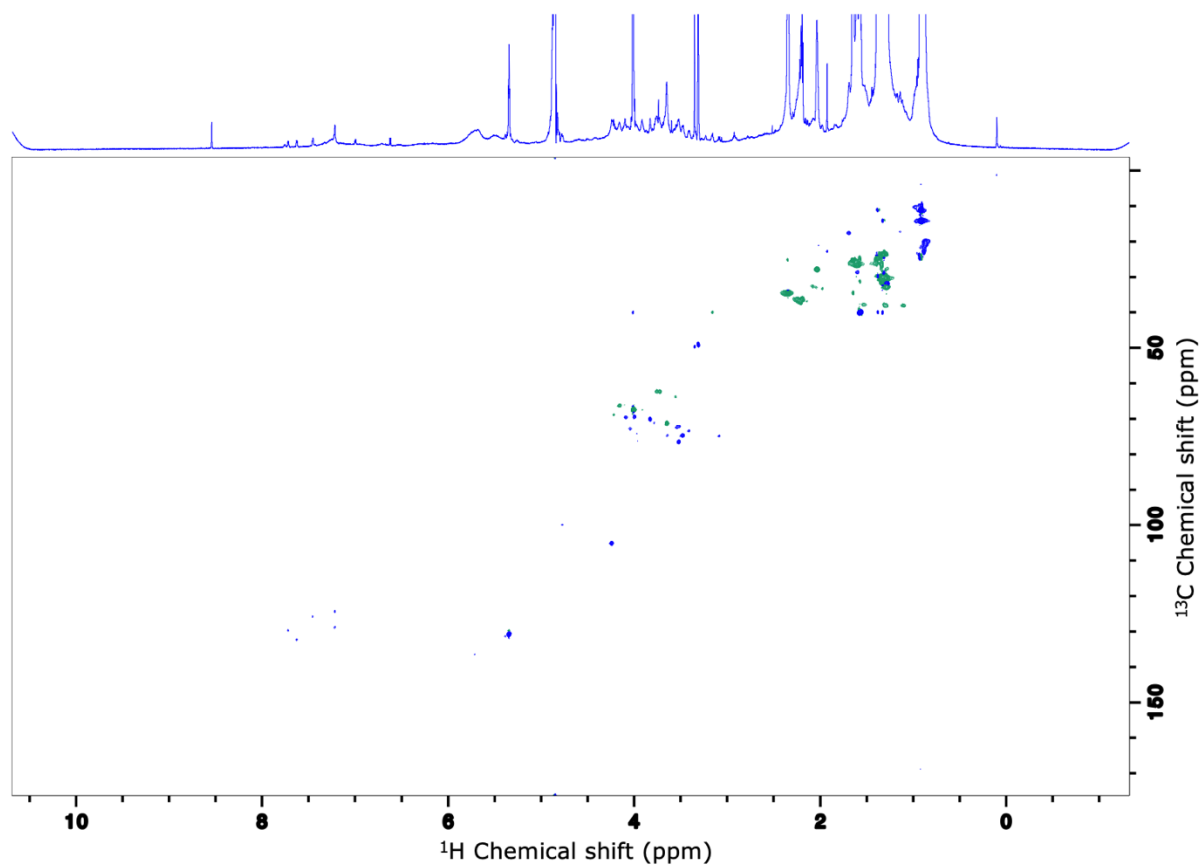


Figure E-21:  $^1\text{H}$ - $^{13}\text{C}$  HSQC of *Saccharina latissima* P5.

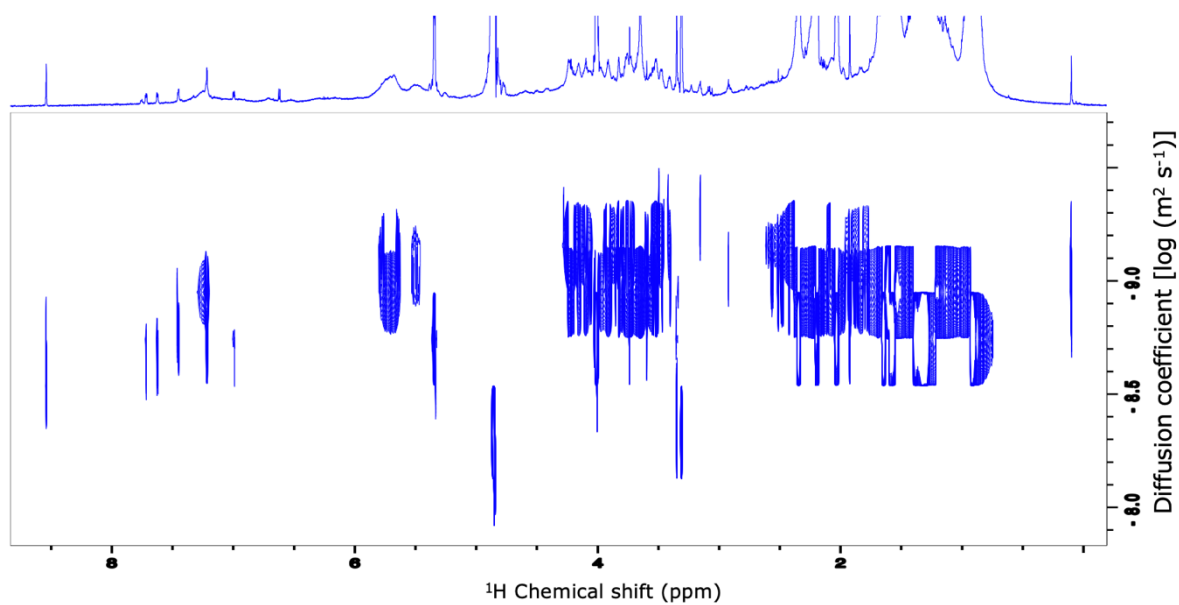
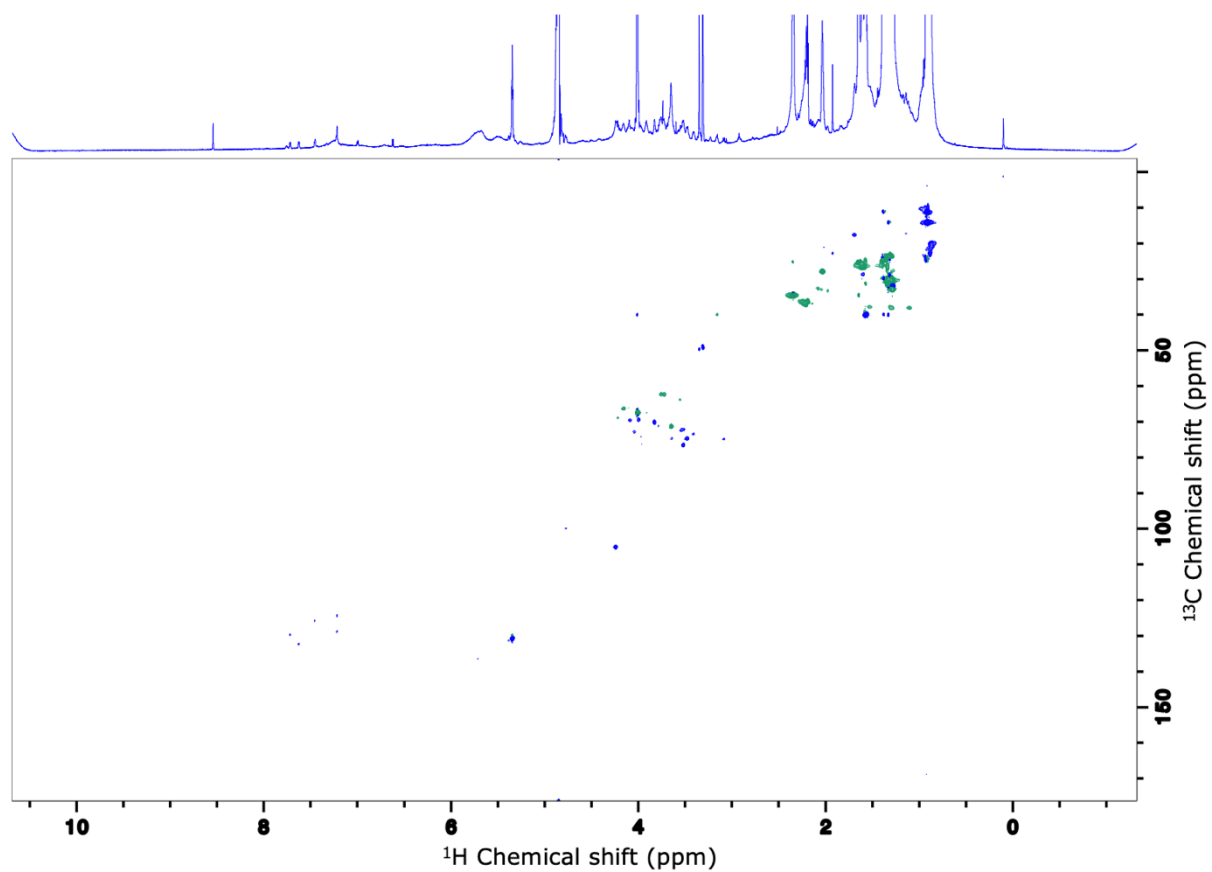
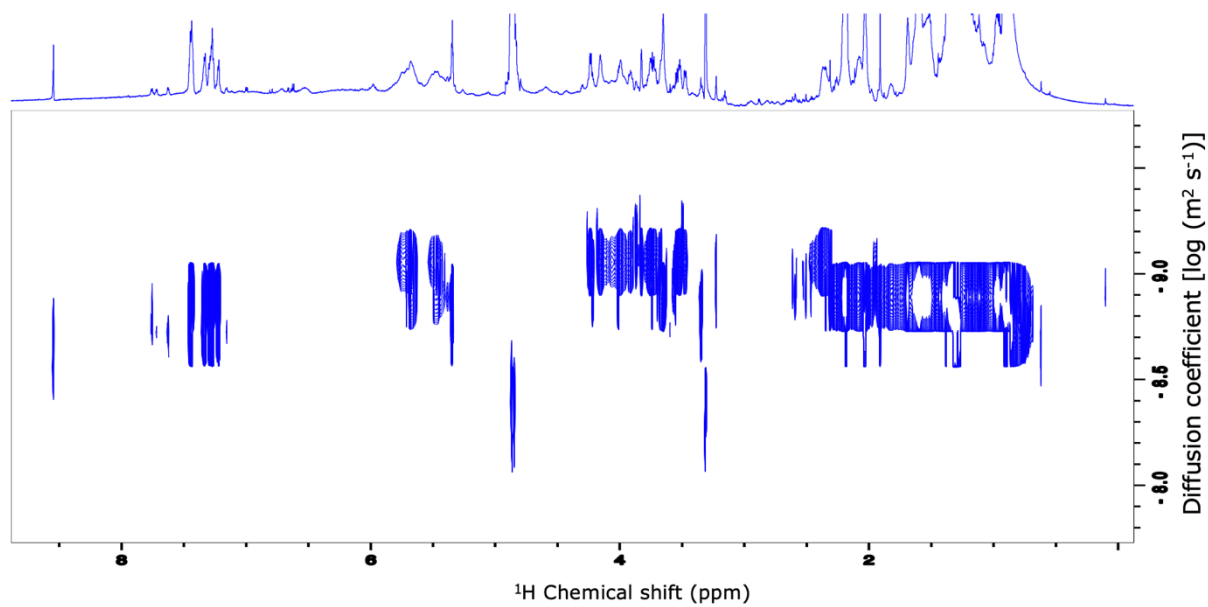


Figure E-22: DOSY HSQC of *Saccharina latissima* P5.



**Figure E-23:  $^1\text{H}$ - $^{13}\text{C}$  HSQC of *Saccharina latissima* P6.**



**Figure E-24: DOSY of *Saccharina latissima* P6.**

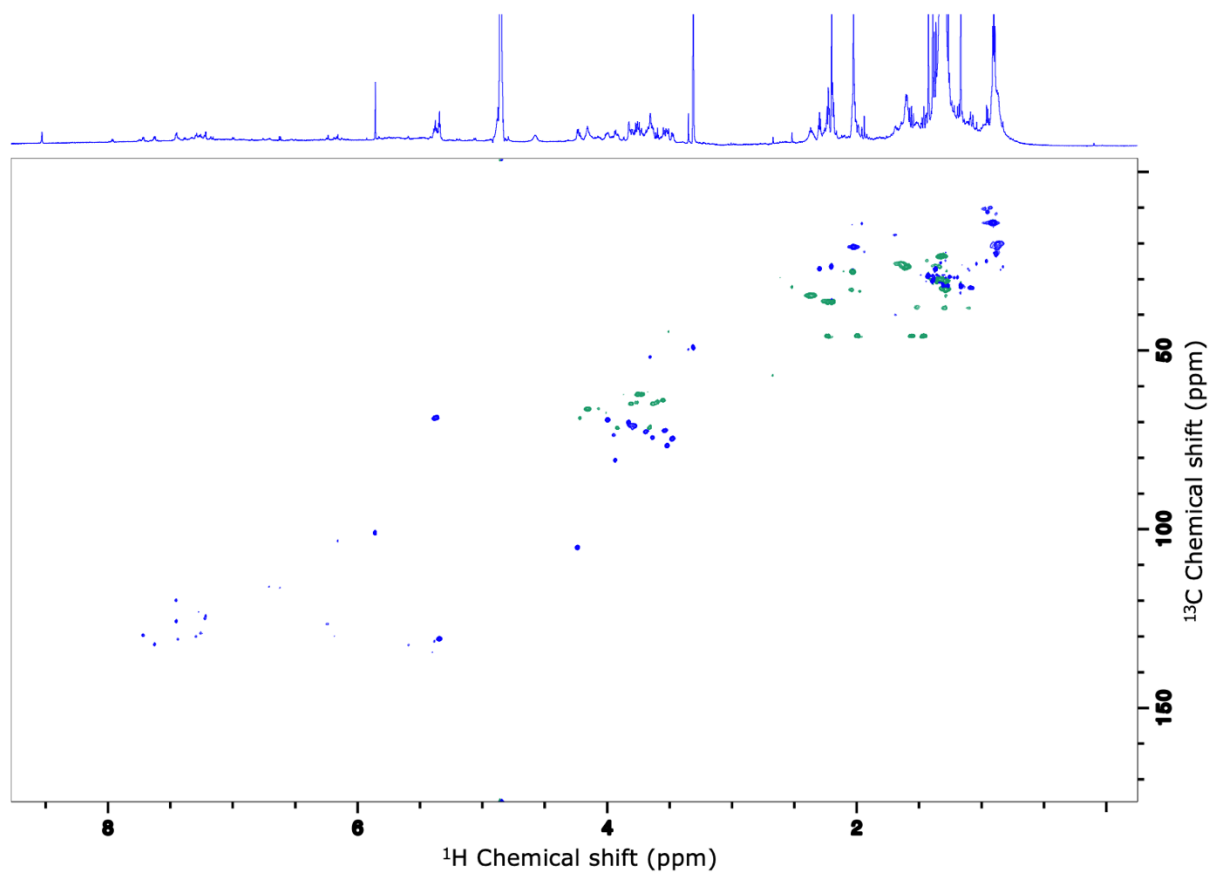


**Figure E-25:  $^1\text{H}$ - $^{13}\text{C}$  HSQC of *Saccharina latissima* P7.**

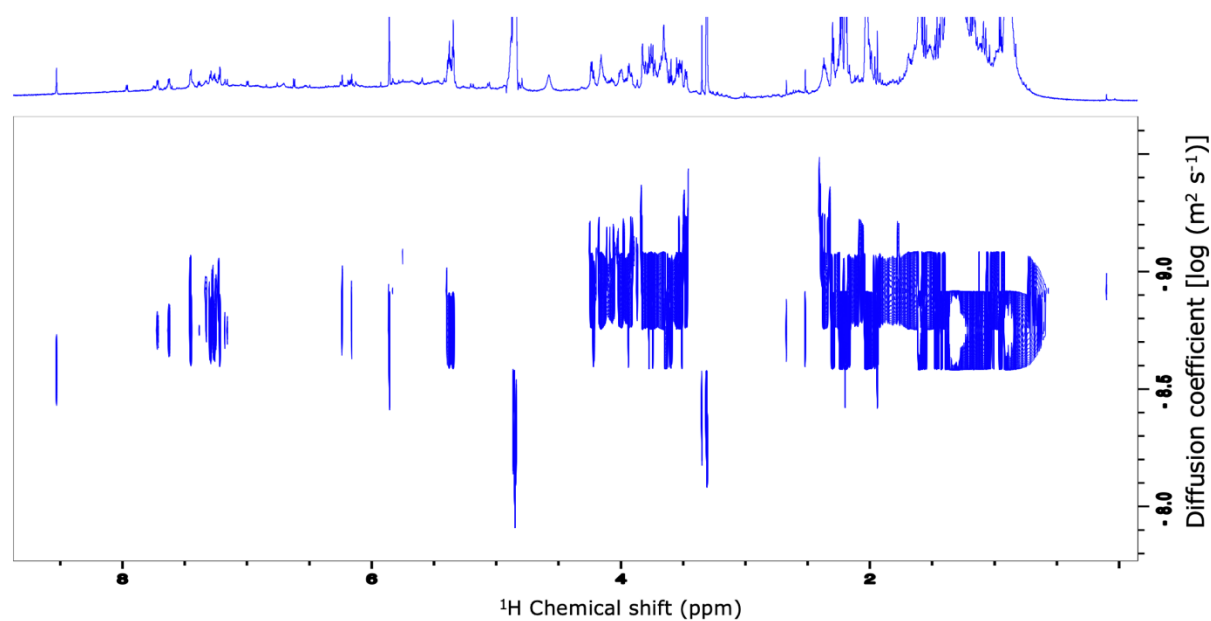


**Figure E-26: DOSY of *Saccharina latissima* P7.**

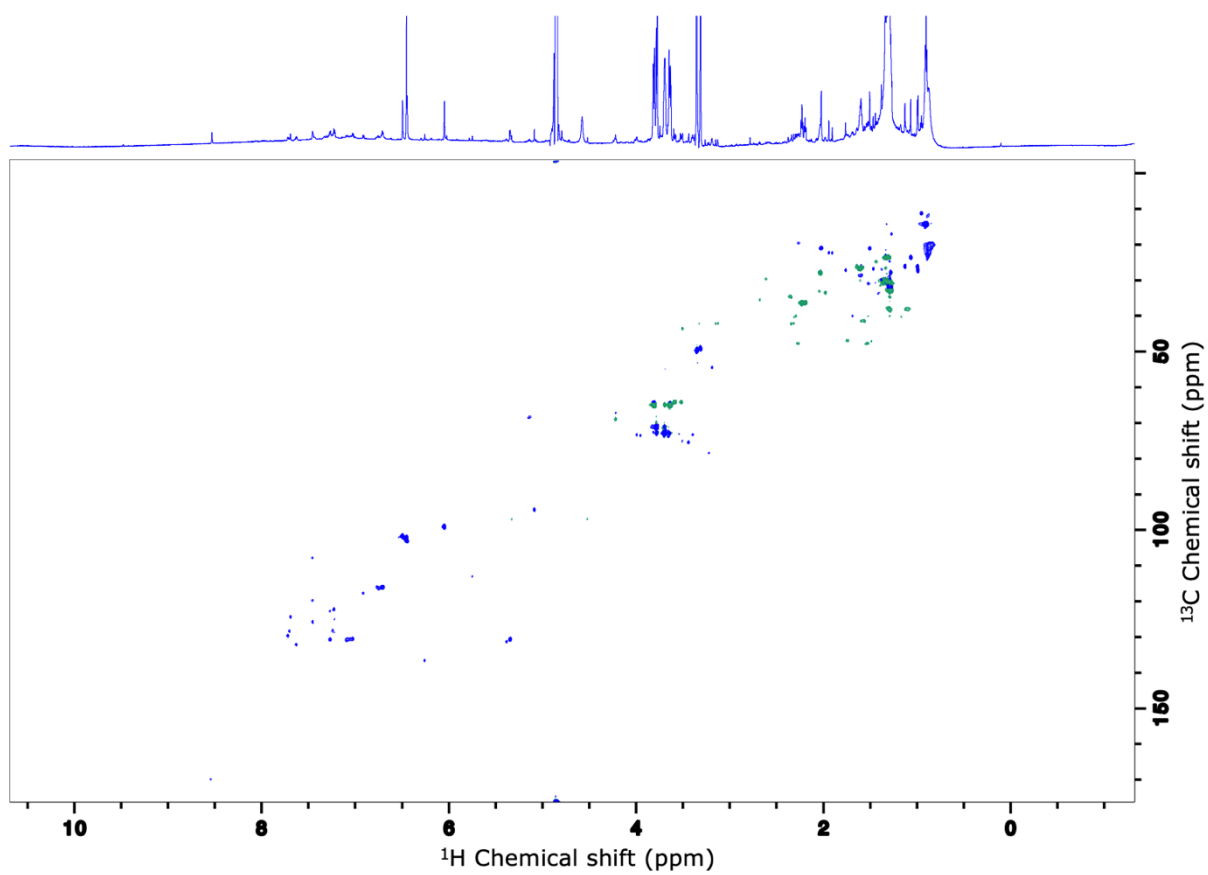


**Figure E-27:  $^1\text{H}$ - $^{13}\text{C}$  HSQC of *Saccharina latissima* P8.**

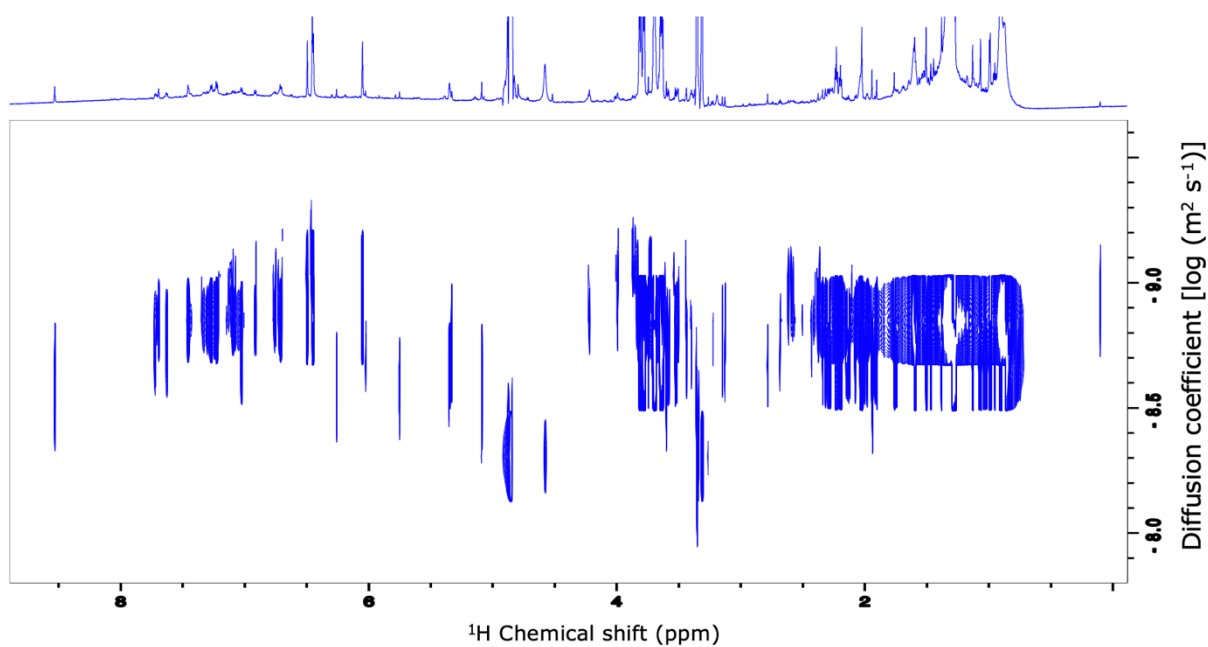


**Figure E-28: DOSY of *Saccharina latissima* P8.**

## Appendix F: NMR spectra FD (DENMARK)

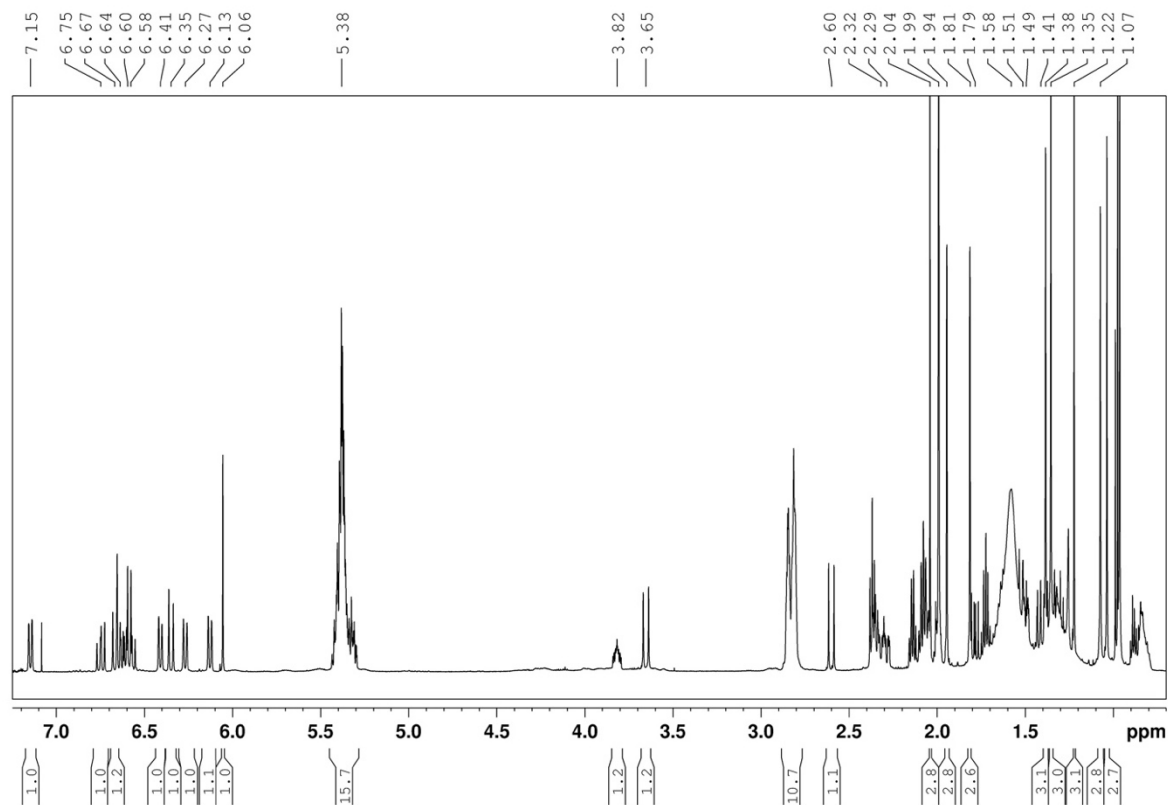


**Figure F-1:**  $^1\text{H}$  NMR spectrum of freeze-dried material of *Alaria esculenta* extracted with acetone and purified with XAD-16 resin.

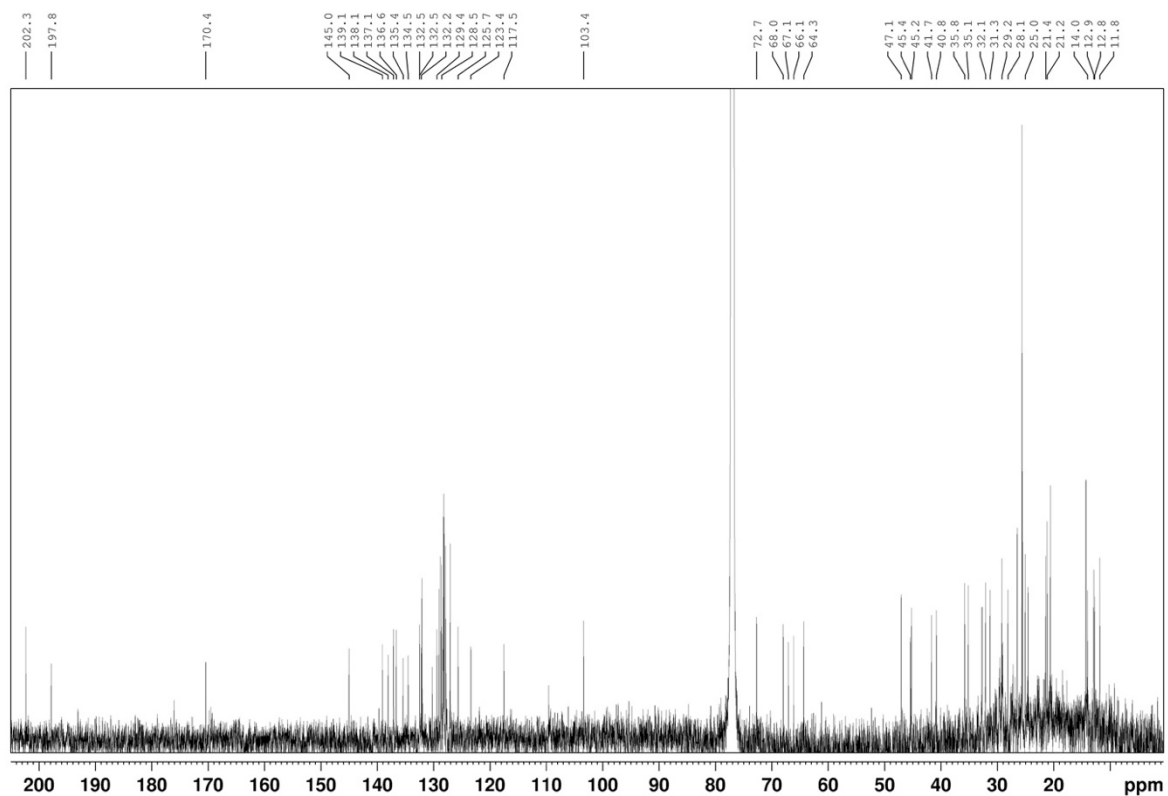


**Figure F-2:**  $^{13}\text{C}$  NMR spectrum of freeze-dried material of *Alaria esculenta* extracted with acetone and purified with XAD-16 resin.

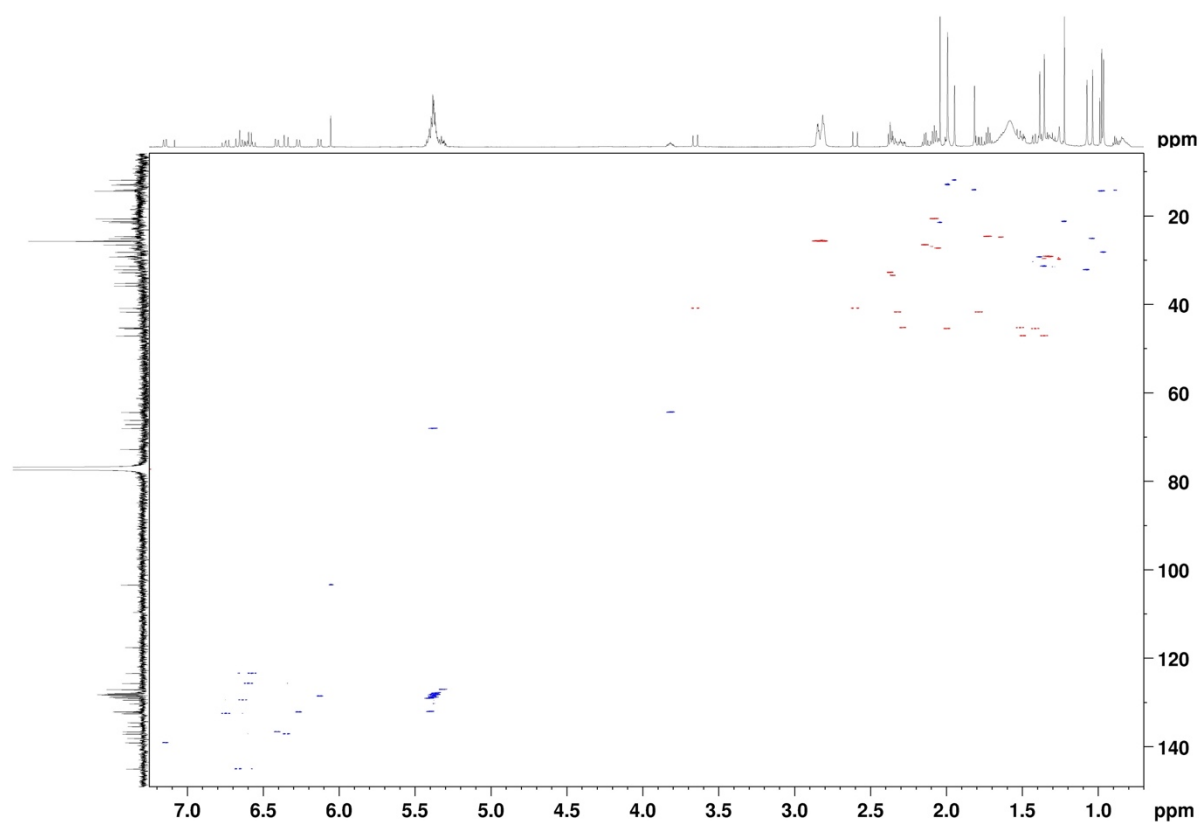


**Figure F-3:**  $^1\text{H}$ - $^{13}\text{C}$  HSQC spectrum of freeze-dried material of *Alaria esculenta* extracted with acetone and purified with XAD-16 resin.

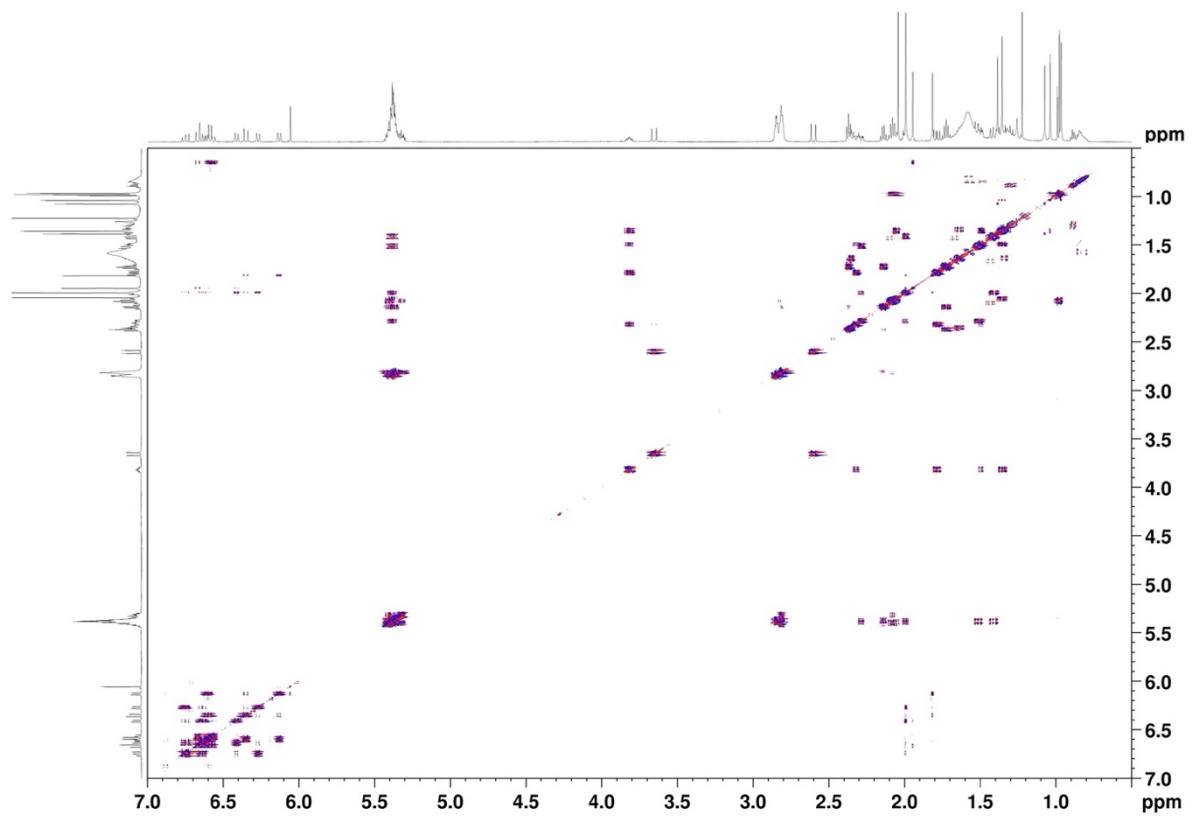


Figure F-4:  $^1\text{H}$ - $^1\text{H}$  COSY spectrum of freeze-dried material of *Alaria esculenta* extracted with acetone and purified with XAD-16 resin.

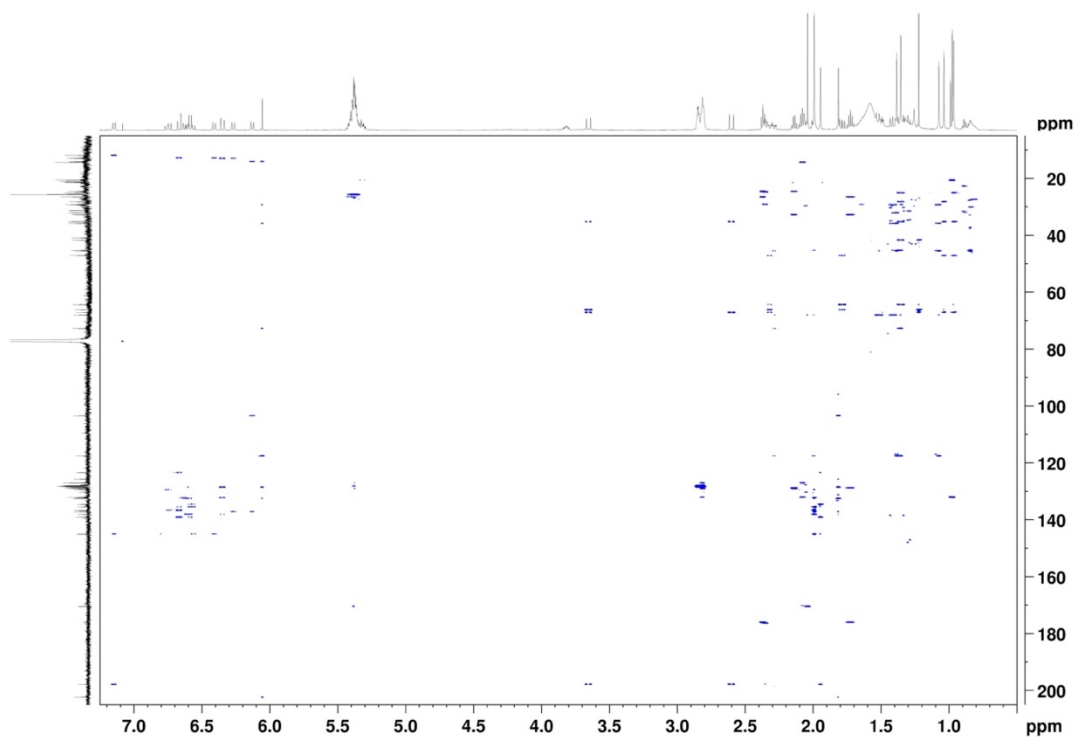
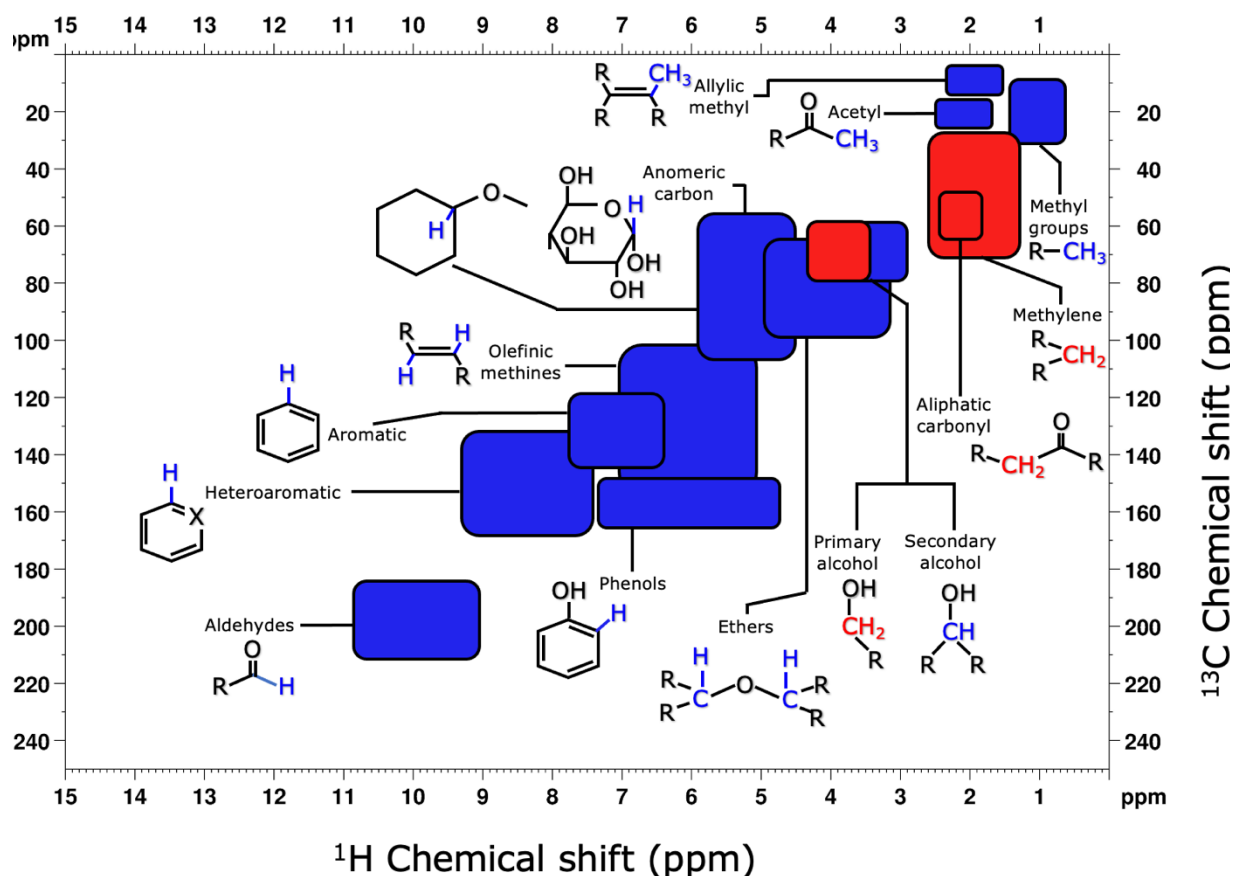


Figure F-5:  $^1\text{H}$ - $^{13}\text{C}$  HMBC spectrum of freeze-dried material of *Alaria esculenta* extracted with acetone and purified with XAD-16 resin.



## Appendix G: HSQC of common moieties in carotenoids and polyphenol

A  $^1\text{H}$ - $^{13}\text{C}$  HSQC (figure G-1) was made for moieties found in carotenoids and polyphenols. It also includes moieties in lipids. The map displays a 2-dimensional spectrum with the chemical shift for protons on the x-axis and for carbons on the y-axis. The areas, where the proton-carbon correlations of the relevant moieties are expected to appear, are marked with squared boxes in either blue or red, depending on the number of protons attached to the carbon. The map was developed by compiling information from samples analyzed in this thesis, and recourses providing typical values for chemical shifts of protons (Organic Chemistry Data, 2005b) and carbons (Organic Chemistry Data, 2005a) in these moieties. The map was further used as a guide when looking at  $^1\text{H}$ - $^{13}\text{C}$  HSQC spectra for carotenoids, polyphenols, and lipids in the samples throughout this thesis.



**Figure G-1:  $^1\text{H}$ - $^{13}\text{C}$  HSQC proton-carbon spin pairs typical for moieties found in carotenoids and polyphenols.** The marked areas (blue and red squares) show typical values for chemical shift of protons and carbons in moieties found in carotenoids and polyphenols. Blue represents methines (CH) and methyl groups ( $\text{CH}_3$ ), red represents methylene groups ( $\text{CH}_2$ ).



